ISSN 2663-2586 (Online)
ISSN 2663-2578 (Print)

1 (203)
2021

Cybernetics and Computer Engineering

КІБЕРНЕТИКА ТА ОБЧИСЛЮВАЛЬНА ТЕХНІКА

The journal is included in the List of Scientific Professional Editions of the Ministry of Education and Science of Ukraine (MESU) for PhD applicants, category "B", in biological and medical sciences, (order of the MES of Ukraine № 409, 17.03.2020), technical and physical-mathematical sciences (order of the MES of Ukraine № 1188, 24.09.2020)

The journal is included in Google Scholar, information resource Scientific Periodicals of Ukraine (V.I. Vernadsky NLU), ULRICHS WEB, Crossref (DOI), ROAD, DOAJ, Index Copernicus, Electronic Journals Library (Germany)

Certificate of State Registration КВ № 12649-1533Р, 14.05.2007

Editorial address:

03187 Kyiv, Acad. Glushkov av., 40
International Research and Training Center
for Information Technologies and Systems of the National Academy of Sciences of Ukraine and the Ministry of Education and Science of Ukraine

Phon: 503 95 62. E-mail: kvt.journal@kvt-journal.org.ua, http://kvt-journal.org.ua/

Executive editor *Pezentsali H.O.*

Editor *Charchiyan N.A.*

Computer layout *Tupalskiy O.V.*

Web-master *Voychenko O.P.*

Підп. до друку 31.03.2021. Формат 70×108/16. Гарн. Times New Roman.
Ум. друк. арк. 10,33. Обл. вид. арк. 9,84. Тираж 66. Зам. №

Віддруковано ВД "Академперіодика" НАН України
01004, Київ 4, вул. Терещенківська, 4.

Свідоцтво про внесення до Державного реєстру суб'єкта видавничої справи

Серії ДК № 544 від 27.07.2001 р.

NATIONAL ACADEMY OF SCIENCES OF UKRAINE
INTERNATIONAL RESEARCH AND TRAINING CENTER FOR INFORMATION TECHNOLOGIES AND SYSTEMS OF THE NAS OF UKRAINE AND OF MES OF UKRAINE
V.M. GLUSHKOV INSTITUTE OF CYBERNETICS OF THE NAS OF UKRAINE

Cybernetics and Computer Engineering

1 (203)/2021

SCIENTIFIC JOURNAL ▪ FOUNDED IN 1965 ▪ PUBLISHED 4 TIMES PER YEAR ▪ KYIV

CONTENTS

NATIONAL ACADEMY OF SCIENCES OF UKRAINE
INTERNATIONAL RESEARCH AND TRAINING CENTER FOR INFORMATION TECHNOLOGIES AND SYSTEMS OF THE NAS OF UKRAINE AND OF MES OF UKRAINE
V.M. GLUSHKOV INSTITUTE OF CYBERNETICS OF THE NAS OF UKRAINE

Cybernetics and Computer Engineering

1 (203)/2021

SCIENTIFIC JOURNAL ▪ FOUNDED IN 1965 ▪ PUBLISHED 4 TIMES PER YEAR ▪ KYIV

CONTENTS

НАЦІОНАЛЬНА АКАДЕМІЯ НАУК УКРАЇНИ
МІЖНАРОДНИЙ НАУКОВО-НАВЧАЛЬНИЙ ЦЕНТР
ІНФОРМАЦІЙНИХ ТЕХНОЛОГІЙ ТА СИСТЕМ НАН УКРАЇНИ І МОН УКРАЇНИ
ІНСТИТУТ КІБЕРНЕТИКИ ІМ. В.М. ГЛУШКОВА НАН УКРАЇНИ

Кібернетика та обчислювальна техніка

1 (203)/2021

НАУКОВИЙ ЖУРНАЛ ▪ ЗАСНОВАНИЙ У 1965 р. ▪ ВИХОДИТЬ 4 РАЗИ НА РІК ▪ КИЇВ

ЗМІСТ

Informatics and Information Technologies

DOI: https://doi.org/10.15407/kvt203.01.005

UDC: 004.67: 543.062

SUROVTSEV I.V.[1], DSc (Engineering), Senior Researcher,
Head of the Ecological Digital Systems Department
e-mail: dep115@irtc.org.ua, igorsur52@gmail.com
ORCID: 0000-0003-1133-6207
GALIMOV S.K.[1], Leading Engineer,
Ecological Digital Systems Department
e-mail: dep115@irtc.org.ua
ORCID: 0000-0001-5716-9454
GALIMOVA V.M.[2]**,** PhD (Chemistry),
Associate Professor, Department of Analytical and Inorganic
Chemistry and Water Quality
e-mail: galimova2201@gmail.com
ORCID: 0000-0001-9602-1006
SARKISOVA M.V.[2] Student
Veterinary Faculty
e-mail: mari.doga2014@gmail.com
ORCID: 0000-0002-5462-6442
[1] International Research and Training Center for
Information Technologies and Systems of the
National Academy of Sciences of Ukraine
and Ministry of Education and Science of Ukraine,
40, Acad. Glushkov av., Kyiv, 03187, Ukraine
[2] National University of Life
and Environmental Sciences of Ukraine,
17, bldg. 2, Heroes of Defense str.,
Kyiv, 03041, Ukraine

METHOD OF CHRONOIONOMETRIC DETERMINATION OF CONCENTRATIONS OF FLUORINE, NITRATE, AMMONIUM IN DRINKING WATER

Introduction. *Using method of chronoionometry and ion-selective electrodes makes it possible to determine quickly the concentrations of chemical elements, which allows you to assess the quality of drinking water and the ecological condition of the environment.*

The purpose *of the paper is to apply the developed method of chronoionometry to measure the concentrations of fluoride, nitrate, ammonium in drinking water and to assess the accuracy of measuring concentrations.*

Methods. *Chronoionometric method of chemical analysis uses the principles of direct potentiometry to measure the concentrations of chemical elements.*

Results. *Methods for detection the concentrations of fluorine, nitrates, ammonium in drinking water were obtained and tests were performed in model aqueous solutions using the device of inversion chronopotentiometry "Analyzer SCP", which testify to the compliance of measurement errors with metrological normative values.*

Conclusions. *Improved analytical system "Analyzer SCP" to determine the concentration of 20 chemical elements (Hg, As, Pb, Cd, Cu, Zn, Sn, Ni, Co, Se, Mn, I, Cr, Fe, K, Na, Ca, F, NO_3, NH_4) in aqueous solutions by inversion chronopotentiometry and chronoionometry, which is sufficient for ecological assessment of drinking water quality and environmental objects. The use of a new method of chronoionometry significantly expands the functionality of the device of inversion chronopotentiometry, increases the reliability and accuracy of measuring the concentrations of chemical elements.*

Keywords: *chronoionometry method, concentration, of fluoride, nitrate, ammonium, ion-selective electrode, inversion chronopotentiometry, drinking water.*

INTRODUCTION

At the present stage of development of society, one of the central places is occupied by the problems of the ecological state of the environment and its pollution by various toxic chemical elements. Therefore, much attention is paid to the control of quality and safety of drinking water and food with the help of cost-effective and highly accurate means of control. According to the WHO, more than 80 % of human diseases can be caused by drinking contaminated water. It is known that the daily human need for water is 2.5–3.0 liters. Along with drinking water, heavy metals, microelements, as well as many salts and macronutrients, in particular, fluoride compounds, nitrate, and ammonium enter the human body.

Therefore, there is a need to develop intelligent methods and tools for environmental monitoring, the introduction of modern information technology that will provide versatility and expressive measurement of concentrations of chemical elements. Such technologies make it possible to obtain, collect and intelligently analyze the obtained environmental information for decision-making on the prevention of human health disorders and carrying out preventive ecological measures.

Thus, in order to perform quality control and assess the ecological state of the environment, primarily water supply sources [1], the International Research and Training Center for Information Technologies and Systems of NAS of Ukraine and MES of Ukraine has developed a highly sensitive analytical system "Analyzer SCP" on the use of electrochemical methods of inversion chronopotentiometry (SCP) and a new chronoionometric method of analysis (CHI).

The analytical system makes it possible to determine in drinking water and in the environment trace concentrations of 17 chemical elements [2], including such ions as potassium (K^+), sodium (Na^+) and calcium (Ca^{2+}), measured by chronoionometric by the method using ion-selective electrodes ISE (ion-selective electrodes). The application of the CHI method allowed to increase the accuracy of the ionometric study and to improve the stability of the potential measurement.

According to the current normative document in Ukraine on the quality of drinking water intended for human consumption [1], in addition to determining the content of heavy metals (Hg, As, Pb, Cd, Cu, Zn, Sn, Ni, Co, Mn, Cr, Fe) and elements (Se, I, K, Na, Ca) it is necessary to determine a number of sanitary and toxicological indicators: ammonium NH_4^+, nitrate NO_3^- and fluorides F^- (hazard class II). The concentration of these macronutrients in drinking water can also be

measured on the device "Analyzer SCP", using our developed method CHI [2, 3], information technology [4] and the corresponding ISE [5], which will expand the functionality of the device.

PROBLEM STATEMENT

The content of fluorine ions, nitrates and ammonium in water has a significant affected human health, so it is important to control them in accordance with sanitary and toxicological standards with the help of modern analytical instruments, fluoride (HF) by passive diffusion [6].
According to the state standards which include the method of CHI.

Fluoride is one of the most important chemical elements that significantly affects human life in general. The daily intake of fluoride anions with food is on average 2–3 mg 90–97 % of which is absorbed in the gastrointestinal tract and blood, from blood plasma fluoride ions are rapidly distributed in intracellular and extracellular fluids, tissues and organs, they are able to penetrate quickly. through biological membranes in the form of hydrogen, the permissible concentration of fluoride in drinking water is 1.5 mg/dm^3 [1]. At concentrations less than 0.7 mg/dm^3 there is a deficiency of fluoride, i.e. hypofluorosis. It provokes the development of caries, most children are prone to it. There are also conventional guidelines for the association of hypofluorosis with rickets, impaired immune status and disorders of calcium metabolism [7].

Increasing the concentration of fluoride in drinking water to 2 mg/dm^3 causes the spread of fluorosis and increases the severity of its course. If the concentration is higher than acceptable (1.5–2 mg/dm^3), then 30–40 % of the population is affected by dental fluorosis, mainly I and II degree. The use of water with such a concentration of fluoride may be temporarily acceptable in terms of local water supply [8, 9]. In the case of centralized water supply, it is necessary to carry out defluoridation or dilution of water. At high concentrations of fluoride in drinking water (2–6 mg/dm^3) the incidence of fluorosis is 30–90 %, and 10–50 % of them have fluorosis of III–IV degree [10]. Among children, there are often cases of developmental delay and bone mineralization [11]. In some people who drink water with a fluoride content of 4–6 mg/dm^3, there is an increase in bone density and impaired conditioned reflex activity.

At very high concentrations of fluoride in drinking water (6–15 mg/dm^3 and more) 90–100 % of the population becomes affected by dental fluorosis with a predominance of severe forms, significantly increased fragility of teeth, mineralization disorders and changes in bones by type of osteosclerosis [12]. There is suppression of thyroid function, changes in the activity of certain enzyme systems of the blood, changes in the myocardium, inhibition of bioelectrical activity of the brain, as well as disorders of other internal organs (e.g. liver), which are detected during functional examination [13].

Fluoride in minimal amounts is necessary for metabolic processes in the body and is the seventh vital trace element after copper, zinc, iron, manganese, iodine and cobalt [14]. Fluoride has a regulatory effect not only on bone cells (osteoblasts and osteoclasts), but also on cells of the endothelium, liver, kidneys, myocardium and nervous system. Excretion of fluoride from the body occurs through the skin, digestive tract and urinary system with an excretion period of 2 to 9 hours. At the cellular level under the action of fluoride in the cells increases the generation of O_2,

H_2O_2, OH^- and nitric oxide NO. Fluoride compounds have been shown to be a cytotoxic factor involved in metabolic alteration, modulation of intracellular signaling pathways and activation of programmed cell death. The mechanisms of physiological or toxic effects of fluoride compounds on the body depend on their concentrations and duration of consumption [15].

Nitrate is inorganic anions (NO_3^-), which are formed due to oxidation of elemental nitrogen. It is an important nutrient for the synthesis of plant proteins, which plays a significant role in the nitrogen cycle of soils and water. Nitrate is formed by natural biological and physical oxidation, they are ubiquitous in the environment [16]. Most nitrate come from inorganic chemicals, especially from fertilizers produced for agriculture. Ammonia from livestock waste can be oxidized to nitrate by soil bacteria under aerobic conditions. It can also be a significant source of nitrate in surface and groundwater, especially near areas where animals are raised [17].

The primary toxic effect of the inorganic nitrate ion (NO_3^-) is due to its reduction to nitrite (NO_2^-). Organic nitrate is metabolized in the liver, which leads to an increas in nitrite in the blood. Nitrate and nitrite are excreted mainly in the urine as nitrate. The main toxic effect of inorganic nitrate is the oxidation of iron in hemoglobin due to an excess of nitrites that form methemoglobin. Infants under 6 months of age make up the most sensitive population. Epidemiological studies have shown that infant formula prepared from drinking water with a nitrate nitrogen content of more than 10 mg/dm^3 can lead to methemoglobinemia, especially in children under 2 months of age [18]. The results show a correlation between the number of congenital malformations of the central nervous system, musculoskeletal system and infants with the amount of inorganic nitrate in drinking water that was consumed. Elderly people, people with anemia, people with respiratory and cardiovascular diseases are also sensitive to nitrate. There are cases of the disease in older children (after consuming water with a high content of nitrate).

Therefore, it is strictly forbidden to use water from wells and catchments where the nitrate content exceeds the norm. Boiling nitrate-contaminated water does not reduce, but increases its toxicity by 39–86 %. Therefore, it is important to determine the nitrate content in drinking water in a timely manner, using analytical measurement methods [19–22].

Organic nitrate is well known for their vasodilating action and is used to treat angina. The possible carcinogenicity of nitrate depends on the conversion of nitrate to nitrite and the reaction of nitrite with secondary amines, amides and carbamates to form carcinogenic nitro compounds.

Ammonium — a substance that is the initial product of decomposition of organic nitrogenous substances, is readily soluble and is always present in water in small concentrations as a mandatory component. Ammonium appears in water due to the dissolution of ammonia in it [23].

Ammonium is one of the most important cations for monitoring, especially in wastewater areas, as large amounts can be toxic to aquatic organisms. Ammonia dissolved in water is formed as a result of anaerobic decomposition of nitrogen-containing compounds from waste streams. Ammonium monitoring is extremely important in determining the quality of drinking water [1] and in open water, in places of wastewater discharge [24].

The increased content of ammonium indicates the deterioration of the sanitary condition of the water. The increase in concentrations is due to the inflow of domestic wastewater, nitrogen and organic fertilizers into groundwater. The content of ammonium in high concentrations in drinking water negatively effects on the human body. Blood pressure may rise, there are various disorders of the liver and kidneys. The toxic effect of ammonium depends on the concentration and duration of consumption of contaminated drinking water, it increases with increasing pH. Short-term consumption of water with a concentration of ammonium salts in the range of 75–360 mg/kg causes an increase in blood pressure. Under conditions of prolonged exposure to drinking water with high levels of ammonium, there is a decrease in calcium in the body, changes in blood pH and weight loss [25].

Electrodes and methods for measuring fluoride, nitrate and ammonium.

Recently, a significant amount of research in the field of electrochemical research is aimed at developing more practical electrodes and biosensors for measuring fluoride, nitrate, ammonium and other elements in the aquatic environment using new technologies and various research methods. The main research directions are aimed at using ISE for the analysis of nitrate in natural objects: in water [9, 17, 19, 23, 24], in different environments [26–28]; application of voltammetric methods of analysis [16, 18, 21, 29, 30]; the use of the element copper in nitrate sensors [18, 20, 22, 30–34]; composite graphite, glass-carbon, graphene electrodes, nanotubes and nanotechnologies for measuring nitrate [33, 35–40]; new sensors and methods for measuring ammonium and nitrate [41–44].

This is by no means a complete list of scientific studies aimed at the application of new technologies and technical means of measuring fluoride, nitrate and ammonium in various fields, but it confirms the current relevance of studying the effects of these chemical elements on human health and the environment.

To ensure control of the content of these chemical elements in water and in the environment, it is necessary to increase the reliability and accuracy of concentrations. Since the performance of electrochemical studies and determination of concentrations of chemical elements in water is quite relevant, so the task is to develop methods for the determination of fluoride ions, nitrate and ammonium in drinking water.

The purpose of the paper is to use a chronoionometric method of measuring concentrations, the principle of which is based on the use of direct potentiometry, to determine the content of fluorides, nitrates and ammonium in drinking water and to determine the metrological characteristics of accuracy.

APPLICATION OF THE CHRONOIONOMETRIC METHOD OF DETERMINATION OF CONCENTRATIONS

The method of chronoionometry is based on the principle of potentiometric analysis, according to which the force difference is measured. The essence of the method is to determine the activity of ions in the mode of direct potentiometry using measuring ISE and comparative silver chloride electrodes. During operation, ISE selectively responds to a certain type of ions, and there is a linear dependence of the electromotive force (EMF) of the electrode system on the concentrations of ions.

The process of measuring potentials by chronoionometry in the analytical system "Analyzer SCP" is performed as follows: during the determination using an electrolyzer with a sample solution, which is installed on a magnetic stirrer, immersed in the solution electrodes (indicator ion-selective and comparative silver chloride), with constant solution at a speed of 4 KHz read the value of the measurement of potentials in the measurement cycle with a duration of one second for a given period of time T [2]. In this case, in the first half of the cycle the signal is stored, and in the second half of the cycle the obtained values are processed and the value of the potential E_i is determined. The obtained values of $E(t)$ in real time in the form of chronopotentiograms are displayed, which allows to monitor the process of determining the constant potential and allows to increase the reliability of determining the concentrations of element ions in the sample solution.

The algorithm of the chronoionometry method consists of five steps: construction of a linear calibration graph at two points; measuring the potential in the sample solution; determination of the mass of the additive; measuring the potential in the sample solution with the additive and calculating the concentrations by the method of multiple additives [2].

MEASUREMENT OF FLUORINE, NITRATE AND AMMONIUM CONCENTRATIONS

Let us determine the relative errors of measuring the concentrations of chemical elements of fluoride, nitrate and ammonium ions in model solutions by the method of chronoionometry.

Fluoride. To measure the concentrations of fluorine ions by chronoionometry, electrochemical parameters of potential measurement (Table 1) and ion-selective electrodes are used: measuring electrode ELIS-131F [5] and comparative silver chloride electrode with double electrolytic key filled with 2 M HCl electrolyte.

Step 1. Determine the constant potentials of calibration solutions of fluoride:

- 1 calibration solution: 10^{-5} M NaF (0, 401 μg/cm^3) + 2 ml $BROIS_F$
- 2 calibration solution: 10^{-1} M NaF (4008 μg/cm^3) + 2 ml $BROIS_F$

$BROIS_F$ is a buffer solution for regulating the total ionic strength: take a sample of 58.5 g NaCl + 15.0 g CH_3COOH + 102.0 g $CH_3COONa \cdot 3H_2O$, transfer to a volumetric flask with a capacity of 1 dm^3, to half filled with distilled water, dissolve and bring to the mark with distilled water.

Construct a calibration graph at two points in the fluorine measurement range (Fig. 1), which shows the determination of the constant potential of the model solution of 10^{-3} M NaF.

Step 2. In a model solution of 10 ml of 10^{-5} M NaF + 2 ml of $BROIS_F$ (C_F= 0.19 mg/dm^3) measure the fluoride potential E_{izm} = -302.0 mV.

Table 1. ***Electrochemical parameters of fluoride measurement***

Ion	Concentration range, μg/cm^3	Interval potential, mV	Duration measurement, s
F^-	0,19–1900	from -500 to -200	60–180

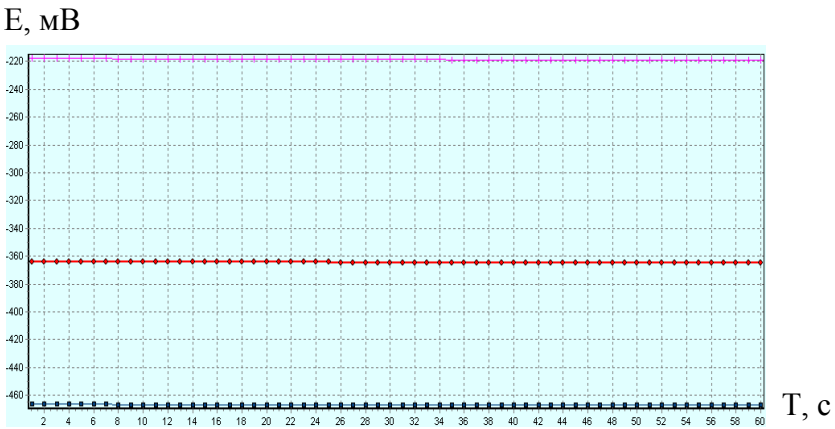

Fig. 1. Chronopotentiograms of potentials of calibration solutions of fluoride ions

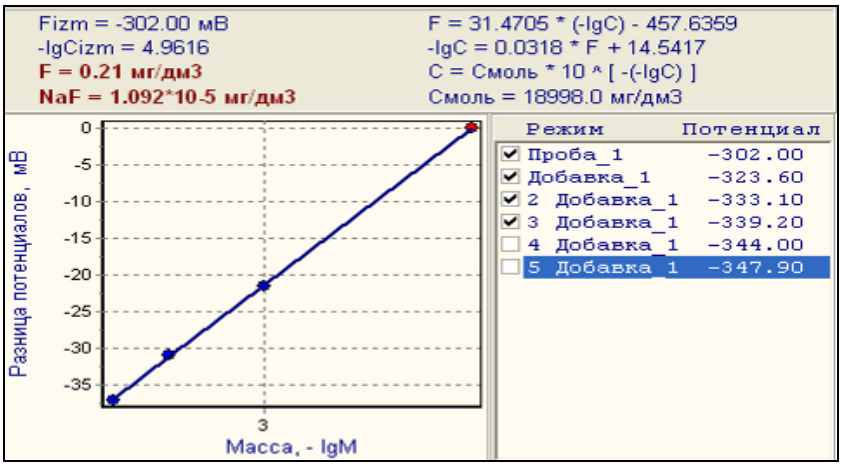

Fig 2. Determination of fluoride ion concentrations

Step 3. Determine the mass of the additive M_F = 19.0 μg of a solution of 10^{-3} M NaF.

Step 4. Measure the constant potential of the fluoride ion in the sample solution for the three additives (Fig. 2).

Step 5. Calculate the concentration of fluoride ions in the model solution and plot the electrode characteristics for the three additives (Fig. 3).

Result. For the model solution of $1.0 \cdot 10^{-5}$ NaF mol/dm^3 (C_F = 0.19 mg/dm^3), according to the calculations (Fig. 2), the concentration of fluorine in the solution is $1.092 \cdot 10^{-5}$ NaF mol/dm^3 (C_F = 0.21 mg/dm^3), with a relative error of 9.2 %.

Nitrate. To measure nitrate concentrations by chronoionometry, electrochemical parameters of potential measurement (Table 2) and ion-selective electrodes are used: measuring electrode ELIS-121NO3 [5] and comparative silver chloride electrode with double electrolytic key filled with 2 M HCl electrolyte.

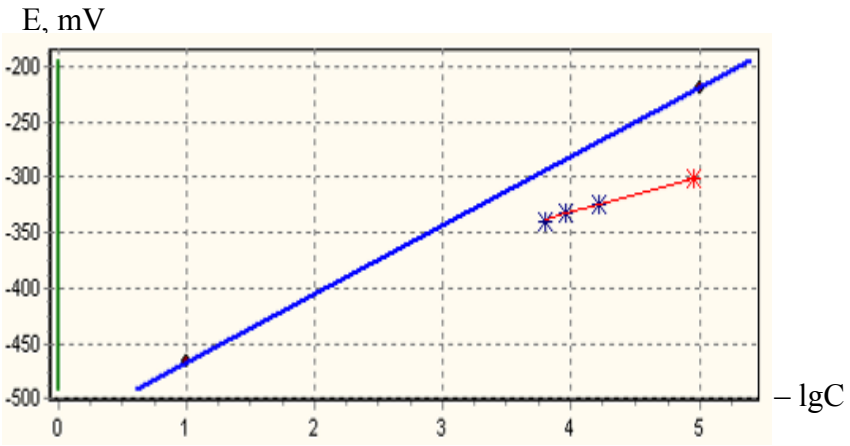

Fig 3. Electrode characteristic of fluoride ion measurement

Table 2. **Electrochemical parameters of nitrate measurement**

Ion	Concentration range, μg/cm^3	Interval potential, mV	Duration measurement, s
NO_3^-	0.62–6200	from 320 to 460	60–180

Step 1. Determine the constant potentials of calibration solutions of nitrates:

- 1 calibration solution: 10^{-5} M KNO_3 (0. 62 μg/cm^3)
- 2 calibration solution: 10^{-1} M KNO_3 (6200 μg/cm^3)

Construct a calibration graph at two points in the range of measurement of nitrates (Fig. 4).

Step 2. In a model solution of 10^{-5} M KNO_3 (C_{NO3} = 0.62 mg/dm^3) measure the potential of nitrates E_{izm} = +444.40 mV.

Step 3. Determine the weight of the additive M_{NO3} = 62.0 μg of a solution of 10^{-3} M KNO_3.

Step 4. Measure the constant values of the potential of nitrates in the sample solution for the three additives (Fig. 5).

Step 5. Calculate the concentration of nitrates in the model solution and plot the electrode characteristics for the three additives (Fig. 6).

Result. For the model solution of $1.0 \cdot 10^{-5}$ KNO_3 mol/dm^3 (C_{NO3} = 0.62 mg/dm^3), according to the calculations (Fig. 5), the concentration of nitrates in the solution is $0.994 \cdot 10^{-5}$ KNO_3 mol/dm^3 (C_{NO3} = 0.62 mg/dm^3), with a relative error of 0.56 %.

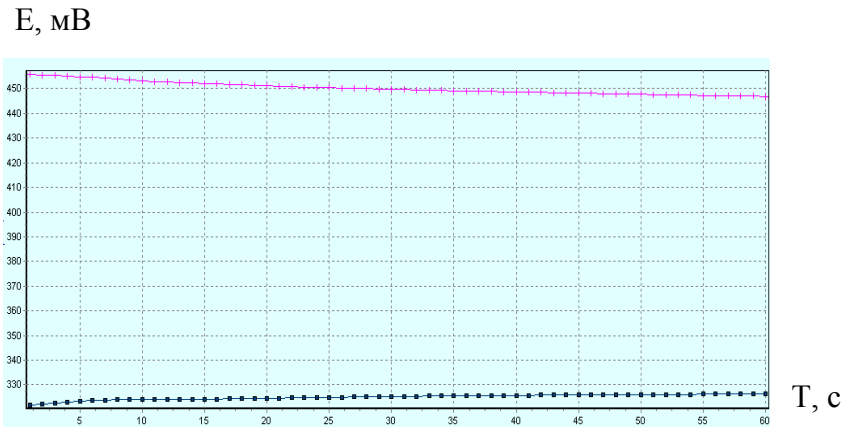

Fig. 4. Chronopotentiograms of potentials of calibration solutions of nitrates

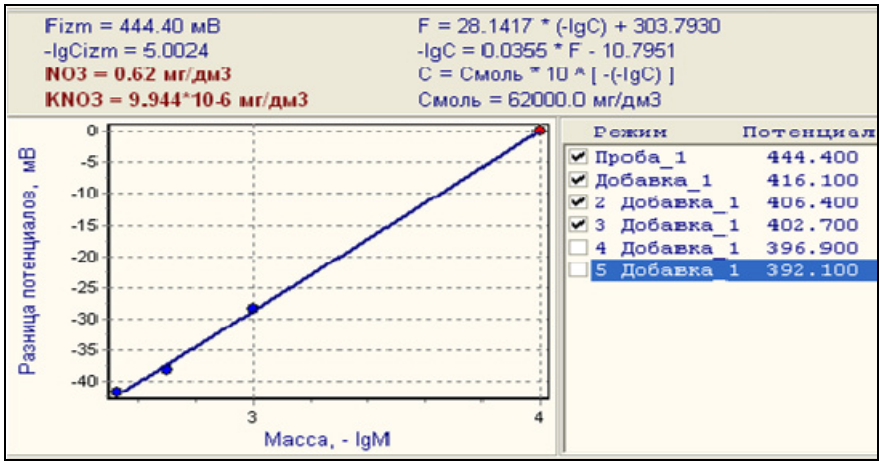

Fig 5. Determination of nitrate ion concentrations

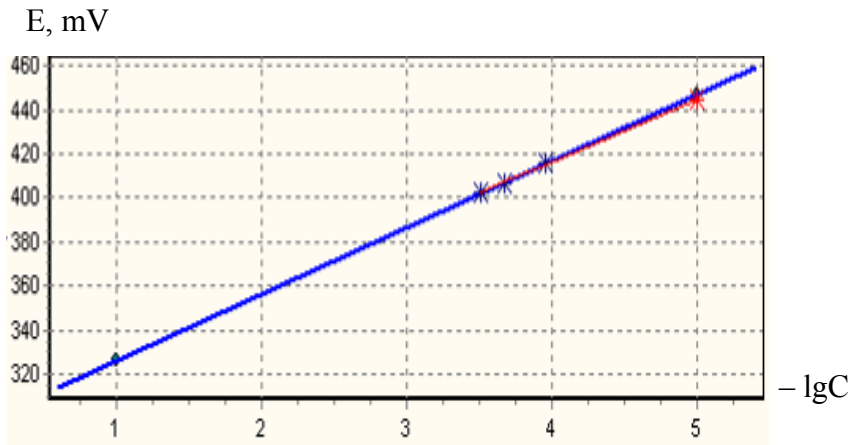

Fig 6. Electrode characteristic of nitrate measurement

Table 3. **Electrochemical parameters of ammonium measurement**

Ion	Concentration range, μg/cm^3	Interval potential, mV	Duration measurement, s
NH_4^+	0.18–1810	from 300 to 550	60–180

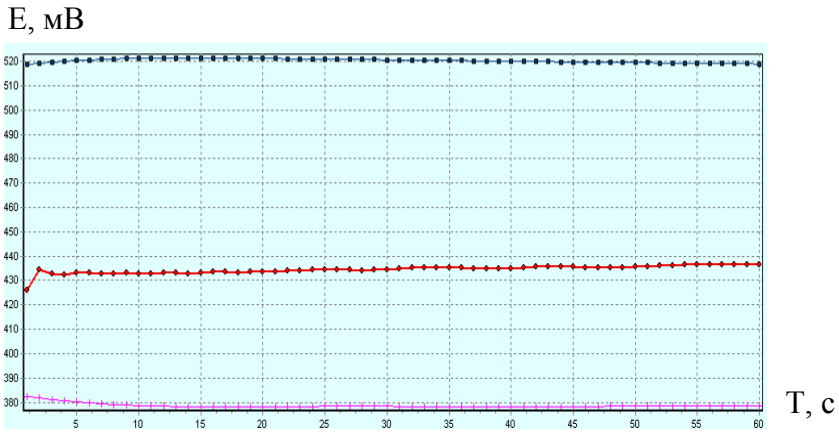

Fig. 7. Chronopotentiograms of potentials of calibration solutions of ammonium

Ammonium. To measure ammonium concentrations by chronoionometry, electrochemical parameters of potential measurement (Table 3) and ion-selective electrodes are used: measuring electrode ELIS-121NH4 [5] and comparative silver chloride electrode with double electrolytic key filled with 2 M HCl electrolyte.

Step 1. Determine the constant potentials of the calibration solutions of ammonium:

- 1 calibration solution: 10^{-5} M NH_4Cl (0.18 μg/cm^3) + 2 ml $BROIS_{NH4}$
- 2 calibration solution: 10^{-1} M NH_4Cl (1810 μg/cm^3) + 2 ml $BROIS_{NH4}$

$BROIS_{NH4}$ — buffer solution to regulate the total ionic strength: take a portion of 110.99 g of $CaCl_2$ (pre-dried), transfer to a volumetric flask with a capacity of 1 dm^3, half filled with distilled water, dissolve and bring to the mark distilled water.

A calibration graph is constructed at two points in the fluoride measurement range (Fig. 7), which shows the determination of the constant potential of the model solution of 10^{-2} M NH_4Cl.

Step 2. In a model solution of 10 ml of 10^{-2} M NH_4Cl + 2 ml of $BROIS_{NH4}$ (C_{NH4} = 181 mg/dm^3) measure the ammonium potential E_{izm} = 408.7 mV.

Step 3. Determine the weight of the additive M_{NH4} = 1810 μg of a solution of 10^{-1} M NH_4Cl.

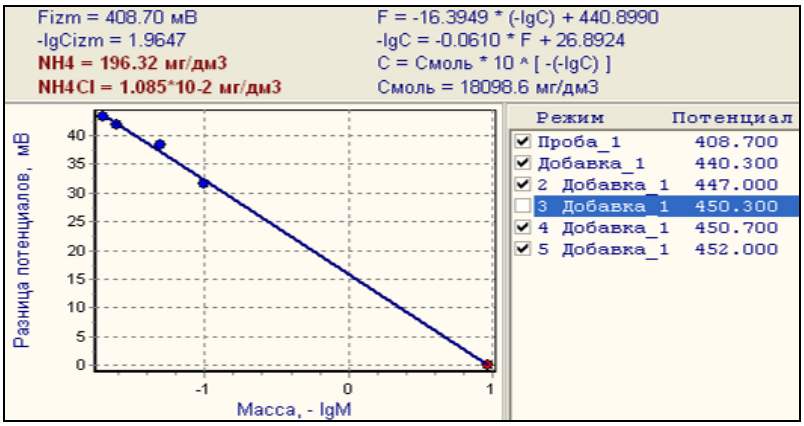

Fig 8. Determination of ammonium ion concentrations

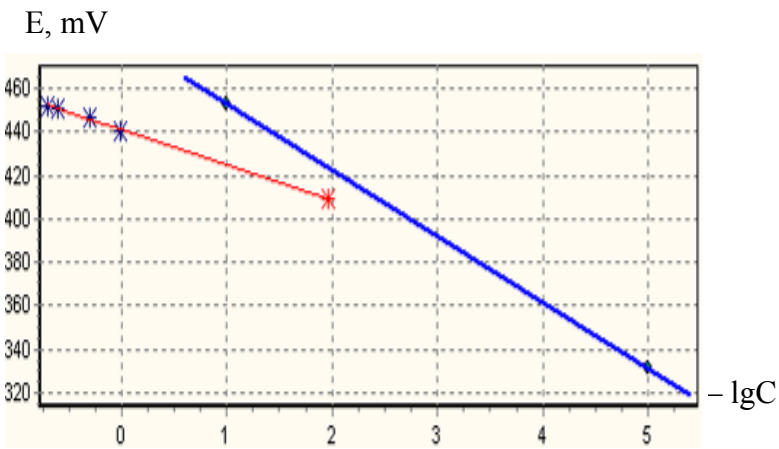

Fig 9. Electrode characteristic of ammonium measurement

Step 4. Perform measurements of constant indicators of the ammonium potential in the sample solution for five additives, additive 3 is not taken into account (Fig. 8).

Step 5. Calculate the concentration of ammonium in the model solution and plot the electrode characteristics for the four additives (Fig. 9).

Result. For the model solution of $1.0 \cdot 10^{-2}$ NH_4Cl mol/dm^3 (C_{NH4} = 181 mg/dm^3), according to the calculations (Fig. 8), the concentration of ammonium in the solution is $1.085 \cdot 10^{-2}$ NH_4Cl mol/dm^3 (C_{NH4} = 196.32 mg/dm^3), with a relative error of 8.5%.

FEATURES OF ALGORITHM IMPLEMENTATION IN INFORMATION TECHNOLOGY

The principles of implementation of the algorithm of the chronoionometry method in the analytical system "Analyzer SCP" are described [2]. Let us dwell on the developed module "Determination of ion concentrations" (Fig. 2, Fig. 5, Fig. 8). The window of this module provides the parameters for calculating the concentrations of the ion of the element, the graph of the potential difference from the logarithm of the mass for the selected potentials of the sample and additives involved in the calculation.

The parameters for calculating the concentrations given in the module window (Fig. 8) have the following values:

F_{izm} — the potential of ammonium (E_{NH4}) in the model solution, mV;

$-lgC_{izm}$ — activity of solution NH_4Cl (pNH_4);

NH_4 — concentration of ions NH_4^+ in the model solution of NH_4Cl, mg/dm^3

NH_4Cl — concentration of model solution, mol/dm^3;

F — record of the linear equation of the calibration graph of the dependence of the potential F on the concentrations (-lgC) of solution NH_4Cl (the coefficient of linear dependence at (-lgC) has the value of the slope of the electrode characteristic, its absolute value should not exceed the passport values for a particular ISE) ;

-lgC — inverse linear equation of the calibration graph of the dependence of the concentrations (-lgC) of the solution NH_4Cl on the potential F;

C — mathematical formula for calculating ion concentration;

Cmol — the value of the molar concentration of ions ammonium, mg/dm^3.

Note: If several potentials are involved in the calculation, the average value of these potentials is taken into account when plotting.

To determine the concentrations of fluoride F^-, nitrate NO_3^-, ammonium NH_4^+ ions in water, methods for measuring chemical elements, confirmed by patents were developed: a device for determining the concentration by CHI [47], a method for determining nitrate ions in aqueous solutions [48], fluoride ions [49] and ammonium ions [50]. These methods have significant scientific value for the development of electrochemical methods of analysis, and can also be used in chemical technology, biotechnology and environmental analysis [51].

The effectiveness of the chronoionometric method for determining the concentrations of fluoride, nitrates and ammonium in drinking water has been proven by comparison with the characteristics of analytical systems developed in other countries.

ANALYSIS OF ACCURACY OF MEASUREMENT OF CONCENTRATIONS BY THE CHRONIONOMETRY METHOD

Assessment of safety and quality of drinking water is carried out according to epidemic safety indicators, sanitary-chemical and radiation indicators, according to hygienic standards [1]. The main principle of practical implementation of chronoionometry methods in determining the quality of drinking water is that the measurement should provide a reliable determination of the concentrations of chemical elements at values that are below the maximum permissible concentrations (MPC). This is due to the fact that the concentrations of chemical elements should not exceed the standardized values of sanitary and toxicological indicators of safety and quality of drinking water, which is an important factor in the prevention of human diseases.

Table 4 shows the normative values of MPC in Ukraine for chemical elements and ranges of measurement of concentrations, according to the methods of measurement in water from different sources: 1 — tap water; 2 — water from wells and catchments of springs; 3 — packaged water from bottling points, ditches; 4 — water of the central drinking water supply; 5 — water of non-central drinking water supply.

The results of the studies to determine the measurement of concentrations of chemical elements fluorine, nitrate and ammonium in water show that the relative errors are in the range from 0.56 % to 9.2 %, which is less than the normalized relative measurement error.

Table 4. **Comparison of measuring ranges of "Analyzer SCP" and sanitary-chemical indicators of safety and quality of drinking water**

Element	Maximum concentration limit for drinking water (mg/dm^3), no more than					Optimal value within[3], mg/dm^3	Measurement ranges "Analyzer SCP" mg/dm^3
	1[1]	2[1]	3[1]	4[2]	5[2]		
Fluoride (F)[4]	0.7	1.5	0.7	0.7	0.7	0.7–1.2	0.2–6000
Nitrate (NO_3)	50	50	10	50	5	-	0.2–6000
Ammonium (NH_4)	-	-	-	0,5	-	-	0,2–6000

Notes:
[1] DSanPiN 2.2.4-171-10 “Hygienic requirements for drinking water intended for human consumption" [1];
[2] DSTU 7525: 2014 Drinking water. Requirements and methods of control (water of centralized and decentralized drinking water supply);
[3] Optimal values of indicators of physiological completeness of mineral composition of drinking water;
[4] Substances of the II class of danger (degree of danger for the person of chemical substances polluting water depending on their toxicity, limiting sign of harm and the ability to cause adverse long-term effects).

Prospects for the development of the method and information technology

The main principle of practical implementation of chronoionometry methods in toxicological research is reliable measurement of fluoride ions, nitrates, ammonium, as well as potassium, sodium and calcium in determining the safety of drinking water and human environment to prevent the most common diseases, the use of the results of analysis of biological fluids in digital medicine, as well as the study of opportunities to improve methods for diagnosing the human condition using the results of analysis of ions of toxic chemical elements and compounds.

The developed method of chronoionometric measurement of ions in drinking water and in various environmental objects can be extended to other inorganic and organic compounds, for which there are ion-selective electrodes and verified methods of their measurement.

The proposed information technology architecture for determining the content of chemical elements in polluted water allows to develop an advanced highly sensitive analytical system based on the use of the device "Analyzer SCP" [52] and new electrochemical research methods that will improve environmental quality monitoring and assess human health risks drinking water.

Further development of information technology will be carried out using modern Internet technologies and a device for express electrochemical analysis of toxic elements, determining the principles of construction of a device for express electrochemical analysis of toxic elements in drinking water and the development of a set of programs for forecasting the risks of disease in terms of consumption of contaminated drinking water.

CONCLUSIONS

In the conditions of intensive anthropogenic impact of heavy metals on the ecosystem it is very important to carry out ecological monitoring of environmental objects, to assess risks for people in case of consumption of polluted drinking water. The possibility of such an analysis provides the use of IT, which is based on the developed algorithm for measuring the mass concentration of chemical elements in drinking and natural water.

The developed analytical system "Analyzer SCP" allows to determine the concentrations of 14 toxic elements in drinking water and in the environment (Hg, As, Pb, Cd, Cu, Zn, Sn, Ni, Co, Se, Mn, I, Cr, Fe) by inversion chronopotentiometry and six elements (K, Na, Ca, NH_4, NO_3, F) by chronoionometry, a total of 20 chemical elements. By chronoionometry, using ion-selective electrodes, you can determine the content of 11 more anions and cations (Ag^+, Cl^-, Br^-, Li^-, Ba^{2+}, ClO^{4-}, CO_3^{2-}, CN^-, CNS^-, S^{2-}, Tl^+), these chemical elements can be added in the future to the analytical system "Analyzer SCP" with the appropriate development of methods for measuring the concentrations and presence of ion-selective electrodes.

REFERENCES

1. DSanPiN 2.2.4-171-10. “Hygienic requirements for drinking water intended for human consumption". Order of the Ministry of Health of Ukraine dated 12.05.2010 No.400. Register. July 1, 2010 for No. 452/17747 (in Ukrainian).
2. Surovtsev I.V., Velykyi P.Y., Galimova V.M., Sarkisova M.V. Ionometric method for determination of concentrations of microelements in research of digital medicine. *Cyb. and comp. eng*., 2020, No.4(220), pp. 25–43. DOI: https://doi.org/10.15407/kvt202.04.025
3. Surovtsev I.V., Galimov S.K. Data processing algorithm of concentration measurement by method chronoionometry. *Control System and Computers*. 2016, No.2, pp. 85–91. DOI: https://doi.org/10.15407/usim.2016.02.085 (in Russian).
4. Surovtsev I.V., Galimov S.K., Tatarinov O.E. Information technology for determining the concentration of toxic elements in environmental objects. *Kibernetika i vyčislitel`naâ tehnika*. 2018, No.1(191), pp. 5–33. DOI: https://doi.org/10.15407/kvt191.01.005 (in Ukrainian).
5. Fenix. Ion-selective electrodes ELIS. 2020, URL: http://www.fenix-trade.kiev.ua/elec_opis1.shtml (in Russian).
6. Zhukova A.G., Mikhailova N.N., Kazitskaya A.S., Alekhina D.A. Contemporary concepts of molecular mechanisms of the physiological and toxic effects of fluorine compounds on an organism. *Medicine in Kuzbass*. 2017, Vol. 16, No 3, pp. 4–11 (in Russian).
7. de Carvalho R.B., Medeiros U.V., dos Santos K.T., Pacheco Filho A.C. Influence of different concentrations of fluoride in the water on epidemiologic indicators of oral health/disease. *Cien. Saude Colet.* 2011 Aug; 16(8): 3509–18. DOI: https://doi.org/10.1590/s1413-81232011000900019. PMID: 21860951
8. Mohd Nor N.A., Chadwick B.L., Farnell D.J.J., Chestnutt I.G. The impact of a reduction in fluoride concentration in the Malaysian water supply on the prevalence of fluorosis and dental caries. *Community Dent Oral Epidemiol*. 2018 Oct;46(5):492-499. DOI: https://doi.org/10.1111/cdoe.12407. Epub 2018 Jul 18.PMID: 30019792
9. Ion I., Ion A.C., Barbu L. Potentiometric determination of fluoride in groundwaters. *Rev. roum. chim*. 2005, Vol. 50, No. 5, pp. 407–412.
10. Trigub V.I. Floride in drinking waters of odessa region and its effect on morbidity of caries and dental fluorosis. *Visnyk of Odessa National University. Series: Geographical and geological sciences.* 2012, Vol. 17, No. 2(15), pp. 71–78. DOI: http://dx.doi.org/10.18524/2303-9914.2012.2(15).186004 (in Ukrainian).

11. Duan Q, Jiao J, Chen X, Wang X. Association between water fluoride and the level of children's intelligence: a dose-response meta-analysis. *Public Health*. 2018 Jan; 154: 87-97. DOI: https://doi.org/10.1016/j.puhe.2017.08.013. Epub 2017 Dec 22. PMID: 29220711
12. O'Mullane D.M., Baez R.J., Jones S., Lennon M.A., Petersen P.E., Rugg-Gunn A.J., Whelton H., Whitford G.M. Fluoride and oral health. *Community Dent Health*. 2016, Jun;33(2), pp. 69–99. PMID: 27352462
13. Kubala E., Strzelecka P., Grzegocka M., Lietz-Kijak D., Gronwald H., Skomro P., Kijak E. A review of selected studies that determine the physical and chemical properties of saliva in the field of dental treatment. *Biomed. Res. Int.* 2018, 2018, 6572381.
14. Buzalaf Mar. Review of fluoride intake and appropriateness of current guidelines. *Adv Dent Res*. 2018 Mar, 29(2), pp. 157-166. DOI: https://doi.org/10.1177/0022034517750850. PMID: 29461104
15. Waugh DT, Potter W, Limeback H, Godfrey M. Risk assessment of fluoride intake from tea in the Republic of Ireland and its implications for public health and water fluoridation. *Int J Environ Res Public Health.* 2016, Feb 26, 13(3), p. 259. DOI: https://doi.org/10.3390/ijerph13030259. PMID: 26927146.
16. Kaminskaya O.V., Zakharova E.A., Slepchenko G.B. Joint voltammetric determination of nitrites and nitrates in waters. *Journal of Analytical Chemistry*. 2004, Vol. 59, No. 11, pp. 1206–1212 (in Russian).
17. Md. Eshrat E. Alahi, Subhas Chandra Mukhopadhyay. Detection methods of nitrate in water: A review. *Sensors and Actuators A Physical*. 2018, Vol. 280, p.210
18. Pan D., Lu W., Zhang H., Zhang L., Zhuang J. Voltammetric determination of nitrate in water samples at copper modified bismuth bulk electrode. *Int. J. Env. Anal. Chem.* Vol. 93, 2013, 935-945, DOI: https://doi.org/10.1080/03067319.2012.690149.
19. DSTU 4725:2007. Soil quality. Potassium, ammonium, nitrate and chloride ion activity determination by potentiometric method. 2007. 34 (in Ukrainian).
20. da Silva Iranaldo S., de Araujo William R., Paixão Thiago R.L.C. Direct nitrate sensing in water using an array of copper-microelectrodes from flat flexible cables. *Sensors and Actuators B Chemical*. 2013, Vol. 188, p. 94.
21. Pan D., Lu W., Zhang H. Voltammetric determination of nitrate in water samples at copper modified bismuth bulk electrode. *International Journal of Environmental & Analytical Chemistry*. 2013, Vol.93, No. 9, p. 935.
22. Yun-Fang Ning, You-Peng Chen, Yu Shen, et al. Directly determining nitrate under wide pH range condition using a Cu-deposited Ti electrode. *Journal of The Electrochemical Society*. 2013, Vol. 160, No.10, H715.
23. Min Zhang, Xuezhi Dong, Xuejun Li, Yongrong Jiang, Yan Li, Ying Liang. Review of separation methods for the determination of ammonium/ammonia in natural water. *Trends in Environmental Analytical Chemistry* (IF 7.059). 2020, DOI: https://doi.org/10.1016/j.teac.2020.e00098
24. Yong Zhu, Jianfang Chen, Dongxing Yuan, Zhi Yang, Xiaolai Shi, Hongliang Li, Haiyan Jin, Lihua Ran. Development of analytical methods for ammonium determination in seawater over the last two decades. *TrAC Trends in Analytical Chemistry*. Vol. 119, October 2019, 115627. DOI: https://doi.org/10.1016/j.trac.2019.115627
25. The effect of ammonium (ammonia) in water on the body. URL: https://ziko.com.ua/ru/all-article-ammoniy-ammiak/ (Last accessed: 27.04.2018) (in Russian).
26. Ammonium — fast and robust determination according to current ISO, EPA, and ASTM standards using direct measurement. URL: https://www.metrohm.com/en-vn/company/news/news-ammonia-ab-133/
27. Yeager J.L., Miller M.D., Ramanujachary K.V. Determination of total fluoride content in electroslag refining fluxes using a fluoride ion-selective electrode. *Ind. and Eng. Chem. Res*. 2006, Vol. 45, No 13, pp. 4525–4529.
28. Electrode for measurement of concentration of nitrate-ions: patent 93137, Ukraine: IPC G01N 27/30 (2006.01). a200907268; claimed 10.07.2009; published 10.01.2011 (in Ukrainian).
29. Wu Y., Fei J., Dang X., Hu S. Determination of ammonium ion in lake water by voltammetry. *Wuhan Univ. J. Natur. Sci*. 2004, Vol.9, No3, pp. 366–370.

30. `Shariar S.M., Hinoue T. Simultaneous voltammetric determination of nitrate and nitrite ions using a copper electrode pretreated by dissolution/redeposition *Analytical sciences november*. 2010, Vol. 26, 1173–1179.
31. Santos Carla S., Lima Alex S., Battistel D. Fabrication and use of dual-function iridium oxide coated gold SECM tips. An Application to pH Monitoring above a Copper Electrode Surface during Nitrate Reduction. *Electroanalysis*. 2016, Vol. 28, No. 7, pp. 1441.
32. Thangamuthu Madasamy, Manickam Pandiaraj, Murugesan Balamurugan, et al. Copper, zinc superoxide dismutase and nitrate reductase coimmobilized bienzymatic biosensor for the simultaneous determination of nitrite and nitrate. *Biosensors and Bioelectronics*. 2014, Vol. 52, p. 209.
33. Hasan Bagheri, Ali Hajian, Mosayeb Rezaei, et al. Composite of Cu metal nanoparticles-multiwall carbon nanotubes-reduced graphene oxide as a novel and high performance platform of the electrochemical sensor for simultaneous determination of nitrite and nitrate. *Journal of Hazardous Materials*. 2017, Vol.324, p. 762.
34. Ying Li, Haitao Han, Dawei Pan, et al. Fabrication of a micro-needle sensor based on copper microspheres and polyaniline film for nitrate determination in coastal river waters. *Journal of The Electrochemical Society*. 2019, Vol.166, No.12, B1038.
35. Hala Araar, Messaoud Benounis, Amani Direm, et al. A new thin film modified glassy carbon electrode based on melaminium chloride pentachlorocuprate(II) for selective determination of nitrate in water. *Monatshefte Chemical Monthly*. 2019, Vol. 150, No. 10, 1737.
36. Manju Bhargavi Gumpu, Noel Nesakumar, Bhat Lakshmishri Ramachandra, et al. Zinc oxide nanoparticles-based electrochemical sensor for the detection of nitrate ions in water with a low detection limit — a chemometric approach. *Journal of Analytical Chemistry*. 2017, Vol.72, No.3, p. 316.
37. Pan D., Lu W., Wu Sh. In situ spontaneous redox synthesis of carbon nanotubes/copper oxide nanocomposites and their preliminary application in electrocatalytic reduction of nitrate. *Materials Letters*. 2012, Vol. 89, p. 333.
38. Remes A., Sonea D., Burtica G., Picken S., Schoonman J. Electrochemical determination of nitrate from water sample using Ag-doped zeolite-modified expanded graphite composite electrode. *Ovidius University Annals of Chemistry.* Vol. 20, No. 1, 2009, pp. 61–65.
39. Catherine M. Fox, Carmel B. Breslin. Electrochemical formation of silver nanoparticles and their applications in the reduction and detection of nitrates at neutral pH. *Journal of Applied Electrochemistry*. 2020, Vol. 50, No.1, p. 125.
40. Junhua Jiang, Lei Zhang, Vinay Shanbhag. Improving electrochemical sensitivity of silver electrodes for nitrate detection in neutral and base media through surface nanostructuration. *Journal of The Electrochemical Society*. 2014, Vol. 161, No.2, B3028.
41. Salatino A. Ammonium ion sensor based on SiO2/ZrO2/phosphate-NH4+ composite for quantification of ammonium ions in natural waters. *J. Braz. Chem. Soc.* 2007, 18(1), 34–40. DOI: https://doi.org/10.1590/S0103 - 50532007000100022
42. Dong Kim Loan, Tran Hong Con, Tran Thi Hong and Luong Thi Mai Ly. Quick determination of ammonia ions in water environment based on thymol color creating reaction. 2013, *Environmental Sciences,* Vol. 1, 2013, no. 2, pp. 83–92, DOI: https://doi.org/10.12988/es.2013.31010
43. Huang Y., Wang T., Xu Z., Hughes E., Qian F., Lee M., Fan Y., Lei, Y., Brückner C., Li B. Real-time in situ monitoring of nitrogen dynamics in wastewater treatment processes using wireless, solid-state, and ion-selective membrane sensors. *Environ. Sci. Technol.* 2019, 53, pp. 3140–3148.
44. Jalalvand Ali R., Mahmoudi M., Goicoechea Hector C. Developing a novel paper-based enzymatic biosensor assisted by digital image processing and first-order multivariate calibration for rapid determination of nitrate in food samples. *RSC Advances*. 2018, Vol. 8, No. 41, 23411.
45. Surovtsev I.V., Tatarinov O.E., Galimov S.K. Device of inversion chronopotentiometry for determining the concentration of heavy metals and toxic elements in water. *Bezpeka zhyttyediyal'nosti.* 2013, No. 12, pp. 37–40 (in Ukrainian).

46. Device for measuring the concentration of toxic elements: patent 107412, Ukraine: IPC (2006) G01N 27/48. a201306295; claimed 21.05.13; published 25.12.14 (in Ukrainian).
47. Device for measuring parameters of aqueous solutions: patent 111689, Ukraine: IPC (2006) G01N 27/48. a201505019; claimed 22.05.15; published 25.05.16 (in Ukrainian).
48. Method for determination of nitrate ions in aqueous solutions: patent 116717, Ukraine: IPC (2006.01) G01N 27/48, G01N 27/49, G01N 27/333, G01N 33/18, G01N 33/20. a201611106; claimed 04.11.2016; published 25.04.2018 (in Ukrainian).
49. Method of determination of fluoride ions in aqueous solutions: patent 116718, Ukraine: IPC (2006.01) G01N 27/48, G01N 27/49, G01N 27/333, G01N 33/18, G01N 33/20. a201611109; claimed 04.11.2016; published 25.04.2018 (in Ukrainian).
50. Method of determining ammonium ions in aqueous solutions: patent 116719, Ukraine: IPC (2006) G01N 27/48, G01N 27/49, G01N 33/18, G01N 33/20. a201611112; claimed 04.11.2016; published 25.04.2018 (in Ukrainian).
51. Kopilevich V.A., Surovtsev I.V., Galimova V.M. Method of measuring the mass concentration of fluorine, ammonium and nitrates in water by chronopotentiometric ionometry. MB 081/12-1023-2016. *Kyiv: Nats. un-t biotekhn. i pryrodokorystuvannya*, 2016, 30 (in Ukrainian).
52. Surovtsev I.V., Babak O.V., Tatarinov O.E., Surovtseva T.V. Hardware and software complex "Analyzer ICP" for measuring the mass concentration of toxic elements. *Nauka ta innovatsiyi*. 2011, Vol. 7, No. 3, pp. 45–46 (in Ukrainian).

Received 03.12.2020

ЛІТЕРАТУРА

1. ДСанПИН 2.2.4-171-10. Державні санітарні норми і правила «Гігієнічні вимоги до води питної, призначеної для споживання людиною.» — Наказ МОЗ України від 12.05.2010 № 400. — Реєстр. 1 липня 2010 р. за № 452/17747.
2. Surovtsev I.V., Velykyi P.Y., Galimova V.M., Sarkisova M.V. Ionometric method for determination of concentrations of microelements in research of digital medicine. *Cyb. and comp. eng.*, 2020. №. 4 (220), 25-43. DOI: https://doi.org/10.15407/kvt202.04.025.
3. Суровцев И.В., Галимов С.К. Алгоритм обработки данных измерения концентрации методом хроноионометрии. *Управляющие системы и машины*. 2016. № 2. 85–91. DOI: https://doi.org/10.15407/usim.2016.02.085
4. Суровцев І.В., Галімов С.К., Татарінов О.Е. Інформаційна технологія визначення концентрації токсичних елементів в об'єктах навколишнього середовища. *Кибернетика и вычисл. техника*. 2018. № 191. 5–31. DOI: https://doi.org/10.15407/kvt191.01.005
5. Fenix. Ионоселективные электроды ЭЛИС. 2020. URL: http://www.fenix-trade.kiev.ua/elec_opis1.shtml
6. Жукова А.Г., Михайлова Н.Н., Казицкая А.С., Алехина Д.А. Современные представления о молекулярных механизмах физиологического и токсического действия соединений фтора на организм. *Medicine in Kuzbass*. 2017. Т. 16. № 3. 4–11.
7. de Carvalho R.B., Medeiros U.V., dos Santos K.T., Pacheco Filho A.C. Influence of different concentrations of fluoride in the water on epidemiologic indicators of oral health/disease. *Cien. Saude Colet.* 2011 Aug; 16(8): 3509-18. DOI: https://doi.org/10.1590/s1413-81232011000900019. PMID: 21860951
8. Mohd Nor N.A., Chadwick B.L., Farnell D.J.J., Chestnutt I.G. The impact of a reduction in fluoride concentration in the Malaysian water supply on the prevalence of fluorosis and dental caries. *Community Dent Oral Epidemiol*. 2018 Oct; 46(5):492-499. DOI: https://doi.org/10.1111/cdoe.12407. Epub 2018 Jul 18.PMID: 30019792
9. Ion I., Ion A.C., Barbu L. Potentiometric determination of fluoride in groundwaters. *Rev. roum. chim*. 2005. Vol. 50. No. 5. 407–412.
10. Тригуб В.І. Вміст фтору в питних водах Одещини та його вплив на захворюваність населення карієсом і флюорозом зубів. *Вісник Одеського національного університету. Серія: Географічні та геологічні науки*. 2012. Vol. 17. No. 2(15). 71–78. DOI: http://dx.doi.org/10.18524/2303-9914.2012.2(15).186004.

11. Duan Q, Jiao J, Chen X, Wang X. Association between water fluoride and the level of children's intelligence: a dose-response meta-analysis. *Public Health*. 2018 Jan; 154: 87–97. DOI: https://doi.org/10.1016/j.puhe.2017.08.013. Epub 2017 Dec 22. PMID: 29220711
12. O'Mullane D.M., Baez R.J., Jones S., Lennon M.A., Petersen P.E., Rugg-Gunn A.J., Whelton H., Whitford G.M. Fluoride and oral health. *Community Dent Health*. 2016 Jun;33(2): 69–99. PMID: 27352462
13. Kubala E., Strzelecka P., Grzegocka M., Lietz-Kijak D., Gronwald H., Skomro P., Kijak E. A review of selected studies that determine the physical and chemical properties of saliva in the field of dental treatment. *Biomed. Res. Int.* 2018, 2018, 6572381.
14. Buzalaf Mar. Review of fluoride intake and appropriateness of current guidelines. *Adv Dent Res*. 2018 Mar; 29(2): 157–166. DOI: https://doi.org/10.1177/0022034517750850. PMID: 29461104
15. Waugh D.T., Potter W., Limeback H., Godfrey M. Risk assessment of fluoride intake from tea in the Republic of Ireland and its implications for public health and water fluoridation. *Int J Environ Res Public Health.* 2016 Feb 26; 13(3): 259. DOI: https://doi.org/10.3390/ijerph13030259. PMID: 26927146.
16. Каминская О.В., Захарова Э.А., Слепченко Г.Б. Совместное вольтамперометрическое определение нитритов и нитратов в водах. *Журнал аналитической химии*. 2004. Т. 59. № 11. 1206–1212.
17. Md. Eshrat E. Alahi, Subhas Chandra Mukhopadhyay. Detection methods of nitrate in water: A review. *Sensors and Actuators A Physical*. 2018, Vol.280, 210.
18. Dawei Pan, Wenjing Lu, Haiyun Zhang, Li Zhang, Jianmei Zhuang. Voltammetric determination of nitrate in water samples at copper modified bismuth bulk electrode. *Int. J. Env. Anal. Chem.* Vol. 93, 2013, 935–945, DOI: https://doi.org/10.1080/03067319.2012.690149.
19. ДСТУ 4725:2007. Якість ґрунту. Визначення активності іонів калію, амонію, нітрату і хлору потенціометричним методом. *Київ: Держспоживстандарт України*. 2007. 34 с.
20. Iranaldo S. da Silva, William R. de Araujo, Thiago R.L.C. Paixão, et al. Direct nitrate sensing in water using an array of copper-microelectrodes from flat flexible cables. *Sensors and Actuators B Chemical*. 2013. Vol. 188. P. 94.
21. Dawei Pan, Wenjing Lu, Haiyun Zhang, et al. Voltammetric determination of nitrate in water samples at copper modified bismuth bulk electrode. *International Journal of Environmental & Analytical Chemistry*. 2013. Vol.93. No.9, 935.
22. Yun-Fang Ning, You-Peng Chen, Yu Shen, et al. Directly determining nitrate under wide pH range condition using a Cu-deposited Ti electrode. *Journal of The Electrochemical Society*. 2013. Vol.160. No.10, H715.
23. Min Zhang; Xuezhi Dong; Xuejun Li; Yongrong Jiang; Yan Li; Ying Liang. Review of separation methods for the determination of ammonium/ammonia in natural water. *Trends in Environmental Analytical Chemistry* (IF 7.059). 2020, DOI: https://doi.org/10.1016/j.teac.2020.e00098
24. Yong Zhu, Jianfang Chen, Dongxing Yuan, Zhi Yang, Xiaolai Shi, Hongliang Li, Haiyan Jin, Lihua Ran. Development of analytical methods for ammonium determination in seawater over the last two decades. *TrAC Trends in Analytical Chemistry*. Volume 119, October 2019, 115627. DOI: https://doi.org/10.1016/j.trac.2019.115627
25. Влияние аммония (аммиака) в воде на организм. URL: https://ziko.com.ua/ru/all-article-ammoniy-ammiak/ (27.04.2018)
26. Ammonium — fast and robust determination according to current ISO, EPA, and ASTM standards using direct measurement. URL: https://www.metrohm.com/en-vn/company/news/news-ammonia-ab-133/
27. Yeager J.L., Miller M.D., Ramanujachary K.V. Determination of total fluoride content in electroslag refining fluxes using a fluoride ion-selective electrode. *Ind. and Eng. Chem. Res*. 2006. Vol. 45. No 13. 4525–4529.
28. Електрод для вимірювання концентрації нітрат-іонів : пат. 93137, України : МПК G01N 27/30 (2006.01). a200907268; заявл. 10.07.2009; опубл. 10.01.2011, Бюл. № 1.

29. Wu Y., Fei J., Dang X., Hu S. Determination of ammonium ion in lake water by voltammetry. *Wuhan Univ. J. Natur. Sci.* 2004. Vol.9. No3. 366–370.
30. Shariar S.M., Hinoue T. Simultaneous voltammetric determination of nitrate and nitrite ions using a copper electrode pretreated by dissolution/redeposition *Analytical sciences november.* 2010. Vol. 26. P. 1173–1179.
31. Carla S. Santos, Alex S. Lima, Dario Battistel, et al. Fabrication and use of dual-function iridium oxide coated gold SECM tips. An Application to pH Monitoring above a Copper Electrode Surface during Nitrate Reduction. *Electroanalysis*. 2016. Vol. 28. No. 7. P.1441.
32. Thangamuthu Madasamy, Manickam Pandiaraj, Murugesan Balamurugan, et al. Copper, zinc superoxide dismutase and nitrate reductase coimmobilized bienzymatic biosensor for the simultaneous determination of nitrite and nitrate. *Biosensors and Bioelectronics*. 2014. Vol. 52. P. 209.
33. Hasan Bagheri, Ali Hajian, Mosayeb Rezaei, et al. Composite of Cu metal nanoparticles-multiwall carbon nanotubes-reduced graphene oxide as a novel and high performance platform of the electrochemical sensor for simultaneous determination of nitrite and nitrate. *Journal of Hazardous Materials*. 2017. Vol.324. P.762.
34. Ying Li, Haitao Han, Dawei Pan, et al. Fabrication of a micro-needle sensor based on copper microspheres and polyaniline film for nitrate determination in coastal river waters. *Journal of The Electrochemical Society*. 2019. Vol.166. No. 12. B1038.
35. Hala Araar, Messaoud Benounis, Amani Direm, et al. A new thin film modified glassy carbon electrode based on melaminium chloride pentachlorocuprate(II) for selective determination of nitrate in water. *Monatshefte Chemical Monthly*. 2019. Vol.150. No.10. 1737.
36. Manju Bhargavi Gumpu, Noel Nesakumar, Bhat Lakshmishri Ramachandra, et al. Zinc oxide nanoparticles-based electrochemical sensor for the detection of nitrate ions in water with a low detection limit — a chemometric approach. *Journal of Analytical Chemistry*. 2017. Vol.72. No.3. P. 316.
37. Dawei Pan, Wenjing Lu, Shijie Wu, et al. In situ spontaneous redox synthesis of carbon nanotubes/copper oxide nanocomposites and their preliminary application in electrocatalytic reduction of nitrate. *Materials Letters*. 2012. Vol. 89. P. 333.
38. Remes A., Sonea D., Burtica G., Picken S., Schoonman J. Electrochemical determination of nitrate from water sample using Ag-doped zeolite-modified expanded graphite composite electrode. *Ovidius University Annals of Chemistry.* Vol. 20. Num 1. 2009. P. 61–65.
39. Catherine M. Fox, Carmel B. Breslin. Electrochemical formation of silver nanoparticles and their applications in the reduction and detection of nitrates at neutral pH. *Journal of Applied Electrochemistry*. 2020. Vol.50. No.1. P. 125.
40. J unhua Jiang, Lei Zhang, Vinay Shanbhag. Improving electrochemical sensitivity of silver electrodes for nitrate detection in neutral and base media through surface nanostructuration. *Journal of The Electrochemical Society*. 2014. Vol.161. No. 2. B3028.
41. A Salatino. Ammonium ion sensor based on SiO2/ZrO2/phosphate-NH4+ composite for quantification of ammonium ions in natural waters. *J. Braz. Chem. Soc.* 2007. 18(1). P. 34-40. DOI: https://doi.org/10.1590/S0103 – 50532007000100022
42. Dong Kim Loan, Tran Hong Con, Tran Thi Hong and Luong Thi Mai Ly. Quick determination of ammonia ions in water environment based on thymol color creating reaction. 2013, *Environmental Sciences*. Vol. 1. 2013. no. 2. P. 83–92, DOI: https://doi.org/10.12988/es.2013.31010
43. Huang, Y.; Wang, T.; Xu, Z.; Hughes, E.; Qian, F.; Lee, M.; Fan, Y.; Lei, Y.; Brückner, C.; Li, B. Real-time in situ monitoring of nitrogen dynamics in wastewater treatment processes using wireless, solid-state, and ion-selective membrane sensors. Environ. Sci. Technol. 2019. 53. 3140–3148.
44. Ali R. Jalalvand, Majid Mahmoudi, Hector C. Goicoechea. Developing a novel paper-based enzymatic biosensor assisted by digital image processing and first-order multivariate calibration for rapid determination of nitrate in food samples. *RSC Advances*. 2018. Vol.8. No.41. 23411.
45. Суровцев І.В., Бабак О.В., Волков Ю.М., Галімов С.К., Татарінов О.Е. Прилад інверсійної хронопотенціометрії для визначення концентрації важких металів та токсичних елементів у воді. *Безпека життєдіяльності*. 2013. № 12. С. 37–40.

46. Пристрій для вимірювання концентрації токсичних елементів : пат. 107412 Україна : МПК G01N 27/48. a201306295; заявл. 21.05.2013 ; опубл. 25.12.2014, Бюл. № 24.
47. Пристрій для вимірювання параметрів водних розчинів: пат. 111689, Україна: МПК G01N 27/48. a201505019; заявл. 22.05.2015; опубл. 25.05.2016, Бюл. № 10.
48. Спосіб визначення нітрат-іонів у водних розчинах : пат. 116717, Україна : МПК (2006.01) G01N 27/48, G01N 27/49, G01N 27/333, G01N 33/18, G01N 33/20. a201611106; заявл. 04.11.2016 ; опубл. 25.04.2018, Бюл. № 8.
49. Спосіб визначення фторид-іонів у водних розчинах : пат. 116718, Україна : МПК (2006.01) G01N 27/48, G01N 27/49, G01N 27/333, G01N 33/18, G01N 33/20. a201611109; заявл. 04.11.2016 ; опубл. 25.04.2018, Бюл. № 8.
50. Спосіб визначення іонів амонію у водних розчинах : пат. 116719, Україна : МПК (2006) G01N 27/48, G01N 27/49, G01N 33/18, G01N 33/20. a201611112; заявл. 04.11.2016; опубл. 25.04.2018, Бюл. № 8.
51. Методика вимірювання масової концентрації фтору, амонію та нітратів у воді методом хронопотенціометричної іонометрії. МВ 081/12-1023-2016 від : введ. 23.12.2016; розробники: В.А. Копілевич, І.В. Суровцев, В.М. Галімова. *К.: НУБіП*, 2016, 30.
52. Суровцев І.В., Бабак О.В., Татарінов О.Е., Суровцева Т.В. Апаратно-програмний комплекс «Аналізатор ІХП» для вимірювання масової концентрації токсичних елементів. *Наука та іннов*. 2011. Т.7. № 3. С.45–46.

Отримано 03.12.2020

Суровцев І.В.[1], д-р техн. наук, старш. наук. співроб.,
зав. відд. екологічних цифрових систем
ORCID: 0000-0003-1133-6207
e-mail: dep115@irtc.org.ua, igorsur52@gmail.com
Галімов С.К.[1], провідний інженер,
відд. екологічних цифрових систем
ORCID: 0000-0001-5716-9454
e-mail: dep115@irtc.org.ua
Галімова В.М.[2], канд. хім. наук,
доцент кафедри аналітичної
і біонеорганічної хімії та якості води
ORCID: 0000-0001-9602-1006
e-mail: galimova2201@gmail.com
Саркісова М.В.[2], студентка,
ветеринарний факультет
ORCID: 0000-0002-5462-6442
e-mail: mari.doga2014@gmail.com
[1] Міжнародний науково-навчальний центр
інформаційних технологій та систем
НАН України та МОН України,
пр. Акад. Глушкова, 40, Київ, 03187, Україна
[2] Національний університет біоресурсів і природокористування
вул. Героїв Оборони, 17, корп. 2, Київ, 03041, Україна

МЕТОД ХРОНОІОНОМЕТРИЧНОГО ВИЗНАЧЕННЯ КОНЦЕНТРАЦІЙ ФТОРУ, НІТРАТІВ, АМОНІЮ У ПИТНІЙ ВОДІ

Вступ. Використання методу хроноіонометрії та іон-селективних електродів дає можливість швидко визначити концентрації хімічних елементів, що дає змогу оцінити якість питної води та екологічний стан об'єктів довкілля.

Мета статті — застосувати розроблений метод хроноіонометрії для вимірювання концентрацій фтору, нітратів, амонію у питній воді та оцінити точність вимірювання концентрацій.

Методи. Хроноіонометричний метод хімічного аналізу використовує принципи прямої потенціометрії для вимірювання концентрацій хімічних елементів.

Результати. Розроблено способи виявлення концентрацій фтору, нітратів, амонію у питній воді та проведено тестування в модельних водних розчинах з використанням приладу інверсійної хронопотенціометрії «Аналізатор ІХП», які свідчать про відповідність похибок вимірювання концентрацій метрологічним нормативним значенням.

Висновки. Удосконалено аналітичну систему «Аналізатор ІХП» для визначення концентрації 20 хімічних елементів (Hg, As, Pb, Cd, Cu, Zn, Sn, Ni, Co, Se, Mn, I, Cr, Fe, K, Na, Ca, F, NO_3, NH_4) у водних розчинах методами інверсійної хронопотенціометрії та методом хроноіонометрії, що цілком достатньо для екологічного оцінювання якості питної води та об'єктів навколишнього середовища. Застосування нового методу хроноіонометрії значно розширює функціональні можливості приладу інверсійної хронопотенціометрії, підвищує надійність та точність вимірювання концентрацій хімічних елементів.

Ключові слова: *метод хроноіонометрії, концентрація, фтор, нітрати, амоній, селективні електроди, інверсійна хронопотенціометрія, питна вода.*

DOI: https://doi.org/10.15407/kvt203.01.026

УДК 004.89

АНІСІМОВ А.В., д-р. фіз.-мат. наук,
член.-кор. НАН України, декан факультету
комп'ютерних наук та кібернетики
ORCID: 0000-0002-1467-2006
e-mail: anatoly.v.anisimov@gmail.com
БЕВЗА М.В., аспірант
ORCID: 0000-0002-2697-4968
e-mail: maksymbevza@gmail.co
БОБИЛЬ Б.В., аспірант,
ORCID: 0000-0002-9612-1071
e-mail: bobylbohdan@gmail.com
Київський національний університет імені Тараса Шевченка,
вул. Володимирська, 60, м. Київ, 01033, Україна

ПРОГНОЗУВАННЯ ВІДГУКІВ НА ВІЗУАЛЬНО-ТЕКСТОВИЙ КОНТЕНТ З ВИКОРИСТАННЯМ НЕЙРОННИХ МЕРЕЖ

Вступ. *Соціальні мережі надають можливість одержувати високо персоналізований досвід для їхніх користувачів, даючи їм змогу підписуватись на сторінки інших користувачів, які публікують релевантний і цікавий контент. Відгук на візуальний і текстовий контент повідомлення одержується від підписників у вигляді поширень, лайків та коментарів. Прогнозування реакції аудиторії на те чи інше повідомлення цих мереж стає чимдалі важливим завданням, оскільки публікація повідомлень носить незворотний характер і перед публікацією необхідно прогнозувати реакцію підписників.*

Метою роботи *є побудова системи, яка може прогнозувати реакцію аудиторії на чергову публікацію, враховуючи особливість кожної сторінки, унікальність її аудиторії та варіативність можливих реакцій.*

Результати. *Проаналізовано структуру контенту і реакцій у соціальних мережах та визначено особливості публікацій, які слід враховувати під час аналізу популярності та відгуку аудиторії на публікацію. Описано процес тренування нейронної мережі, що дає можливість натренувати нейронну мережу для кожної сторінки з урахуванням особливостей аудиторії. Характеристики текстової частини контенту попередньо сформовано за допомогою нейронної мережі BERT, а характеристики візуальної частини контенту — нейронної мережі VGG-16. Створено модель класифікації для трьох груп показників: лайків, поширень та емоційної направленості коментарів. Розроблено алгоритм передбачення реакції аудиторії на повідомлення, який об'єднує роботу компонентів нейронної мережі для екстракції візуально-семантичних ознак зображення, текстово-семантичних ознак текстових даних та*

мета-інформації досліджуваного повідомлення. Розроблено систему, яка опрацьовує у поєднанні візуальну і текстову частину контенту і таким чином дає можливість отримати повний контекст публікації. Аналіз роботи розробленої системи показав, що найкраще прогнозовано сентимент коментарів аудиторії, якість прогнозування лайків і репостів була дещо нижчою.

Висновки. *Використання розробленої нейронної мережі, яка складається з трьох повнозв'язних шарів і на вхід отримує характеристики текстової та візуальної частин контенту та мета-дані про досліджувану сторінку, дає змогу комплексно оцінити реакцію користувачів на чергову публікацію конкретної сторінки в соціальній мережі.*

Ключові слова: *штучний інтелект, оброблення природної мови, комп'ютерний зір, соціальні мережі, прогнозування реакції аудиторії, текстовий та візуальний контент.*

ВСТУП

Соціальні мережі надають можливість одержувати високоперсоналізований досвід для їхніх користувачів, даючи їм змогу підписуватись на сторінки інших користувачів, які публікують релевантний і цікавий контент.

Комерціалізація цих мереж теж відбулась за лічені роки після їхнього створення. Реклама в цих мережах є дуже популярною. Рекламою також займаються користувачі, що ведуть власні сторінки і мають велику кількість підписників, які регулярно отримують нові повідомлення. Прогнозування реакції аудиторії на те чи інше повідомлення у цих мережах стає чимдалі важливим завданням, оскільки публікація повідомлень носить незворотний характер і перед публікацією необхідно прогнозувати реакцію підписників.

Попередні дослідження з прогнозування реакції аудиторії орієнтовано на великі веб-ресурси і не беруть до уваги контекст, за яким здійснюється прогнозування реакції.

ПОСТАНОВКА ПРОБЛЕМИ

Реакція аудиторії зазвичай розглядається в контексті різних жанрів і способу побудови історії та тексту для отримання різних реакцій [1]. Відзначено необхідність визначення, як саме спосіб викладення контенту впливає на те, чи прочитає аудиторія контент до кінця і, відповідно, чи будуть реакції на нього. Таку залежність між способом викладення інформації і майбутньою активністю читачів проаналізовано у [1] та зазначено значне підвищення цієї активності, якщо учасники мають справу з контентом у жанрі розповідання історій.

У дослідженнях емоційного окрасу реакцій користувачів соціальних мереж на події широкого масштабу (державного і глобального) є корисним використовувати не тільки бінарну позитивно-негативну, а й детальну класифікацію цих реакцій. Проведений аналіз афективних виразів у Twitter, зібраних авторами у Німеччині на основі схеми кодування [2], надав змогу зрозуміти спосіб сприйняття користувачами соціальних мереж загальної ситуації під час інциденту забруднення харчових продуктів ЕНЕС 2011 р. Аналіз їхньої детальнішої реакції допомагає визначати загальні настрої в суспільстві та оцінювати цілі, які постають перед людьми у соціумі, і мотиви, якими вони керуються.

Треба зазначити дослідження немаркованих даних для створення класифікатора настроїв Twitter за допомогою мереж Convolutional Neural Networks (CNN) та Long Short Term Memory (LSTM) [3]. Авторами використано метод оцінювання сентименту для повідомлень у соціальній мережі

Twitter за допомогою моделі згорткових та рекурентних нейронних моделей. Використано дві категорії сентименту — позитивний і негативний. Ця робота описує state-of-the-art з сентимент аналізу повідомлень.

Дуже цікаве завдання ще не знайшло свого розв'язання, а саме прогнозування реакції користувачів у вигляді «лайк» та «поширення» для конкретного повідомлення на сторінці користувача з певною тематикою.

Сучасні методи оброблення текстових даних базуються на застосуванні рекурентних нейронних мереж (RNN), а також системи Transformer [4].

Рекурентна нейронна мережа (RNN) може отримувати на вхід наперед невизначену кількість вхідних даних у послідовності і опрацьовувати їх послідовно. Щоправда, є практичні обмеження щодо кількості вхідних даних в одній послідовності, що зумовлено обмеженим розміром прихованого шару мережі. Рекурентні нейронні мережі мають велику популярність у сучасних методах оброблення текстів за рахунок їхньої можливості «пам'ятати» контекст речення у разі подання їм на вхід послідовності слів. Найпоширеніші реалізації рекурентних нейронних мереж є системи Long Short-Term Memory (LSTM) [3].

Ще один з підходів навчання нейронних мереж використано в мережі Transformer [4]. Ця нейронна мережа складається з багатьох повнозв'язних шарів, а також має вбудовану систему Attention, яка дає можливість нейронній мережі фокусуватися на найважливіших частинах речення на кожному рівні нейронної мережі.

Отже, наведені дослідження сконцентровано на аналізі окремих характеристик візуально-текстової інформації, таких як емоційне навантаження тексту, категоризація за темами та/або жанрами, класифікація зображень тощо.

Мета роботи — розробити систему, яка дасть можливість для будь-якої сторінки веб-ресурсу з великою популярністю (більше 5000 підписників) передбачити відгук читачів на чергове повідомлення. Наша робота має фокус на підлаштування під кожну окрему сторінку і на врахування деталей та попередніх коментарів саме з цієї сторінки, щоб максимально точно передбачати реакцію аудиторії конкретної сторінки.

ПІДГОТОВКА ВХІДНИХ ДАНИХ ДЛЯ АНАЛІЗУ ТА ПРОГНОЗУВАННЯ РЕАКЦІЇ АУДИТОРІЇ НА ПОВІДОМЛЕННЯ НА ПЕРСОНАЛЬНІЙ СТОРІНЦІ КОРИСТУВАЧА

Дані для тренування. Збір даних для тренування накладає значні обмеження на процес тренування. Автоматичне завантаження даних користувачів, які не дали на це безпосередньої згоди, не є дозволеним. Тому дані для тренування та валідації було завантажено у напівавтоматичному режимі з даних авторів цієї статті та обмеженого кола осіб, що дали свою згоду на вивантаження їхніх даних.

Структура об'єкту дослідження — контенту і реакцій у соціальних мережах. У контексті соціальних медіа, таких як "Facebook" та "Instagram" публікований контент може складатися з трьох компонентів:

- візуальний контент — набір зображень або відео;
- аудіо контент;
- текстовий контент — текстові публікації та коментарі користувачів.

Рис. 1 Схематичне подання опублікованого контенту і реакції аудиторії на різних соціальних платформах (Facebook, Instagram)

Також соціальні платформи підтримують можливість для аудиторії виражати реакцію та ставлення до опублікованого контенту. Наразі способи вираження реакції аудиторії до контенту є стандартними практично для всіх соціальних платформ і можна виділити такі інструменти:

- лайк — інструмент для швидкого вираження позитивного ставлення до контенту, що зазвичай реалізовано у вигляді кнопки з лічильником;
- дизлайк — інструмент для швидкого вираження негативного ставлення до контенту, що зазвичай реалізовано у вигляді кнопки з лічильником;
- текстовий коментар;
- поширення (репост) — інструмент, який дає змогу аудиторії копіювати контент, публікувати і поширювати його на власних сторінках.

Схематично структуру опублікованих у соціальних мережах даних та реакції ауді торії надано на рис. 1.

Отже, аудиторія має багато способів виразити своє ставлення до опублікованого контенту. У схемі (Рис. 1) наведені найпоширеніші інструменти, проте варто враховувати, що будь-яка соціальна платформа може мати свої специфічні засоби для вираження ставлення аудиторії до інформації, що публікується.

Прогнозування популярності та відгуку аудиторії на публікацію є складною та комплексною задачею у загальному випадку за таких причин:

1) публікація складається зі слабоструктурованої інформації, яка має складну природу;

2) структура публікації може відрізнятися за різних платформ і може як включати, так і не включати ті чи інші засоби; наприклад можливість ставити дизлайки на деяких платформах відсутня, коментарі до публікації можуть бути відключеними автором тощо;

3) модерація контенту може бути різною, тобто автори можуть видаляти коментарі, деякі платформи підтримують можливість налаштування відображення публікації тільки для певної частини аудиторії тощо;

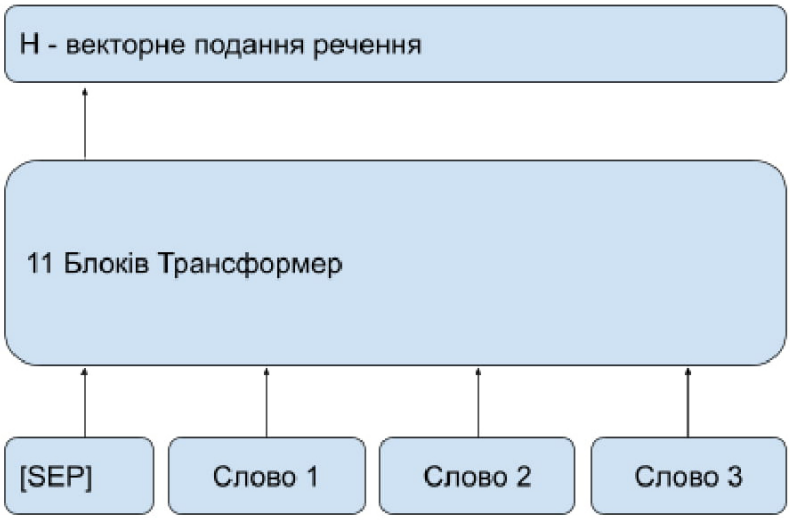

Рис 2. Схема роботи нейронної мережі BERT

4) аналіз кожної частини публікації (текст, зображення, відео) є нетривіальним завданням.

У цій роботі пропонується система для аналізу візуально-текстового контенту публікації, що базується на нейронних мережах та основна ідея якої — це побудова швидкої для тренування нейронної мережі, специфічної для кожного автора, яка буде прогнозувати такі значення для нової публікації: кількості лайків, кількості поширень та емоційну направленість коментарів аудиторії (позитивна/негативна).

Отримання характеристик з текстової частини контенту. Для генерації ознак з текстових даних було використано нейронну мережу, побудовану на основі архітектури Transformer [4]. Оскільки навчання нейронної мережі для оброблення потребує величезних обсягів даних, то цю систему ми тренували на основі попередньо навченої мережі на мовних моделях системи BERT [5].

На рис. 2 зображено схему нейронної мережі BERT. Ця система дає змогу приймати на вході ціле речення, розраховувати 12-рівневу нейронно-мережеву архітектуру і отримати контекстно-залежні репрезентації слів. Цей підхід має перевагу над підходом незалежного оброблення слів, оскільки враховує контекст, в якому кожне слово використовується.

Для розв’язання цього завдання використано тільки перші 11 рівнів нейронної мережі задля того, щоб отримати репрезентацію слів з усіма контекстними ознаками, але без ознак, які потрібні для обчислення ймовірності появи слова у мовній моделі.

Кожне слово має 768-розмірний вектор, який відповідає його числовій репрезентації. Для побудови єдиного значення для всього тексту здійснено усереднення за всіма словами в тексті як спосіб узагальнення.

Отримання характеристик з візуальної частини контенту. Для генерації ознак із зображення використано згорткову нейронну мережу VGG-16 [6], а саме частину мережі зі згортковими шарами, які відповідають за екстракцію

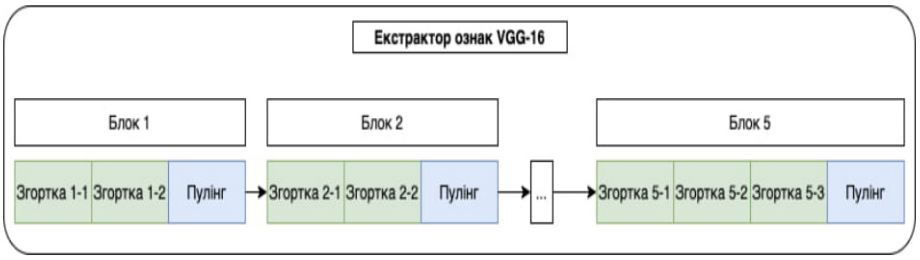

Рис. 3. Структура згорткових шарів мережі VGG-16

ознак, що описують вміст зображення. Вибір такої архітектури зумовлено тим, що її тренування було здійснено на наборі даних ImageNet [7] і ваги мережі для цього набору даних знаходяться у відкритому доступі. Альтернативний спосіб ініціалізації ваг мережі — це ініціалізація випадковими значеннями, що мають нормальний розподіл, параметри якого є математичним сподіванням та дисперсією, залежать від кількості вхідних значень та кількості вихідних значень шару [8]. Структуру згорткових шарів надано на рис. 3. Ця мережа дає наразі найкращі результати на наборі даних ImageNet, але простота її структури і ознаки, вивчені в процесі тренування на ImageNet, дають змогу швидко адаптувати її до інших завдань та дотреновувати за короткий час, що є значною перевагою для нашого завдання.

Нормалізація зображення здійснюється таким чином. Перед тим, як подати зображення в мережу, його розмір зменшується до 224x224 пікселів (стандартний розмір для задач класифікації зображень). Ця трансформація робиться для того, щоб пришвидшити оброблення даних та зменшити використання пам'яті. Після цього здійснюється нормалізація значень зображення — від нього віднімається середнє значення за кожним кольоровим каналом та ділиться на 255 — всі трансформації робляться по-піксельно. Після цих дій, зображення подається в мережу.

Результатом роботи мережі, в нашому випадку — останнього згорткового шару, буде карта ознак — 3-х вимірний тензор розмірністю 7 x 7 x 512. Перші дві розмірності є просторовими та відповідають за прояви тих чи інших ознак на сегменті зображення. Остання розмірність — це розмірність ознак, тобто мережа видала на вихід вектори розмірністю 512 для кожного з 7 * 7 = 49 пікселів вхідного зображення. Просторові розмірності є непотрібними для подальшої роботи алгоритму, тому, щоб зменшити кількість обчислень, використовується Global Average Pooling — усереднення ознак за просторовими координатами карти ознак. Отже, результатом мережі буде вектор ознак розмірністю 512 для всього зображення.

АЛГОРИТМ ПЕРЕДБАЧЕННЯ РЕАКЦІЇ АУДИТОРІЇ НА ПОВІДОМЛЕННЯ

Розроблена нейронна мережа прогнозує порядок значення реакції користувачів на певне повідомлення, а не цю конкретну величину, оскільки ці значення мають значну дисперсію в лінійній шкалі і незначну в логарифмічній. Порядок величин, які нейронна мережа буде передбачати — це кількість лайків і кількість поширень. Таке обмеження дає можливість запропонованій мережі навча-

тися ефективніше. Однак прогнозування порядку, а не точної кількості реакцій не обмежує використання мережі з практичною метою, оскільки інформації про порядок кількості "лайків" та "поширень" достатньо для того, щоб прийти до рішення про публікацію чи відмову від публікації контенту.

Компоненти моделі. Зведемо регресійну задачу прогнозування лайків і репостів до задачі класифікації. Здійснюється це таким чином. Для кожної сторінки та автора є відомим розмір його аудиторії, який позначимо як N. Кількісні параметри i-ї публікації (P_i) — лайки та репости, позначимо як l_i та r_i відповідно. Для кожної публікації розрахуємо нормовані параметри відносно розміру аудиторії:

$$\forall P_i : l_i^* = \frac{l_i}{N}, r_i^* = \frac{r_i}{N}.$$

Маючи сукупність нормованих лайків для кожної публікації, рівномірно розіб'ємо їх на C_l інтервалів, довжина яких дорівнює $\frac{max(l_i^*)}{C_l}$. Таким розбиттям ми фактично зводимо задачу регресії для лайків до задачі класифікації на C_l класів.

Аналогічно зводимо задачу регресії для поширень до задачі класифікації на C_r класів.

В наших експериментах використано такі значення: $C_l = 5$, $C_r = 5$.

Емоційна направленість коментарів, або сентимент-аналіз, також є задачею класифікації. Для тренування запропонованої моделі є необхідним здійснення розмітки коментарів за їхньою емоційною направленістю. Для збору цих даних використано вже відомий підхід, що базується на глибоких нейронних мережах. Дані опрацьовували таким чином. Кожен коментар публікації подавався на вхід мережі, яка видавала ймовірність p_j того, що коментар виражає позитивне ставлення користувача до контенту. Далі рахували середнє значення всіх ймовірностей p^* за всіма коментарями і, якщо $p^* > 0{,}5$, то загальна реакція аудиторії в коментарях на публікацію вважалась позитивною, інакше — негативною.

Отже, в рамках цієї роботи розв'язували три незалежні завдання класифікації відповідно до предмета аналізу — визначення та передбачення:

1) кількості лайків;
2) кількості поширень;
3) сентименту коментарів реакцій.

Дані трьох типів було надано на вхід алгоритму: зображення, додане в публікації; текст публікації; мета-інформація про сторінку та автора — математичне сподівання та дисперсія для лайків, поширень.

На вхідні дані накладено деякі обмеження: 1) обробляються публікації, що складаються з текстового опису і одного зображення, якщо зображень декілька — лише одне вибирається для аналізу; 2) аудіо та відео контенти ігноруються.

Ці обмеження не зменшують узагальненого характеру методу, а лише спрощують завдання і дають змогу простіше аналізувати поведінку моделі. Система може бути узагальнена для оброблення як відео-, так і аудіо-контенту.

Під час тренування моделі на дані накладалося додаткове обмеження — мережа тренувалася лише на тих публікаціях, для яких є не менше за 3 коментарі від аудиторії.

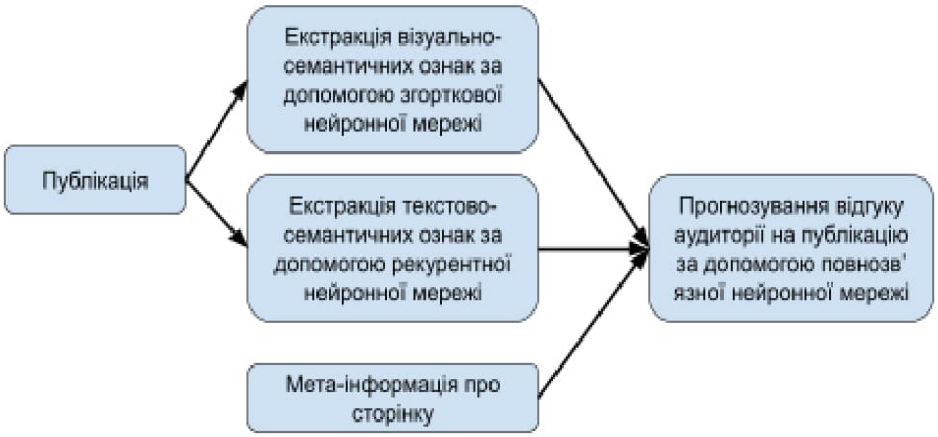

Рис. 4. Схема роботи алгоритму прогнозування реакції аудиторії

Розроблений алгоритм складається з функціонування трьох головних компонентів (Рис. 4):

1) згорткова нейронна мережа для екстракції візуально-семантичних ознак для зображення;

2) рекурентна нейронна мережа для екстракції текстово-семантичних ознак для текстових даних;

3) повнозв'язна нейронна мережа, що приймає мета-інформацію про сторінку та ознаки, отримані на попередніх кроках та генерує остаточне прогнозування.

Алгоритм працює таким чином.

1. Зображення нормалізується та подається на вхід згорткової нейронної мережі, результатом роботи якої буде згенерований вектор ознак розмірності 512.

2. Передоброблений текстовий вміст публікації подається на вхід рекурентної нейронної мережі, результатом роботи якої буде згенерований вектор ознак розмірності 768.

3. Отримані вектори та мета-інформація про сторінку об'єднуються в один вектор. Об'єднання візуально-текстових ознак та мета-інформації для прогнозування відбувається таким чином. Ознаки у вигляді векторів, отриманих на попередніх кроках, конкатенуються. Також до ознак додається ще 4 параметри — математичні сподівання та дисперсії кількості лайків та поширень, розраховані на основі попередніх публікацій автора. В результаті отримуємо фінальний вектор ознак розмірністю 1284.

4. Згенерований вектор ознак подається на наступний блок — нейронну мережу, що складається з трьох послідовних повнозв'язних шарів, основна мета яких — комбінувати візуальні, текстові ознаки та мета-інформацію про сторінку між собою і згенерувати фінальний вектор ознак. Далі три незалежні шари нейронної мережі на основі цих ознак прогнозують необхідні значення — порядок лайків і репостів та оцінку емоційної направленості коментарів аудиторії.

Для реалізації алгоритму використано мову програмування Python та бібліотеку PyTorch.

АПРОБАЦІЯ ПРОГНОЗУВАЛЬНОЇ МОДЕЛІ

Мережа тренувалася в end-to-end манері, за допомогою алгоритму оптимізації Adam. Оскільки задачу прогнозування було зведена до задачі класифікації трьох різних параметрів, використано категоріальну крос-ентропію як функція втрат:

$$CE = -\sum_{i=1}^{C} y_i \log(p_i),$$

де C — кількість класів; y_i — вектор, в i-й позиції якого буде 1, якщо об'єкт класифікації належить класу i, інакше 0; p_i — вектор, в i-й позиції якого буде ймовірність, що за якою об'єкт класифікації належить класу i.

Отже, якщо функцію втрат для прогнозування лайків позначити як L_{like}, репостів — L_{repost}, емоційної направленості — $L_{\text{sentiment}}$, то кінцева функція втрат буде:

$$L_{\text{total}} = \alpha_1 L_{\text{like}} + \alpha_2 L_{\text{repost}} + \alpha_3 L_{\text{sentiment}},$$

де α_1, α_2, α_3 — вагові коефіцієнти, що вказують на те, як сильно мережа має концентруватися на відповідному предметі прогнозування.

У експериментах з апробації прогнозувальної моделі значення параметрів були $\alpha_1 = 1$, $\alpha_2 = 0{,}5$, $\alpha_3 = 1$. Ці параметри вибрано такими, бо зазвичай прогнозувати поширення значно складніше у зв'язку з тим, що користувачі рідше поширюють публікації, ніж ставлять лайки і пишуть коментарі. Тому сильно штрафувати мережу за помилку, тобто збільшувати значення функції втрат, в цьому випадку є недоцільним.

Для аналізу процесу навчання мережі використовувався моніторинг зміни значень функції втрат в залежності від часу навчання, а саме — кількості епох навчання. Одна епоха — це епізод зміни ваг мережі, у якому кожен об'єкт з тренувального набору даних було використано один раз для коригування ваг мережі. Обчислення значення функції втрат на тренувальному наборі даних використовується для отримання значення помилки навчання та за викостання валідаційного набору даних для отримання значення помилки узагальнення. У разі оптимального вибору моделі та алгоритму навчання, тренувальна і валідаційна помилки зменшуються за збільшення кількості епох навчання аж до порогового значення епохи, де вона максимально наближується до асимптотичного значення.

Під час тренування модель досягла мінімального значення на епосі навчання 17 і через 3 епохи навчання було зупинено, оскільки значення метрики функції втрат не покращувалось. Значення функції втрат на тренувальному та валідаційному наборах даних зі зростанням кількості епох навчання надано на рис. 5.

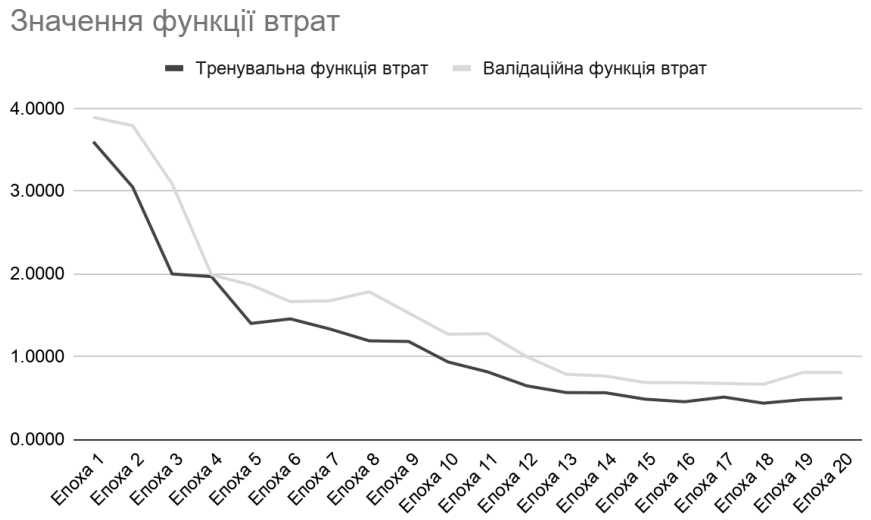

Рис. 5. Динаміка зміни значення функцій втрат (вісь *y*) в залежності від ітерації навчання (вісь *x*)

Методика оцінювання якості алгоритму прогнозування реакції аудиторії. Для оцінювання якості роботи запропонованого алгоритму, а саме — якості прогнозування кількості лайків, поширень та сентимент-аналізу коментарів, використано такі метрики — точність (precision) та повнота (recall) [9]. Ці метрики використовуються у випадку, коли є дисбаланс у кількості даних різних класів. Метрики розраховуються для кожного класу, об'єкти, які належать до вибраного класу, називатимемо позитивами, а об'єкти інших класів — негативами. Для підрахунку метрик використано такі формули:

$$Precision = \frac{TP}{TP + FP}, \quad Recal = \frac{TP}{TP + FN},$$

де *TP* — кількість об'єктів, які є позитивами, і модель класифікувала їх як позитиви, *FP* — кількість об'єктів, які є негативами, але модель їх класифікувала як позитиви; *FN* — кількість об'єктів, які є позитивами, але модель їх класифікувала як негативи.

Ці метрики показують якість роботи алгоритму з урахуванням помилок 1-го та 2-го роду (помилки типу "хибна тривога" та "пропуск цілі" відповідно).

Оцінювання якості роботи алгоритму здійснюється за такою методикою.

Крок 1 — встановлення мінімального порогу ймовірності віднесення об'єкту до певного класу. На основі розрахунків за моделлю для кожного підзавдання встановлюється такий мінімальний поріг ймовірності для певного класу, який має бути, щоб класифікувати досліджуваний об'єкт як об'єкт цього конкретного класу. Значення мінімального порогу лежить у діапазоні (0;1).

Крок 2 — побудова графіку залежності "точність-повнота" (precision-recall curve) за заданим мінімальним порогом. Варіюючи цей поріг, домагаємося зміни метрик кожного класу. Підвищення мінімального порогу зазвичай підвищує точність (precision), водночас повнота не зростає або спадає. Аналогічна ситуа-

ція виникає, якщо мінімальний поріг ймовірності знизити, тоді зростає повнота, а точність зменшується. Перебираючи значення мінімальних порогів для кожного класу, отримуємо графік залежності "точність-повнота" (precision-recall curve). Площа під кривою цього графіка — це число від 0 до 1; чим воно ближче до одиниці, тим якісніше працює алгоритм.

Крок 3 — визначення усередненої точності алгоритму для певного підзавдання (AP — average precision), яка розраховується як площа під кожною кривою певного підзавдання.

Крок 4 — визначення загальної усередненої точності алгоритму (mAP - mean average precision), яка є усередненням за усіма завданнями кожного класу. Значення загальної усередненої точності алгоритму є показником якості роботи запропонованого алгоритму.

Аналіз результатів якості роботи. Кінцеві результати розрахунків за зазначеною методикою показано у таблиці 1.

Ми порівняли результати роботи розробленого нашого алгоритму з базовим алгоритмом, який видає випадковий результат на тестову публікацію.

За отриманими результатами визначено, що модель показала високу якість роботи під час прогнозування сентименту коментарів аудиторії. Якість прогнозування лайків і репостів є нижчою. Причини цього — великий рівень суб'єктивності, прояви можливої емоційності та упередженості аудиторії, небажання або відсутність можливості надати свою оцінку у вигляді лайка чи поширень, що збільшує дисперсію і не дає змогу точно спрогнозувати відповідне значення кількості лайків чи поширень.

Отже, побудовано нейронну мережу для прогнозування реакції аудиторії на контент, що створюють користувачі в соціальних мережах Фейсбук та Інстаграм. Для побудови і навчання нейронної мережі використано найточніші на сьогодні системи з автоматичного оброблення природної мови, а також оброблення візуальних даних (зображень). Кожна з цих систем була наперед навчена на великих обсягах даних і в цій роботі ми використали ці напрацювання для підвищення точності роботи запропонованої мережі.

Проведено аналіз контенту за набором даних і визначено необхідність окремого тренування нейронної мережі для кожної сторінки в соціальній мережі. Процес тренування оптимізовано таким чином, щоб тренування відбувалось тільки для набору зображень і текстів конкретно заданої сторінки.

Особливістю цієї розробки є те, що допомогою запропонованої нейронної мережі реалізовано можливість поєднаного дослідження візуального і текстового контентів для прогнозування реакції аудиторії.

Табл. 1. **Якість роботи алгоритму на різних підзадачах**

Задача	**Загальна усереднена точність**	
	Базовий алгоритм (%)	**Запропонований алгоритм (%)**
Прогнозування лайків	20	69,7
Прогнозування поширень	20	63,4
Сентимент-аналіз коментарів	50	91,2

ВИСНОВКИ

Використання розробленої нейронної мережі, яка складається з трьох повнозв'язних шарів і на вхід отримує характеристики текстової та візуальної частин контенту та мета-дані про досліджувану сторінку, дає змогу оцінити реакцію користувачів на чергову публікацію конкретної сторінки в соціальній мережі. Характеристики текстової частини контенту попередньо формуються за допомогою нейронної мережі BERT, а характеристики візуальної частини контенту — за допомогою нейронної мережі VGG-16.

За аналізом результатів роботи нейронної мережі визначено такі обмеження поточної системи, зазначені у порядку зменшення їхньої значущості:

а) необхідність врахування загального інформаційного контексту щодо явища і/або предмету публікації в момент її створення;

б) необхідність врахування темпоральної інформації — порядку публікацій і часові проміжки між публікаціями.

ЛІТЕРАТУРА

1. De Fina A. Storytelling and audience reactions in social media. *Language in Society*. 2016. № 45. P. 473–498.
2. Gaspar R., Pedro C., Panagiotopoulos P., Seibt B. Beyond positive or negative: Qualitative sentiment analysis of social media reactions to unexpected stressful events. *Comput. Human Behav*. 2016. No.56. P. 179-191.
3. Cliche, M. (2017). BB_twtr at SemEval-2017 task 4: *Twitter sentiment analysis with CNNs and LSTMs.* Proceedings of the 11th international workshop on semantic evaluations (SemEval-2017). P. 573–580.
4. Vaswani A., Shazeer N., Parmar N., Uszkoreit J., Jones L., Gomez A.N., Kaiser L., and Polosukhin I. *Attention is all you need.* In Advances in Neural Information Processing Systems. 2017. P. 6000–6010.
5. Devlin J., Chang M-W, Lee K., Toutanova K. *Bert: Pre-training of deep bidirectional transformers for language understanding.* arXiv preprint arXiv:1810.04805. 2018.
6. Simonyan K., Zisserman A., *Very Deep Convolutional Networks for Large-Scale Image Recognition*, arXiv e-prints. 2014.
7. Russakovsky O., *ImageNet Large Scale Visual Recognition Challenge*, arXiv e-prints, 2014.
8. He K., Zhang X., Ren S., Sun S. *Delving Deep into Rectifiers: Surpassing Human-Level Performance on ImageNet Classification.* IEEE International Conference on Computer Vision (ICCV), 2015. P. 1026–1034.
9. Glorot X., Bengio Y. 2010. *Understanding the difficulty of training deep feedforward neural networks*. [Electronic resource] Journal of Machine Learning Research.
10. Bishop C. M. Neural networks and machine learning. Berlin: Springer, 1998. 353 p. (Nato ASI Subseries F).
11. He K., Zhang X., Ren S., Sun S. *Deep Residual Learning for Image Recognition.* 2016 IEEE Conference on Computer Vision and Pattern Recognition (CVPR). Las Vegas, NV:IEEE. 2016. P. 770–778.

Отримано 30.11.2020

Anisimov A.V., DSc (Phys & Math), Corresponding member
of National Academy of Sciences of Ukraine,
Dean of the Faculty of Computer Science and Cybernetics
ORCID: 0000-0002-1467-2006
e-mail: anatoly.v.anisimov@gmail.com
Bevza M.V., PhD student
ORCID: 0000-0002-2697-4968
e-mail: maksymbevza@gmail.com
Bobyl B.V., PhD student
ORCID: 0000-0002-9612-1071
e-mail: bobylbohdan@gmail.com
Taras Shevchenko National University of Kyiv
60, Volodymyrska st., Kyiv, 01033, Ukraine

PREDICTION OF AUDIENCE REACTION ON TEXT-VISUAL CONTENT USING NEURAL NETWORKS

Introduction. *Social networks provide an ability to receive highly personalized experiences for their users, giving them an opportunity to follow pages of other users that publicize relevant and interesting content for them. Feedback on visual and textual content of the message is being received from followers by shares, likes and commentary. Prediction of the audience reaction on a particular message in social media becomes more and more of an important task, because the message is irreversible and there's a need to predict audience reactions before its publication.*

The purpose *of the paper is to build a system that can predict the reaction of the audience on the post and account for all the specialties of the page itself, its audience, the author and variety of possible reactions.*

Results. *We analyzed structure of the content and reactions in the social media and defined specialities of the messages, that should be accounted for during the analysis of the message popularity and reactions of the audience on it. We explain the process of the neural network training, that gives the ability to train the neural network for each particular page and audience to get better quality of the algorithms work. Features of the textual part of the content were o-btained using the BERT neural network, whereas features of the visual part were obtained with the VGG-16 neural network. We've created the model that performs classification for three types of values: likes, shares and emotional focus of the commentaries. We have created a system that processes both visual-semantical and text-semantical parts as well as meta-information of the content and gives the program the full context of the publication that algorithm will process. Analysis of the developed system shows that model performs on emotional focus prediction better than amount of likes and shares.*

Conclusions. *The developed system uses three neural network layers and features from textual and visual parts of the content as well as meta-data of the message provides ability to predict reaction of the users on a particular message in the social media.*

Keywords*: artificial intelligence, natural language processing, computer vision, social n-etworks, audience reaction prediction.*

Intelligent Control and Systems

DOI: https://doi.org/10.15407/kvt203.01.039

UDC 519.688

MISHCHENKO M.D. [1], PhD Student,
Department of Mathematical Methods in System Analysis
ORCID: 0000-0001-6135-2569
e-mail: mishenkomihailo@gmail.com
GUBAREV V.F. [2], DSc (Engineering),
Corresponding Member of NAS of Ukraine,
Head of the Dynamic Systems Control Department
ORCID: 0000-0001-6284-1866
e-mail: v.f.gubarev@gmail.com
[1] Institute for Applied Systems Analysis,
National Technical University of Ukraine
"Igor Sikorsky Kyiv Polytechnic Institute"
37, Peremohy av., Kyiv, 03056, Ukraine
[2] Space Research Institute of the National Academy
of Sciences of Ukraine and the State Space Agency of Ukraine
40, Acad. Glushkova, Kyiv, 03187,Ukraine

HORIZON LENGTH TUNING FOR MODEL PREDICTIVE CONTROL IN LINEAR MULTI INPUT MULTI VARIABLE SYSTEMS

Introduction. *There is wide range of systems describable as linear Multi Input Multi Variable systems evolving in discrete time. This mathematical model is often used in engineering, but it can also be applied in many other fields. The problem of stabilization of this kind of system frequently arises. In this paper we consider the Model Predictive Control approach to this problem. Its main principle is to generate control signals by optimizing consequent system's future dynamics on limited prediction horizon. While it demonstrates some good results, in practice we are always limited in terms of computational resources. Thus, we can optimize outcomes of our future control sequence only for limited horizon lengths. That is why it is valuable to understand how this limit affects control quality.*

The purpose of the paper *is to propose a way to appraise drawbacks of limiting of the prediction horizon to certain length for a particular system, so that we can make informed choice of such limit and therefore choose controller's microprocessor with sufficient computing power.*

Methods. *Several indexes which characterize the stabilization process are defined. Their heatmaps built against system's initial state are used as a convenient visualization of how system's stabilization dynamics changes depending on its initial state and of drawbacks induced by prediction*

horizon length limiting. Such heatmaps were built for several prominent example systems with different structures by performing corresponding series of computational experiments.

Results. *Drawbacks of prediction horizon length limiting vary from severe to completely nonexistent depending on the system's structure and representation. These drawbacks relax with increase of this limit.*

Conclusions. *The stabilization dynamics depends largely on the system's structure. Therefore, it is advised to take it into account and build heatmaps of aforementioned indexes to decide on prediction horizon length limit. A good system's representation can improve stabilization time with limited prediction horizon length.*

Keywords: *MPC, MIMV, heatmap, control synthesis, discrete controllable system, linear system, moving horizon, stabilization.*

INTRODUCTION

The object of this study is the Model Predictive Control (MPC) based control process. The aim of the considered control process is to stabilize a system, e. g. for a system with non-zero state vector x at initial point of time to bring its state to zero with specially crafted sequence of control signals. In this paper we are working with discrete-time linear Multi Input Multi Variable (MIMV) systems with constrained input values, which can be described as

$$x_{k+1}=\boldsymbol{A}x_k+\boldsymbol{B}u_k,\ k \in \mathbb{Z}, \tag{1}$$

$$|u_k[j]| \le u_{max},\quad k \in \mathbb{Z},\quad j \in 1..r \tag{2}$$

where x is the system's state at a particular point of time represented as n-dimensional real-valued vector, u is the control applied to the system at a particular point of time, k is a sequential number of a related point of time, j is an index of a particular element of the control vector u, $u_{\max}$ is a positive value representing constraint on control signal values, $\boldsymbol{A}$ and $\boldsymbol{B}$ are real-valued matrices of corresponding dimensions.

The aforementioned formalization is applicable to wide variety of systems. First of all, the system dynamics equation (1) can be obtained as a result of discretization of a model of a continuous-time system by transforming its differential equation into a difference equation with certain sampling rate. This transformation is indispensable if we want to control such system with digital controller, which perceives continuously changing values through analog-to-digital converters. Usage of programmable controllers is essential in various fields where we need precise online control, i. e. for operating industrial plants or various mechanisms and engines.

There are also applications outside of traditional engineering scope. Various naturally-formed (e. g. not engineered by someone) complex systems can be represented in form of weighted digraphs, as discussed in subsection 4.3 of [1]. We can also think of them as of cognitive maps. The pulse process model described further in subsection 4.4 of [1] allows us to model dynamics of such systems. Coincidentally, dynamics of the so-called pulses (differences between current system state vector and previous) can also be described with equation (1). This gives us opportunity to control them in the same way as ordinary linear systems, as it is proposed in [2–3].

It is a common problem to stabilize the system by influencing it with control signals. In this context "to stabilize" means to make system's state x equal (or at least nearly equal) to zero at some point of time. This problem was thoroughly studied within the framework of the control theory. For textbook description of the control theory approach to this problem see, for example, [4–5]. But this conventional approach also have its drawbacks. One of them is that in real-life (not simulated) systems there is always a constraint on control signal values in one form or another, which can't be directly taken into account with the control theory. The other drawback is that control loops produced this way require fine-tuning to ensure its stability and satisfy other requirements at the same time, such as high response speed and satisfaction of the aforementioned control signal constraints.

To mitigate this and some other drawbacks the MPC approach to this problem was introduced in [6]. The MPC-based feedback loop is organized similarly to ones employed in the control theory. The main difference is that control signals are calculated not by multiplying the current system's state (or its estimation) by a matrix, as in the control theory, but by solving a mathematical optimization problem. The solution of this optimization problem is a sequence of future control signals, which would result in the best predicted future system's states in terms of employed objective function. This leads to another significant difference: this way we generate a whole sequence of control signals instead of just one next control signal. Thus, there are many possible ways to employ generated control sequences. For example, we can apply the whole control sequence as is, or just use the first control signal value from each generated control sequence. Different optimization problem variants, approaches to their solving and ways to integrate their solutions into the control loop were proposed in [6–7].

PROBLEM STATEMENT

While showing some promising results [6–7], this approach requires significant computational resources, especially in comparison with control theory based controllers. Moreover, the required computational resources rapidly grow with prediction horizon length increase. Considering the fact, that there is no such thing as infinite computational resources, the prediction horizon we can implement consequentially becomes limited by hardware we use for computations and by system's sampling rate (which enforces hard limit on time we have to compute next control signal value).

As actual prediction horizon length required to produce ideal (in terms of stabilization time) control sequence differs from one situation to another, it is valuable to understand what actual drawbacks to expect from its limiting. This would give us the required information to make informed choice of such limit and therefore to choose controller's microprocessor with sufficient computing power.

The purpose of this paper is to propose a way to represent drawbacks of prediction horizon limiting in a meaningful and understandable way. Since the stabilization dynamics is essentially different for systems with different structure, it is required to perform such investigation for any particular system we are considering. In other words, in general case we can only say that the bigger horizon length limit, the better. So, in this paper we propose a way to appraise this drawbacks for a particular system and analyze some example systems to explore the impact of system's structure.

The proposed method is essentially series of system stabilization computational experiments and a way to visualize their results. So, the rest of the paper is organized as follows. The Experiment Design section describes exactly what, how and for what purpose are we doing in the computational experiments. The Experiment Results section shows some examples of application of the proposed method to perform the discussed analysis for some example systems with essentially different structures. In the Analysis of Results section we discuss our findings derived from the experiment results. Lastly, the Conclusions section provide a brief summary of obtained results.

EXPERIMENT DESIGN

Our goal here is to evaluate effects of horizon length limiting alone, in isolation from other additional factors, which can influence the quality of control process for a given horizon length limit. That is why we implement the most basic feedback loop scheme and consider the system being deterministic, even though in most real-world cases systems suffer from random perturbations.

Assumptions about the system. We consider matrices $\boldsymbol{A}$ and $\boldsymbol{B}$ having full ranks, because otherwise there is a roughly equivalent representation of the system with full-ranked matrices and reduced dimensions.

For the same reason we also consider that $r \leq n$, i. e. that number of control vector's dimensions is not greater than number system state vector dimensions.

As it was already mentioned, the system is deterministic, i. e. there are no noises affecting the system.

Structure of matrix $\boldsymbol{A}$. The linear system representation (1–2) is not invariant, since for every invertible linear transformation of the state space we have corresponding alternative representation in the same form, but with different matrices $\boldsymbol{A}$ and $\boldsymbol{B}$. In most examples in the Experiment Results section we construct $\boldsymbol{A}$ matrices for subject systems in our computation experiments using real-valued modification of Jordan normal form (with rotation, rotation-shrinking or rotation-expanding block corresponding to complex eigenvalues) to be sure to examine most distinct variants of stabilization dynamics. But even though linear transformations of state-space do not affect stabilization process if the prediction horizon length is not limited, it may have its impact otherwise. Thus, we also added an example described in non-canonical form for comparison.

Heatmap experiment result representation. It is obvious, that for given system and controller the system's future depends on its initial state. For deterministic systems it is fully determined by its initial state. Thus, if there are some significant numeric characteristics (indicators) of the system's dynamics, it is valuable to plot them against system's initial state.

Of course, the system's state vector x may have many dimensions, but it is not very meaningful to try to analyze a heatmap built for more than two dimensions manually. It may be possible to do with machine learning techniques, but we will not touch this topic in this paper. Thus, we propose to plot heatmaps of indicators for initial system states residing on a certain 2-dimensional (hyper-) plane.

As it is obvious that the system model's equation (1) and control synthesis algorithm we use does not have any fractal properties, it is enough to calculate the indicators we consider (by performing corresponding computational experiments) only for a finite subset of possible initial states uniformly distributed on a (hyper-)plane patch we build heatmap for. This way if we have two direction vectors e_1 and e_2, and a grid step $g \in (0,+\infty]$, then the grid will consist of points $g\,(ie_1 + je_2)$, $i, j \in \mathbb{Z}$.

The last significant thing about the heatmap structure which should be mentioned is that all heatmaps we build here demonstrate point symmetry with its center in zero. It is due to properties of the considered system structure (1—2). That is why we plot heatmaps only for a half-plane to reduce computation time required to produce such plot and to fit them on page.

Control synthesis. We compute series of controls as a solution for an optimization problem

$$\min_{u_k, u_{k+1}, \ldots, u_{k+s-1}} \left\| x_{k+s}\left(x_k, u_k, u_{k+1}, \ldots, u_{k+s-1}\right) \right\| \tag{3}$$

$$\left| u_k[j] \right| \le u_{\max}, \quad i \in 1..s-1, \quad j \in 1..r \tag{4}$$

where s is the prediction horizon length. This is a convex quadratic program, which we solve with the CVXOPT coneqp solver [8]. We apply computed control vector sequences as is, without correcting them at each next point of time, which would be natural if we were working with non-deterministic systems, i. e. when there are random noises affecting the system. Such intermediate control sequence corrections would require more sophisticated optimization problem and/or structure of the feedback loop. Obviously, the combination of the optimization problem and the way its solutions are used for control is not the most optimal, but the most simplistic one. It is because one of our aims is to demonstrate a way to benchmark such combination in general. The analysis of this basic combination should also give some valuable insights which hopefully will help in development of better ones in future.

Indicators and corresponding control strategies (controllers). As we said, we will plot heatmaps for different indicators representing significant information about system's properties regarding the stabilization process. And to calculate them we need to simulate stabilization process with different control strategies.

Stabilization time with unlimited horizon length. Our goal is to explore negative effects of prediction horizon length limiting, so firstly we need to determine what actually happens if the horizon length is unlimited to have a basis to compare with. So, for each considered initial state x_0 we sequentially try to solve the problem (3–4) for $s = 1$, $s = 2$ and so on, until the corresponding optimal final state $x_s(x_0, u_0, \ldots, u_{s-1})$ is zero. This way we obtain the first index we will plot: minimal number of iterations needed to stabilize the system with corresponding initial state.

Of course, this is just a simplification. In practice, all computations are performed with floating point numbers, which by itself causes numerical errors and thus introduces otherwise negligible perturbations, which nevertheless make obtaining a state vector *exactly* equal to zero highly improbable. In addition, the CVXOPT solver computes a numeric estimation of problem's solution, rather than its precise value. That is why we follow a common practice to check if the

final state vector $x_s(x_0, u_0, \ldots, u_{s-1})$ resides in a certain small ε-neighborhood of zero instead of checking for strict equality.

The other peculiarity we must address here is that if the system is unstable, i. e. $\rho(\boldsymbol{A}) > 1$, then for such system there are initial states, for which stabilizing control does not exist. And, obviously, the aforementioned optimal control synthesis procedure will never meet its stop condition for such initial states. In addition, the solver faces computational difficulties when we try to find a solution of the problem (3–4) for really huge values of s. Thereby, we stop the procedure when the next horizon length s exceeds a certain huge value `huge_s`.

We will call the simulated model controller implementing aforementioned principles "the ascending controller" for short.

Stabilization time with limited horizon length. The next index we will plot as a heatmap is stabilization time obtainable with a controller, whose solver is unable (or prohibited) to solve problems with s higher than certain value s_{max}. We will call corresponding simulated model controller "the descending controller". This controller will generate control sequences of limited length and apply them to the simulated system as is in loop, until the ε-neighborhood of zero is reached.

It initially will try to solve the problem (3–4) for maximum allowed horizon length $s_{\max}$. But if the controller will just apply generated control sequences as is, the stabilization time that we would measure would be a multiple of $s_{\max}$. The value measured in this way would often overestimate the required stabilization time, because the last generated control sequence (which finally leads the system to the aimed ε-neighborhood of zero) could have been shorter. So, in this situation the descending controller will check if the next generated control sequence would finally stabilize the system. If it is the case, the controller will try to solve the problem (3–4) for $s = s_{\max} - 1$, $s = s_{\max} - 2$ and so on until corresponding $x_{k+s}(x_k, u_k, u_{k+1}, \ldots, u_{k+s-1})$ will fall out of the ε-neighborhood of zero, or until s = 1 inclusive. Hence the name of this controller: the descending controller. The shortest stabilizing sequence will be applied to the system. This way we will obtain more adequate measurement of required stabilization time.

Stabilization time loss for limited horizon length. To compare the stabilization time measured with the descending and ascending controllers, we will calculate their difference, which is another index we will plot heatmap for. It is expected that this difference will be nonnegative.

There are three implicit values which originate from the fact that this is a computational experiment and which affect this experiment's outcome. The first one was already mentioned. It is the radius of the zero's neighborhood we compare system's state x with: ε. The other two are related to the CVXOPT solver, namely `reltol` and `abstol`, which control relative and absolute accuracy of results returned by the solver. These three values need to be finely tuned to obtain meaningful results. Too small ε or too big `reltol` and/or `abstol` leads to overestimation of minimal stabilization time (measured for ascending controller). Too big ε leads to its underestimation. Too small `reltol` or `abstol` leads to computational difficulties in the solver.

Such overestimation becomes apparent if we see negative values on the stabilization time loss heatmap. This gives us required information to manually tune these implicit variables.

Distance loss for limited horizon length. There is one more index we measure. It has less obvious construction. It measures minimum distance from zero

achievable by a controller with solver with limited horizon length at the point of time, when the same system with the same initial state would have been stabilized by the ascending controller.

To measure this index we use another specific emulated controller. Let us call it "the distance controller". As in the descending controller, this controller will generate control sequences of limited length. The main difference is that it does not check whether the generated control sequence would stabilize the system (i. e. would lead the system's state to the ε-neighborhood of zero). Instead it calculates and applies control sequences of maximum allowed length until it can do so without exceeding number of system's iterations $s_{opt}(x_0)$ needed by the ascending controller to stabilize the same system from the same initial state. When such situation eventually occurs at certain point of time k, it solves the problem (3–4) for horizon length $s = s_{opt}(x_0) - k < s_{max}$ and applies generated control sequence to the system. This way this controller executes the same number of iterations, as it was done by the ascending controller for the same system with the same initial state x_0.

In the beginning the distance controller has the same behavior as the descending one, e. g. they both generate control sequences for horizon length $s = s_{max}$, so we reuse them to reduce computation time.

EXPERIMENT RESULTS

In this section indicator heatmaps we built for systems of various structures will be shown, and how their structure affects stabilization process will be discussed. As it can be seen from the Experiment Design section, the computational experiment get a number of input variables, which can be divided into four groups.

The first group describes the system itself: the $\boldsymbol{A}$ and $\boldsymbol{B}$ matrices. The spectral radius of $\boldsymbol{A}$, which is denoted as $\rho(\boldsymbol{A})$, is also shown in tables next to them, because its value determines, whether the system is stable or not. The second group is constraints on control values and horizon length, denoted as u_{max} and s_{max}. The third group consists of plotting parameters, namely the direction vectors e_1 and e_2 of the heatmap grid and its grid step g. On heatmap plots e_1 and e_2 correspond to the horizontal and vertical axes. The last group consists of some experiment parameters concerning caveats of numeric computations: ε, `reltol`, `abstol` and `huge_s`. All following computational experiments were performed with ε = 1E-6, `reltol` = 1E-12, `abstol` = 1E-10.

Stable systems. In this subsection results obtained for stable systems, e. g. whose matrix $\boldsymbol{A}$ have spectral radius $\rho(\boldsymbol{A})$ less than 1, will be presented. In this case systems can stabilize themselves even without any control, so the purpose of the controller is to make the system stabilize faster.

Stable system with real-valued eigenvalues. Let us begin with the most obvious case demonstrated on Fig. 1. As can be seen from the sysem's structure on Table 1, dimensions of the state space do not influence each other and can be controlled separately. So, on the heatmaps of stabilization time the maximum of required times for both dimensions can be seen. The border on which the stabilization times of each dimension are equal can also be seen on the plots. In this particular case this lines are straight and form 45° and 135° angles with absciss. This is because the self-stabilization speeds (defined by eigenvalues of the matrix $\boldsymbol{A}$) and control impact magnitudes (defined by coefficients of the matrix $\boldsymbol{B}$) are equal for both dimensions. In other case this border would be curvilinear.

It is also worth to notice, that the time loss in this case is always nonexistent (equal to 0) and therefore the distance loss is always smaller than ε.

The horizon length limit s_{max} was set to 1, so, considering such good results it would be a waste to use bigger horizon length limit for such a trivial case.

Rotation-shrinking stable system. On heatmaps on Fig. 2 built for a stable system with complex-valued eigenvalues we can see the same results as for the one with real-valued eigenvalues. The only difference is the peculiar shape of them. The used $\boldsymbol{A}$ matrix represents combination of the following two operations: rotation by 45° counterclockwise and shrinking by a constant. If we use rotation by a degree, which is not a divisor of 360°, then the heatmap shape will become circular, rather than edged. We suppose that this edgedness is a consequence of the shape of the set of allowed control signals defined in (2).

As in the previous example, the system's structure and some other variables are presented on Table 2.

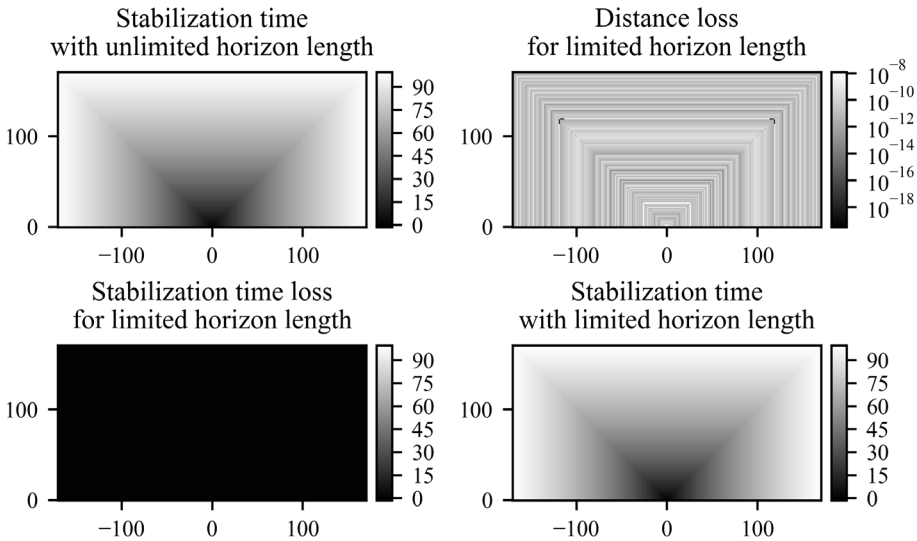

Fig. 1. Index heatmaps for a stable system with real eigenvalues

Table 1. **Computational experiment input values corresponding to heatmaps on Fig. 1**

Variable	Value	Variable	Value
System		**Plotting parameters**	
$\boldsymbol{A}$	$\begin{pmatrix} 0.99 & 0 \\ 0 & 0.99 \end{pmatrix}$	e_1	$\begin{pmatrix} 0 \\ 1 \end{pmatrix}$
$\boldsymbol{B}$	$\begin{pmatrix} 1 & 0 \\ 0 & 1 \end{pmatrix}$	e_2	$\begin{pmatrix} 1 \\ 0 \end{pmatrix}$
$\rho(\boldsymbol{A})$	0.99	grid step (g)	1.0

Constraints			
u_{max}	1.0	s_{max}	1

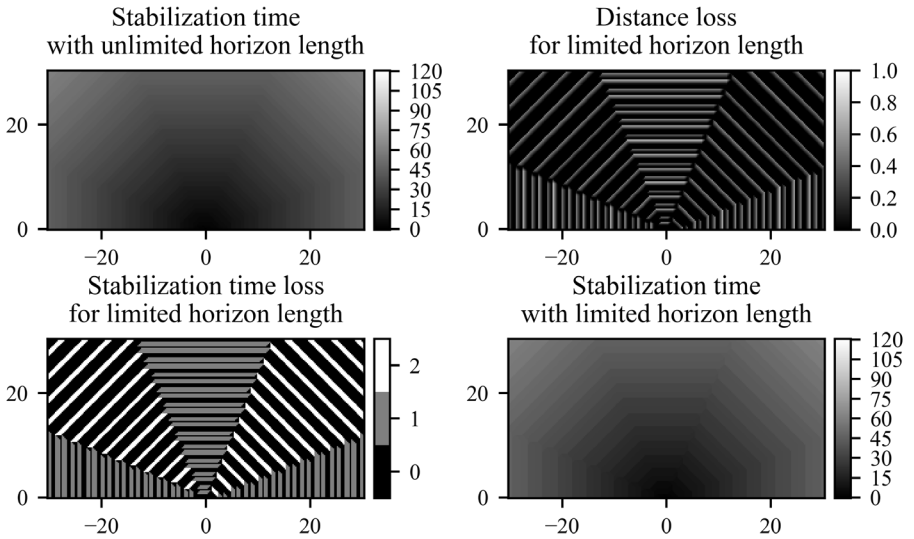

Fig. 2. Index heatmaps for a rotation-shrinking stable system

Table 2. **Computational experiment input values corresponding to heatmaps on Fig. 2**

Variable	**Value**	**Variable**	**Value**
System		**Plotting parameters**	
$\boldsymbol{A}$	$\begin{pmatrix} 0.7036 & -0.7036 \\ 0.7036 & 0.7036 \end{pmatrix}$	e_1	$\begin{pmatrix} 0 \\ 1 \end{pmatrix}$
$\boldsymbol{B}$	$\begin{pmatrix} 1 & 0 \\ 0 & 1 \end{pmatrix}$	e_2	$\begin{pmatrix} 1 \\ 0 \end{pmatrix}$
$\rho(\boldsymbol{A})$	~0.995	grid step (g)	1.0

Constraints			
$u_{\max}$	1.0	$s_{\max}$	1

Uncontrollable stable linear system. It is also interesting to see what happens if we can't control two different components of the state space separately. If these components correspond to two different real-valued eigenvalues, as in the system defined in Table 3, it is obvious that the system becomes uncontrollable. Nevertheless, on Fig. 3 we can see, that if the uncontrollable system is stable, then trying to control such system is not completely useless, because depending the initial state we still can make the stabilization process a bit faster. And for some particular initial states, whose set depends on structure of the matrix $\boldsymbol{B}$, we can make it stabilize significantly faster. But we had to use a system with significantly smaller $\rho(A)$ for this example to make stabilization time small enough to be able to compute it in reasonable time.

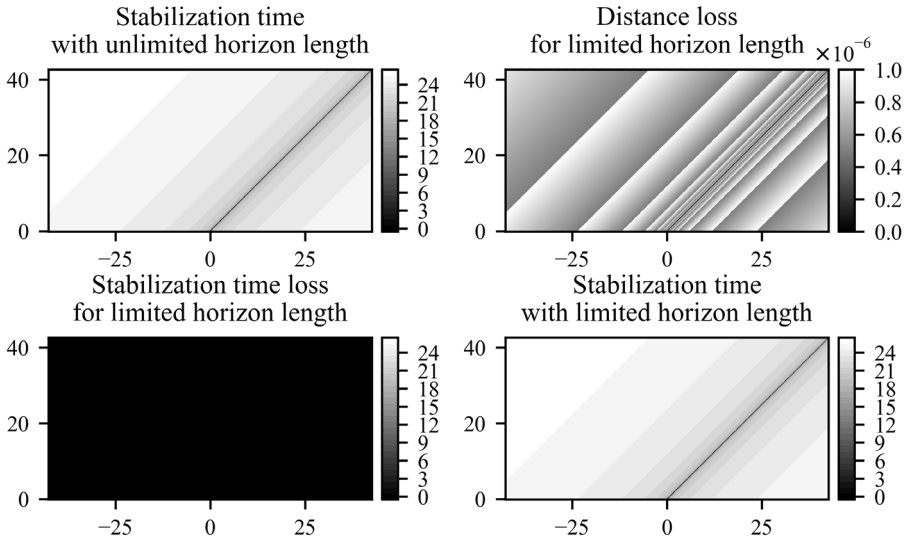

Fig. 3. Index heatmaps for uncontrollable stable linear system

Table 3. **Computational experiment input values corresponding to heatmaps on Fig. 3**

Variable	Value	Variable	Value
System		**Plotting parameters**	
$\boldsymbol{A}$	$\begin{pmatrix} 0.5 & 0 \\ 0 & 0.5 \end{pmatrix}$	e_1	$\begin{pmatrix} 0 \\ 1 \end{pmatrix}$
$\boldsymbol{B}$	$\begin{pmatrix} 1 & 0 \\ 0 & 1 \end{pmatrix}$	e_2	$\begin{pmatrix} 1 \\ 0 \end{pmatrix}$
$\rho(\boldsymbol{A})$	0.5	grid step (g)	0.25

Constraints			
$u_{\max}$	1.0	$s_{\max}$	1

As in the previous examples, here the control with prediction horizon length equal to 1 has no drawbacks in comparison with control with unlimited horizon length.

Rotation-shrinking stable system with intertwined control. Significantly different picture can be seen if we can influence only one component of the state space among the two corresponding to the Jordan matrix cell for complex-valued pair of eigenvalues, as in Fig. 4, Table 4 and Fig. 5, Table 5. When we limit horizon length, the control synthesis algorithm becomes greedy by its nature, consequences of which can be clearly seen on the stabilization time and distance loss plots on Fig. 4 and Fig. 5.

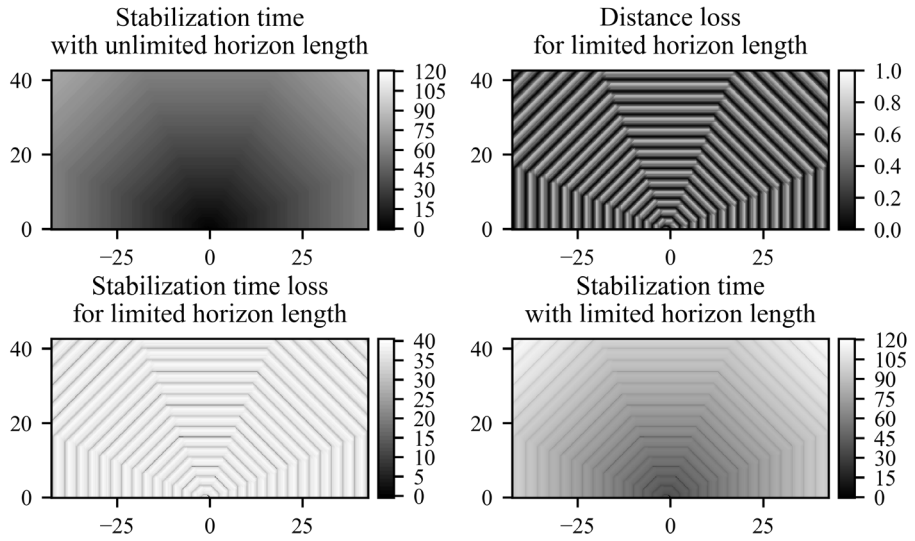

Fig. 4. Index heatmaps for rotation-shrinking stable system with intertwined control and smax = 1

Table 4. **Computational experiment input values corresponding to heatmaps on Fig. 4 and Fig. 6**

Variable	Value	Variable	Value
System		**Plotting parameters**	
$\boldsymbol{A}$	$\begin{pmatrix} 0.7036 & -0.7036 \\ 0.7036 & 0.7036 \end{pmatrix}$	e_1	$\begin{pmatrix} 0 \\ 1 \end{pmatrix}$
$\boldsymbol{B}$	$\begin{pmatrix} 1 & 0 \\ 0 & 1 \end{pmatrix}$	e_2	$\begin{pmatrix} 1 \\ 0 \end{pmatrix}$
$\rho(\boldsymbol{A})$	~0.995	grid step (g)	0.25

Constraints			
$u_{\max}$	1.0	$s_{\max}$	1

In this example matrix $\boldsymbol{B}$ does not allow to influence both components. This makes it similar to the previous example on Fig. 3, Table 3, where matrix $\boldsymbol{B}$ does not allow to control both components separately, because in both cases we can "push" the system only along one single direction, which intertwines control of two different state-space components. While it is so, the $\boldsymbol{A}$ is effectively a rotation-shrinking matrix. That is why influences on one of the components consequentially influence dynamics of both of them. In other words, the system does not become uncontrollable, like in the previous example. Instead, this peculiarity lets the greediness of the algorithm manifest.

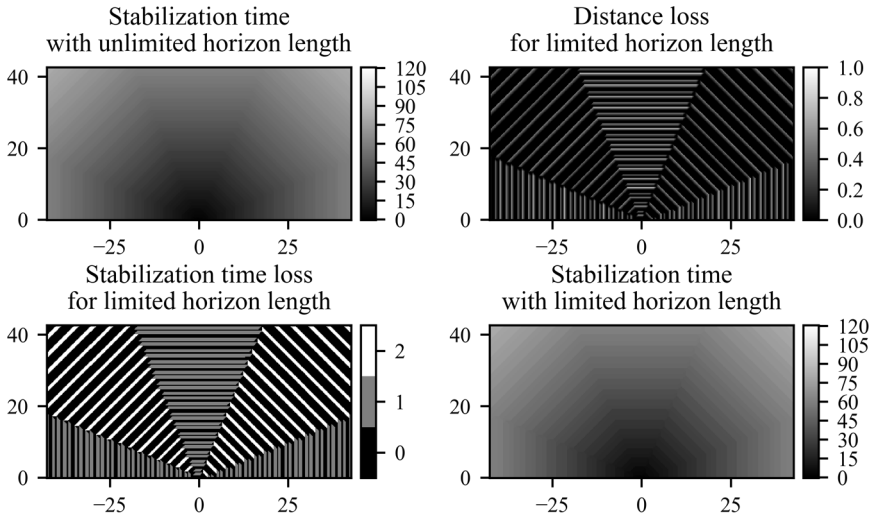

Fig. 5. Index heatmaps for rotation-shrinking stable system with intertwined control and $s_{\max} = 2$

Table 5. **Computational experiment input values corresponding to heatmaps on Fig. 5**

Variable	Value	Variable	Value
System		**Plotting parameters**	
$\boldsymbol{A}$	$\begin{pmatrix} 0.7036 & -0.7036 \\ 0.7036 & 0.7036 \end{pmatrix}$	e_1	$\begin{pmatrix} 0 \\ 1 \end{pmatrix}$
$\boldsymbol{B}$	$\begin{pmatrix} 1 \\ 0 \end{pmatrix}$	e_2	$\begin{pmatrix} 1 \\ 0 \end{pmatrix}$
$\rho(\boldsymbol{A})$	~0.995	grid step (g)	0.25

Constraints			
$u_{\max}$	1.0	$s_{\max}$	2

Even though there are visible losses from horizon length limiting, it is clearly seen that they are limited and do not worsen indefinitely for initial states further from zero, as we can see on Fig. 4 and Fig. 5. In addition, the time loss improves greatly when we increase horizon length limit from 1 to 2: its maximum drops from 39 to 2. At the same time, the distance loss does not improve with horizon length increase. We also tested other horizon lengths up to 8, but both loss indices did not improve further.

It is also interesting, that if we expand this heatmaps to another half-plane, we will see that both loss heatmaps have a shape of double spiral, which we can see on Fig. 6.

Rotation-shrinking stable system in sheared space. Until now we have seen systems with canonical blocks used as matrix $\boldsymbol{A}$. But, as it was already mentioned, the controller becomes greedy when the prediction horizon is limited. Thus, linear transformation of the state-space in form (5–6) can distract it into choosing not the best intermediate aims.

$$x'_k = Px_k, \ k \in \mathbb{Z} \tag{5}$$

$$x'_{k+1} = PAP^{-1}x'_k + PBu_k, \ k \in \mathbb{Z} \tag{6}$$

To demonstrate this effect we transformed the state-space for the system described in Table 2 with shearing matrix (7) and repeated the experiment. Full specification of it, as always, can be seen in Table 6.

$$P = \begin{pmatrix} 1 & 2 \\ 0 & 1 \end{pmatrix} \tag{7}$$

As we can see on Fig. 7, after this transformation the duration loss is not limited, but instead it grows along certain directions, unlike what we see in the example on Fig. 2, Table 2.

Stable system with one real-valued eigenvalue and two generalized eigenvectors. The most interesting results we have when the matrix $\boldsymbol{A}$ is defective, as in example on Fig. 8, Table 7. On the heatmap for stabilization time with unlimited horizon length we can clearly see that initial positive values of the component corresponding to e_1 (which is the ordinary eigenvector of the matrix $\boldsymbol{A}$) compensate for initial negative values of the other component corresponding to e_2 (which is the generalized eigenvector of rank 2 of the matrix $\boldsymbol{A}$). Considering that the heatmaps are point-symmetric, we can also say, that negative values of the former also compensate for positive values of the latter.

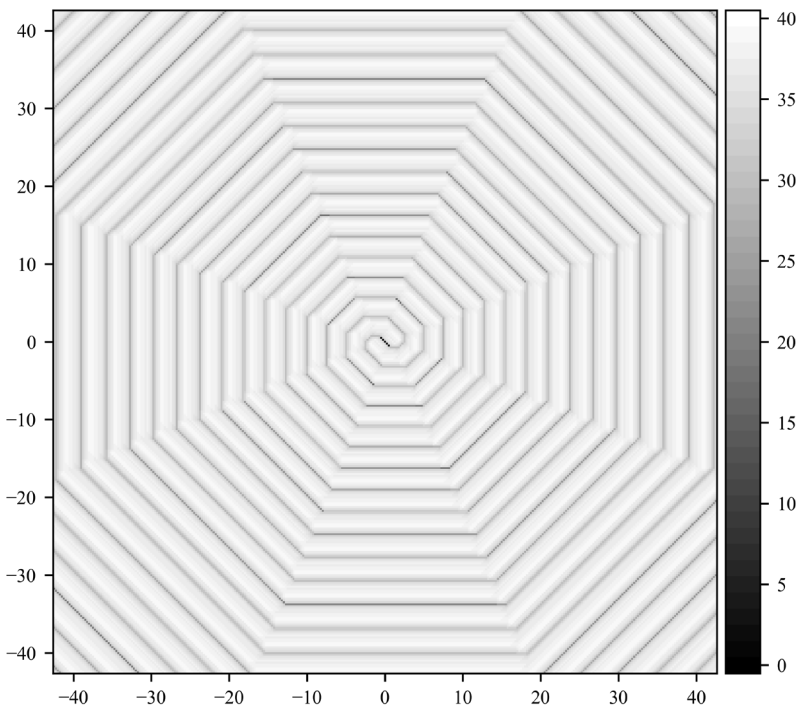

Fig. 6. Stabilization time loss for rotation-shrinking stable system with intertwined control and $s_{\max}$ =1, both half-planes

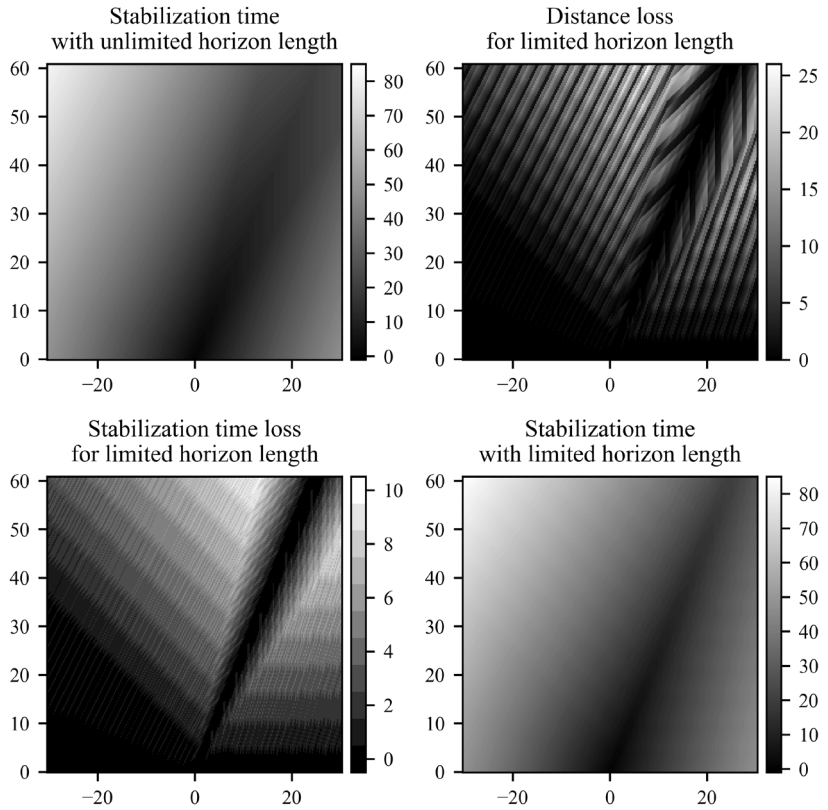

Fig. 7. Index heatmaps for rotation-shrinking stable system in sheared space

Table 6. **Computational experiment input values corresponding to heatmaps on Fig. 7**

Variable	Value	Variable	Value
System		**Plotting parameters**	
$\boldsymbol{A}$	$\begin{pmatrix} 2.1108 & -3.5180 \\ 0.7036 & -0.7036 \end{pmatrix}$	e_1	$\begin{pmatrix} 0 \\ 1 \end{pmatrix}$
$\boldsymbol{B}$	$\begin{pmatrix} 1 & 2 \\ 0 & 1 \end{pmatrix}$	e_2	$\begin{pmatrix} 1 \\ 0 \end{pmatrix}$
$\rho(\boldsymbol{A})$	~0.9950	grid step (g)	1.0

Constraints			
$u_{\max}$	1.0	$s_{\max}$	1

Other significant difference is that, unlike in previous examples, the greediness of the algorithm for limited horizon lengths has significant impact, even though we can directly influence both components of the state-space. Even more, the losses are not limited - they increase indefinitely the further the initial state is from certain "free-fall trajectory", which is clearly visible on the corresponding heatmap, and along which the time loss is zero. Also, the stabilization time (either with or without horizon length limiting) grows the slowest along the same trajectory.

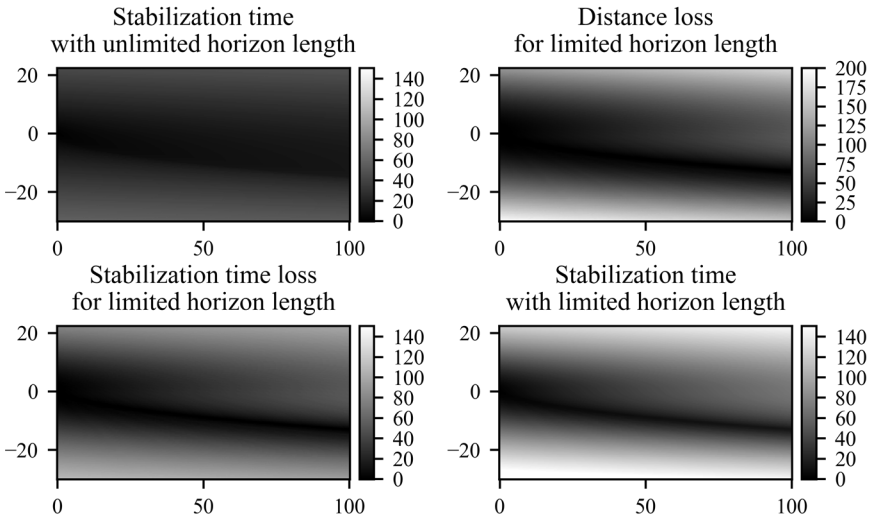

Fig. 8. Index heatmaps for stable system with defective matrix $\boldsymbol{A}$

Table 7. **Computational experiment input values corresponding to heatmaps on Fig. 8**

Variable	Value	Variable	Value
System		**Plotting parameters**	
$\boldsymbol{A}$	$\begin{pmatrix} 0.99 & 1 \\ 0 & 0.99 \end{pmatrix}$	e_1	$\begin{pmatrix} 1 \\ 0 \end{pmatrix}$
$\boldsymbol{B}$	$\begin{pmatrix} 1 \\ 0 \end{pmatrix}$	e_2	$\begin{pmatrix} 0 \\ 1 \end{pmatrix}$
$\rho(\boldsymbol{A})$	0.99	grid step (g)	0.25

Constraints			
$u_{\max}$	1.0	$s_{\max}$	1

This heatmaps are built for $s_{max} = 1$, but the dynamics looks the same for its bigger values, even though the losses' growth becomes somewhat slower.

It is important to note, that in this example we can influence both components of the state-space separately, but this does not help much, like in some previous examples, even though the system is controllable.

Unstable systems. In this subsection unstable systems, e. g. whose matrix $\boldsymbol{A}$ has spectral radius $\rho(\boldsymbol{A})$ bigger than 1, will be discussed. In this case systems can not stabilize themselves.

Moreover, if they are left by themselves without any control, the slightest disturbance can make initially equal to zero system's state trend to infinity. This makes stabilizing control even more important for unstable systems, than for stable ones.

It is well-known, that if the control resources are limited (for example, as in (2)), then for an unstable system there are initial states, for which this system can not be stabilized, e. g. the stabilizing control sequence does not exist. Thus, it is expected that a certain border surface in state-space exist, inside of which stabilization is still possible, while outside of which it is not. These our expectations were corroborated with our

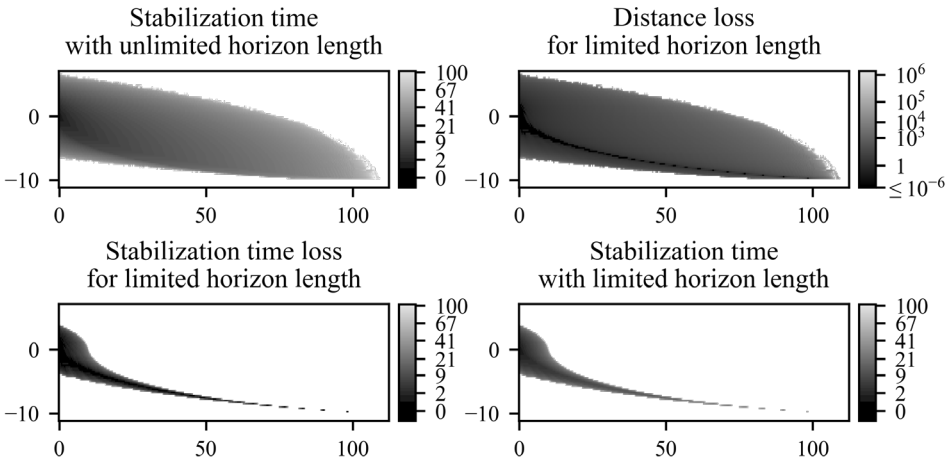

Fig. 9. Index heatmaps for unstable system with defective matrix $\boldsymbol{A}$

Table 8. **Computational experiment input values corresponding to heatmaps on Fig. 9**

Variable	Value	Variable	Value
System		**Plotting parameters**	
$\boldsymbol{A}$	$\begin{pmatrix} 1.1 & 1 \\ 0 & 1.1 \end{pmatrix}$	e_1	$\begin{pmatrix} 1 \\ 0 \end{pmatrix}$
$\boldsymbol{B}$	$\begin{pmatrix} 1 \\ 0 \end{pmatrix}$	e_2	$\begin{pmatrix} 0 \\ 1 \end{pmatrix}$
$\rho(\boldsymbol{A})$	1.05	grid step (g)	0.25

Constraints			
$u_{\max}$	1.0	$s_{\max}$	1

experiment results. The unstable systems demonstrate the same dynamics as equivalent stable ones, except the aforementioned border that can be clearly seen on plots.

When we talk about the border surface, it is natural to imagine it being bounded when projected on those state-space components, which correspond to unstable Jordan matrix's cells. According to results of our computational experiments, this intuition is indeed true, but only for systems with non-defective matrix $\boldsymbol{A}$. If this matrix is defective, then the "free-fall trajectory" similar to ones for stable systems with defective matrix $\boldsymbol{A}$ also exist. But, unlike in stable system, it does not continue indefinitely, which can be clearly seen on Fig. 9, Table 8.

It is also worth noticing that the stabilization time with unlimited horizon length near the boundary starts to increase so abruptly, that with the chosen grid step this growth was captured only by some of its cells near the border, even though not reaching the `huge_s`, which in this particular case was set to 130.

ANALYSIS OF RESULTS

As there is inexhaustible variety of possible linear discrete-time systems which can be defined in form (1–2), we limited the examples shown in the Experiment Result section to those displaying some prominent characteristics of the stabilization process. And now let us discuss our findings.

One of expected and rather obvious effects which was confirmed in this research is that stabilization time improves with increase of the prediction horizon limit if the objective function optimizes distance of the future system's state at the end of the horizon, as it was described in (3). The question was in what cases and to what degree it can be limited without significant losses, and how can the controller be modified to alleviate this losses.

As it was demonstrated in the examples from the Experiment Results section, for some systems losses do not grow indefinitely for initial states further from zero. In these cases a certain rather small horizon length limit can be safely assigned. At the same time, there are examples where this is not the case, and thus we need to consider the area in which initial states of the system are likely to occur. The most noticeable among them are the examples with defective matrix $\boldsymbol{A}$.

A valuable finding upon which we have stumbled is that a particular system's representation (among equivalent ones) has significant impact on efficiency of generated controls under limited prediction horizon. This leads us to a conclusion, that we should transform the system's representation (1) in some way, as it was described in equations (5–6), to get the most efficient controller and to minimize required computational resources at the same time.

As it was demonstrated in our experiments, in some trivial cases the prediction horizon can be limited to impressive one or two steps. Thus, it is tempting to just transform the matrix $\boldsymbol{A}$ into the real-valued modification of the Jordan normal form and transform matrix $\boldsymbol{B}$ accordingly. But the shape of possible controller's impacts on the system's state (the Bu_k part in (1)), which originates from values of matrix $\boldsymbol{B}$ and constraints (2), may (and in many cases — will) make it more optimal to sacrifice stabilization speed of some state's components to speed-up it for others in long term. So, even in this simplified representation the controller with limited prediction horizon may not catch the most fast stabilization trajectory. That is why it is still not obvious which transformation of the state-space would be the most efficient for a particular system.

For the same reason we can't neglect the structure of matrix $\boldsymbol{B}$ and decompose the system into independent subsystems by transforming matrix $\boldsymbol{A}$ into block-diagonal form and using each block as a subsystem's matrix $\boldsymbol{A}$ — this way we would reduce the aforementioned set of possible controller's impacts on the system's state, and thus we would not be able to use its full potential.

The other possible approach is to construct a different objective function, which does not blindly optimize the distance of predicted future system's state at some point of time. It leads us to a question, what the most efficient objective function looks like.

In this research we obtained an instrument to see the very limits of possible improvement of time required for stabilization process. Even though the most simplistic variant of controller was used, it still produces the most optimal stabilizing control sequence possible if we set the prediction horizon to appropriate length and have required computational resources to compute it. It gave us an

opportunity to see how exactly the minimum possible stabilization time change depending on initial system's state. It is valuable to see the limits of what is possible so that we will not waste time trying to do the impossible. It also gave us valuable hints about how to improve stabilization time while not allocating ridiculously big amount of computational resources.

From our observations in the Experiment Results section it becomes obvious, that the most efficient objective function is the one which optimizes the time which will be required to stabilize the system from next intermediate state. And this time is actually plotted on the "Stabilization time with unlimited horizon length" plots throughout the Experiment Results section. As we can see on the plots, this ideal objective function is not convex in most cases. This complicates controller development in various ways. Firstly, with such objective function we no longer can use convex optimization algorithms. Secondly, we need to somehow represent such rather intricate function to work with it. It would also be good to have a relatively fast way to calculate coefficients of this representation from matrices $\boldsymbol{A}$ and $\boldsymbol{B}$, similarly to how we can do it for objective function (3).

Of course, this ideal objective function can be, for example, precomputed for some set of points in state-space and in order to interpolation, but this way the flexibility of digital controllers would be lost because this way the system's model no longer can be fixed on the fly. This is a significant drawback, because in some cases coefficients of the system drift and so we do need to fix the model used in controller.

Thus, the question about computationally-efficient controller which would give the best possible stabilization speed is still open. Thus, we propose to test new variants of controllers in a way described in this paper to have a comprehensive picture of their strong points and limitations. While examples in this paper are, in fact, two-dimensional, this approach can also be extended for systems with more dimensions. We can build heatmaps for different two-dimensional slices of state-space, as it was described in the Experiment Design section. This way we can see more comprehensive picture of stabilization dynamics, than a single slice can give us. Considering all the uncertainties mentioned above, it is advised to do so and not to approximate behavior of more complex systems with behavior of previously explored more simple ones.

CONCLUSIONS

In this paper we proposed a way to appraise and visualize negative effects of prediction horizon length limiting for particular system, objective function and scheme of feedback loop used in controller. We also demonstrated stabilization dynamics for some example systems with distinctive structures in case when the most basic variant of MPC-based feedback loop is used. These observations gave us some valuable insights about the stabilization dynamics with MPC-based controller in general.

It was shown that in many cases the losses from horizon length limiting can grow indefinitely for initial system's states further from zero if the used objective function optimize norm of predicted future state. Nevertheless, at least in some cases this growth can be prevented with certain good state- space transformation. It was also confirmed that for such objective function the losses decrease with increase of the prediction horizon length limit.

As a side result, we were able to plot minimum required stabilization time for various example systems, which can be used as the most efficient objective function if

found. This objective function was shown to have an intricate structure which largely depends on system's structure and representation. In our case the plots of this objective function were obtained with excessive amount of computations, so how to efficiently find and use it in practice remains an open question.

As there is an inexhaustible variety of possible modifications of the MPC-based feedback loop, it is important to have an instrument to analyze how a particular variant performs. The proposed method provides a convenient visualization for this purpose. This way we can compare the already existing stabilization methods and those to be developed with each other and with the very limits of possible performance.

This visualization also gives an opportunity to fine-tune a particular stabilization method and to determine amount of computational resources required for it to achieve required performance.

The proposed visualization also allowed to have a glimpse of how the best possible stabilization performance would look like. While in this work it required an amount of computations inadequate for usage in online controllers, we hope that the obtained results will help in future research in this direction to achieve best possible stabilization times with reasonable computational resources.

REFERENCES

1. Roberts F. Discrete Mathematical Models with Applications to Social, Biological, and Environmental Problems. Englewood Cliffs, Prentice-Hall, 1976. 559 p.
2. Romanenko, V. D., Milyavskiy, Yu. L. Ensuring the sustainability of pulse processes in cognitive maps on the basis of the models in the states space. *System research and information technologies*. 2014. № 1. P. 26–42. (In Russian)
3. Romanenko V.D., Milyavskiy Y.L. Impulse Processes Stabilization in Cognitive Maps of Complex Systems Based on Modal State Regulators. *Kibernetika i vyčislitelnaâ tehnika*. 2015, Iss. 179, pp 60–71. (In Russian)
4. Kailath, T. *Linear systems*. Englewood Cliffs, NJ: Prentice-Hall, 1980
5. Chen, C.-T. *Linear system theory and design.* NY: Oxford University Press. 1999/
6. Gubarev V.F., Mishchenko M.D., Snizhko B.M. Model Predictive Control for Discrete MIMO Linear Systems. In: Kondratenko Y., Chikrii A., Gubarev V., Kacprzyk J. (eds) Advanced Control Techniques in Complex Engineering Theory and Applications. Studies in Systems, Decision and Control, 2019 vol 203. pp 63–81 Springer, Cham. https://doi.org/10.1007/978-3-030-21927-7_4
7. Mishchenko M.D., Gubarev V.F. Methods of Model Predictive Control for Discrete Multi-Variable Systems with Input. *Cybernetics and Computer Engineering*, 2020, 1(199), pp 39–58.
8. Vandenberghe, L. The cvxopt linear and quadratic cone program solvers. March 2010 URL: http://www.ee.ucla.edu/~vandenbe/publications/coneprog.pdf, (Last accessed: 20.12.2020)

Received 24.12.2020

ЛІТЕРАТУРА

1. Roberts F. Discrete Mathematical Models with Applications to Social, Biological, and Environmental Problems. Englewood Cliffs, Prentice-Hall, 1976. 559 p.
2. Романенко В.Д., Милявский Ю.Л. Обеспечение устойчивости импульсных процессов в когнитивных картах на основе моделей в пространстве состояний. *Системні дослідження та інформаційні технології*. 2014. № 1. С. 26–42.
3. Романенко В.Д., Милявский Ю.Л. Стабилизация импульсных процессов в когнитивных картах сложных систем на основе модальных регуляторов состояния *Киб.и выч. техн.*. 2015, Вып. 179, С 60–71.

4. Kailath, T. *Linear systems*. Englewood Cliffs, NJ: Prentice-Hall, 1980
5. Chen, C.-T. *Linear system theory and design.* NY: Oxford University Press. 1999/
6. Gubarev V.F., Mishchenko M.D., Snizhko B.M. Model Predictive Control for Discrete MIMO Linear Systems. In: Kondratenko Y., Chikrii A., Gubarev V., Kacprzyk J. (eds) Advanced Control Techniques in Complex Engineering Systems: Theory and Applications. Studies in Systems, Decision and Control, 2019 vol 203. pp 63–81 S-pringer, Cham. https://doi.org/10.1007/978-3-030-21927-7_4
7. Mishchenko M.D., Gubarev V.F. Methods of Model Predictive Control for Discrete Multi-Variable Systems with Input. *Cybernetics and Computer Engineering*, 2020, 1(199), pp 39–58.
8. Vandenberghe, L. The cvxopt linear and quadratic cone program solvers. March 2010 http://www.ee.ucla.edu/~vandenbe/publications/coneprog.pdf, (Last accessed: 20.12.2020)

Отримано 24.12.2020

Міщенко М.Д.[1], аспірант,
кафедра математичних методів системного аналізу
ORCID: 0000-0001-6135-2569
e-mail: mishenkomihailo@gmail.com
Губарєв В.Ф.[2], д-р. техн. наук, чл.-кор. НАН України,
зав. відд. керування динамічними системами
ORCID: 0000-0001-6284-1866
e-mail: v.f.gubarev@gmail.com
[1] Інститут прикладного системного аналізу,
НТУУ «Київський політехничний інститут імені Ігоря Сікорського»
пр. Перемоги, 37, м. Київ, 03056, Україна,
[2] Інститут космічних досліджень НАН України та ДКА України,
пр. Акад. Глушкова 40, корп. 4/1, Київ, 03187, Україна

ВИБІР ДОВЖИНИ ГОРИЗОНТУ ДЛЯ КЕРУВАННЯ ЗА ПРОГНОЗНОЮ МОДЕЛЛЮ У ЛІНІЙНИХ СИСТЕМАХ З БАГАТЬМА ЗМІННИМИ ТА ВХОДАМИ

Вступ. Є широкий спектр систем, які можуть бути описані як лінійні системи з багатьма змінними та входами, що функціонують у дискретному часі. Ця математична модель часто застосовується в інженерії, але також може бути застосована у багатьох інших сферах. Завдання стабілізації систем такого типу є досить розповсюдженим. У статті розглядається підхід до керування за прогнозною моделлю у розв'язанні цієї задачі. Його головний принцип полягає у генеруванні керуючих сигналів шляхом оптимізації майбутніх станів, у які перейде система внаслідок цих керувань, на обмеженому прогнозному горизонті. Хоча цей підхід демонструє непогані результати, на практиці завжди є обмеження в обчислювальних ресурсах. Через це оптимізувати наслідки майбутньої послідовності керувань є можливим лише на горизонтах обмеженої довжини. Тому важливо розуміти, як це обмеження впливає на якість керування.

Метою статті є запропонувати спосіб оцінювання негативних впливів обмеження прогнозного горизонту до певної довжини для конкретної системи, аби можна було зробити поінформоване рішення щодо цієї максимальної довжини і таким чином вибирати для контролера мікропроцесор з достатньою обчислювальною потужністю.

Методи. Було задано декілька індексів, що характеризують процес стабілізації. Теплові карти їхньої залежності від початкового стану системи використовуються як зручна візуалізація змін динаміки стабілізації системи у залежності від початкового стану, а також негативних впливів, спричинених обмеженням довжини прогнозного горизонту. Такі теплові карти було побудовано для кількох визначних прикладів систем з різними структурами шляхом виконання відповідних обчислювальних експериментів.

Результати. Втрати від обмеження довжини прогнозного горизонту варіюються від значних до повної їх відсутності у залежності від структури системи і її подання. Ці втрати зменшуються, якщо збільшити межу довжини прогнозного горизонту. Проста цільова функція, що мінімізує норму майбутнього стану, дає найкращі результати для таких систем, матриця природнього відгуку яких є діагоналізовною над полем комплексних чисел і є поданою у дійсночисловій Жордановій формі. Інакше результати сильно погіршуються.

Висновки. Динаміка стабілізації суттєво залежить від структури системи. Тому варто брати це до уваги і будувати теплові карти індексів втрат для процесу стабілізації аби визначитись з обмеженням на довжину прогнозного горизонту. Вдале представлення системи може зменшити час стабілізації за умов обмеження на довжину прогнозного горизонту. Також, функція найменшого необхідного часу стабілізації для початкового стану може розглядатись як ідеальна цільова функція, але знаходження цієї функції для конкретної системи є проблематичним.

Ключові слова: *керування за прогнозною моделлю, система з багатьма змінними та входами, теплова карта, синтез керування, дискретна керована система, лінійна система, рухомий горизонт, стабілізація.*

Medical and Biological Cybernetics

DOI: https://doi.org/10.15407/kvt203.01.060

UDC 519.8.812.007

ARALOVA N.I.[1], DSc (Engeniring), Senior Researcher,
Senior Researcher of Optimization of Controlled Processes Department,
ORCID: 0000-0002-7246-2736
e-mail: aralova@ukr.net
KLYUCHKO O.M.[2], PhD (Biology), Associate Professor,
Associate Professor, Faculty of Air Navigation,
ORCID: 0000-0003-4982 7490
e-mail: kelenaXX@nau.edu.ua
MASHKIN V.I.[1], PhD (Engeniring), Senior Researcher,
Senior Researcher of Optimization of Controlled Processes Department,
ORCID: 0000-0002-4479-6498
e-mail: mashkin_v@ukr.net
MASHKINA I.V.[3], PhD (Engeniring), Associate Professor,
Associate Professor, Faculty of Information Technology and Management
ORCID: 0000-0002-0667-5749
e-mail: mashkina@kubg.edu.ua
[1] V.M. Glushkov Institute of Cybernetics of National Academy of Sciences of Ukraine.
40, Acad.Glushkov av., Kyiv, 03680, Ukraine
[2] Electronics and Telecommunications National Aviation University,
1, Lubomyr Huzar av., Kyiv, 03058, Ukraine
[3] Borys Grinchenko Kyiv University,
18/2, Bulvarno-Kudriavska str., Kyiv, 04053, Ukraine

MATHEMATICAL MODEL OF FUNCTIONAL RESPIRATORY SYSTEM FOR THE INVESTIGATION OF HARMFUL ORGANIC COMPOUNDS INFLUENCES IN INDUSTRIAL REGIONS

Introduction. *The areas around industrial objects, and now in regions of military actions are characterized by a high content of pollutants. Qualitative spectrum of these pollutants is extremely broad and contains both inorganic and organic elements and compounds. In particular, environmental pollution is caused by hydrocarbons with wide range of chemical structures, the study of which is very important due to their harmful and toxic influences on living organisms. The methods, currently used in medicine, give only a "thin slice" of current pathological state of organism, but they cannot predict the long-term consequences of such lesions. That is why it seems appropriate to use mathematical models that simulate the*

movement of organic compounds in the respiratory and circulatory systems and thus to predict possible pathologies in organs and tissues caused by hypoxic states that occur when these organs and tissues are affected.

***Purpose of the paper is** to create a mathematical model of functional respiratory system, which simulates the influence of external environment on the parameters of self-organization of human respiratory system in the dynamics of respiratory cycle; and thus to predict hypoxic conditions during tissue damage by hydrocarbons.*

***Results.** The mathematical model for respiratory gases transport and mass transfer in human organism is represented as a system of differential equations, which is a controlled dynamic system, and the states of which are determined by oxygen and carbon dioxide stresses in each structural link of the respiratory system (alveoli, blood, and tissues) at each moment of time. The model is supplemented by the equations of transport of the substances in each structural link as well as by the mathematical model of organism oxygen regimes regulation. The model includes seven groups of tissues - brain, heart, liver and gastrointestinal tissues, kidneys, muscle tissue etc. The algorithm of the work and iterative procedure of research with application of suggested complex are given.*

***Conclusion.** The proposed mathematical model for studying of the transport of organic substances in human organism which consists of differential equations of respiratory gases transport and mass transfer in it, and for the transport of organic compounds is theoretical only for today. However, in the presence of appropriate array of experimental data, it will be able to monitor the state of functional respiratory system after the pathogenic organic compounds inquiry, which may be useful in choosing of strategies and tactics for the treatment of particular lesion.*

***Keywords:** functional respiratory system, regulation of organism oxygen regimes, harmful organic substances, hypoxic state, mathematical model of respiratory system, transport of gases by blood, self-regulation of respiratory system.*

INTRODUCTION

In contemporary reality the great attention is attracted to problems of environmental pollution, and numerus researchers, environmentalists study effects of toxic and harmful environmental substances influence on living organisms. Industrial polluted territories are characterized by high content of contaminating substances, the qualitative spectrum of which is extremely wide, containing both inorganic and organic elements and compounds. Among such environmental chemical pollutants there are hydrocarbons (with linear and/or cyclic structures) for example, the derivatives of phenols with polyamine radicals of different lengths and branches. Such substances were registered among a wide range of environmentally harmful pollutants appeared as a result of industrial objects functioning, as well as damages of chemical plants, contamination of accident sites by fuels and lubricants, consequences of air crashes, fires at objects of oil and gas industries etc. Numerous works are devoted to study of these problems [1, 2], but many questions still are unanswered [2].

Numerical facts of environment industrial pollution with hydrocarbons of wide range of chemical structures were described [1, 2, 3], as well as the facts of their harmful and toxic effects on living organisms. However, the studies of mechanisms of such compounds influences on organisms, details of their physiological effects, results of monitoring of their pressure on organisms over long time periods are absolutely insufficient because of number of reasons. Such reasons are: the great diversity of such compounds in pollutant emissions, their insufficient chemical identification, variability of chemical structures of such compounds over time as a result of their continued chemical transformation in

the environment, other. The grounding of such substances computer identification with further studying was already done [4].

The practice of contemporary science demonstrates that usage of mathematical methods, including the methods of mathematic modeling permits to overcome such difficulties. Such methods have to be used in cases when direct experimental study is or impossible, or rather expensive [5]. The methods existing in medicine for such substances influences studying give only imagination about current pathological state of organism, which, of course, is very important for the treatment of specific lesions, but cannot predict the long-term consequences of such lesions for organism. Therefore, it is advisable to use mathematical models that allow ones to simulate the processes, pathways of organic compounds transportation by respiratory and/or blood circulation systems; and thereby to predict possible pathologies in organs and tissues. In this research we use mathematical model of functional respiratory system [6–8], which is supplemented by the equations of substances transportation in organism [9, 10].

The purpose of the paper is to develop mathematical models to study the influences of organic pollutants (derivatives of aromatic hydrocarbons) on the state of functional systems of living organisms.

Problem of environment pollution by harmful and toxic organic substances in industrial regions. Hydrocarbons are the major component of liquid and gaseous fuels that cause toxic effects on living organisms. Different types of fuels (gasoline, kerosene etc.) differ in their content of paraffin, petroleum and aromatic hydrocarbons [1, 2, 3]. The wastewater of production areas of airports, other aviation industry objects contains benzene, petroleum products that occur damaging effect on organisms of these enterprises service personnel and surrounding population. For example, an increased risk for the health of population was registered within the 10 km wide band surrounding the aviation objects [2]. Hydrocarbons are sources of environmental pollution by carcinogens, the most powerful of which are polycyclic hydrocarbons, as well as aromatic amines, which are products of functioning and emissions of aviation industry, chemical and petrochemical industries [3]. Hydrocarbons are also the components of transport fuels, their quantity is growing in metropolitan areas and, consequently, the risk of related diseases of population is increased in Ukrainian cities [3].

Oil pollution of sewages is especially noticeable in industrial regions, however, the molecular mechanisms of action of these hydrocarbons have not been studied yet [3]. At the same time, it is known that oil and petroleum products are too harmful for water reservoirs in nature (sea, lakes etc.), their physiological toxic effects on living organisms are widely known [1, 2, 3]. The authors tried to investigate effects of such hydrocarbons derivatives, which are parts of the abovementioned pollutants. Namely, the effects of aromatic hydrocarbons influence on organism (phenol derivatives with hydrocarbon radicals of different length and structure) were investigated. In previous works by Klyuchko O.M. was demonstrated that investigated molecular mechanisms of such substances action are common to a broad class of such compounds. In addition, the differences in properties of the action of toxic substances depending on the length of the polyamine radical were demonstrated [4, 5].

It should be noted that the most common of coal products are indene-coumar resins containing chemical compounds with similar structure of molecules. Inden-coumar resins are products of polymerization of non-organic compounds of xylene fraction ($T_{кип} = 160^0 – 180^0$ C): coumarone, indene, styrene and their homologues. These resins are used to increase the stickiness of the rubber mixtures. There are no fundamental differences between such compounds - low molecular weight and high molecular weight polymers [11]. The results obtained by some authors [1–3, 11] can be used to improve the safety of personnel working in coal mining or processing enterprises, chemical plants, places of industrial accidents etc.

Mathematical model of respiratory system. Using a systematic approach to describe the process of mass transfer of respiratory gases in organism, lets imagine the respiratory system in the form of controlled system in which the mass transfer of oxygen, carbon dioxide and nitrogen is going, and the controlling system, which produces certain effects that ensure the normal course of the process of mass transfer of gases. The mathematical model of controlled part of respiratory system is represented by a system of ordinary differential equations that describe the dynamics of oxygen tensions at all stages of its ways in organism.

We represent the mathematical model of the functional respiratory system in following form.

The block diagram of the model is shown in Fig. 1.

Let's denote as pO_2, pCO_2, and pN_2 partial pressures of oxygen, carbon and nitrogen respectively in breathing mixture, taking into account that

$$B = pO_2 + pCO_2 + pN_2, \tag{1}$$

where B is a value of atmospheric pressure.

Lets suppose that $p_{j_{RW}}$, $j = \overline{1,3}$ are the partial pressures of oxygen, carbon dioxide and nitrogen in the respiratory tract, and p_{j_A}, $j = \overline{1,3}$ — in the alveolar space.

Then the equation describing the dynamics of respiratory gases in the respiratory tract can be represented as:

$$\frac{dp_{j_{RW}}}{d\tau} = \frac{\dot{V}}{V_{RW}}(\vec{p}_{j_{RW}} - \overline{p}_{j_A}), \tag{2}$$

where the gas number corresponds to the index j — oxygen, carbon dioxide, nitrogen, V_{RW} — airway volume, $\dot{V}$ — lung ventilation.

$$\dot{V} = \begin{cases} \dfrac{RV \cdot \tau}{T_a} \sin \dfrac{\tau - \tau 0}{T_a} n_i, \textit{during a breathing act (inhalation and expiration)} \\ 0, \textit{during a breathing pause} \end{cases} \tag{3}$$

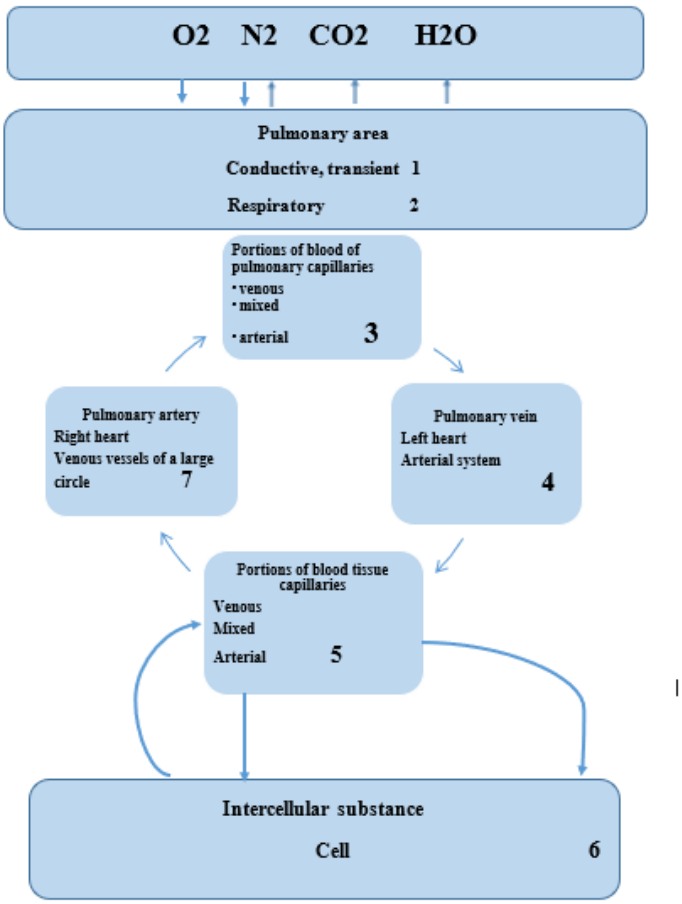

Fig. 1. Block diagram of the model

$$\text{and} \quad p_{jRW} = \begin{cases} p_j, at\, \dot{V} > 0 \\ p_{jRW}, at\, \dot{V} \le 0 \end{cases} \tag{4}$$

$$p_{j_A} = \begin{cases} p_{j_{RW}}, at\, \dot{V} > 0 \\ p_{j_A}, at\, \dot{V} \le 0 \end{cases}, \tag{5}$$

where T_α is the duration of the respiratory act, τ_0 — the time of its onset, RV — the respiratory volume. Using the same principles of material balance and flow continuity, we can write the equation for the dynamics of respiratory gases in the alveolar space:

$$\frac{dp_{j_A}}{d\tau} = \frac{1}{n_j(V_L - V_{RW})}[n_j \cdot p_{j_A} \cdot \widetilde{V} - G_{j_A} - n_j p_{j_A} \frac{dV_L}{d\tau}], \tag{6}$$

where G_{jA} is the flow of gas through the alveolar-capillary membrane, V_L is the lungs' volume, n_j — transfer coefficients. The algebraic analogue of Fick's law is used for G_{jA}:

$$G_{j_A} = k_j \cdot n_j \cdot S \cdot (p_{j_A} - p_{j_{Lc}}), \tag{7}$$

where *k, n* are coefficients of gases permeability through the membrane, *S* — is the surface area of mass transfer.

The peculiarities of mass transfer of gases convectively should be taken into account during obtaining of equations for the transport of respiratory gases by the blood. Oxygen is transported being dissolved in blood plasma as well as being chemically coupled to hemoglobin (*Hb)*; carbon dioxide — being dissolved as well as chemically coupled to hemoglobin and blood buffer bases *(BH);* nitrogen — being only dissolved in blood plasma.

Let suppose that p_aO_2, p_aCO_2, p_aN_2 — are the tensions of respiratory gases in the arterial blood; $p_{\bar{v}}O_2$, $p_{\bar{v}}CO_2$, $p_{\bar{v}}N_2$ — in mixed venous blood, ($p_{Lc}O_2$, $p_{Lc}CO_2$, $p_{Lc}N_2$) — in pulmonary capillary blood; ($p_{ct_i}O_2$, $p_{ct_i}CO_2$, $p_{ct_i}N_2$) — in tissue capillary blood; and ($p_{t_i}O_2$, $p_{t_i}CO_2$, $p_{t_i}N_2$)— in tissue fluid, respectively.

Applying the principles of material balance and continuity of flows, we can obtain the equation for changes of gases tensions in the blood of pulmonary capillaries as follows:

$$\frac{dp_{Lc}O_2}{d\tau} = \frac{1}{V_{Lc}(\alpha_1 + \gamma \cdot Hb \frac{\partial \eta_{Lc}}{\partial p_{Lc}O_2})}[\alpha_1(Q - Q_{sh})(p_a - p_{Lc}O_2) - \tag{8}$$

$$-\gamma \cdot Hb \cdot (Q - Q_{sh})(\eta_{\bar{v}} - \eta_{Lc}) + G_AO_2]$$

$$\frac{dp_{Дc}CO_2}{d\tau} = \frac{1}{V_c(\alpha_2 + \gamma_{BH} \cdot BH \frac{\partial z_{Lc}}{\partial p_{Lc}CO_2} + \gamma \cdot Hb(1 - \eta_{Lc}) \frac{\partial z_{Lc}}{\partial p_{Lc}CO_2})} \cdot \tag{9}$$

$$\cdot[\alpha_2(Q - Q_{sh})(p_{\bar{v}}CO_2 - p_{Lc}CO_2) + G_ACO_2 + (Q - Q_{sh}) \cdot \gamma_{BH} \cdot BH \cdot Q_{t_i} \cdot (z_{\bar{v}} - z_{Lc}) +$$

$$+ (1 - \eta_{Lc}) \cdot \gamma_{BH} \cdot BH \cdot (Q - Q_{sh}) \cdot z_{\bar{v}} - z_{Lc}] + \tag{10}$$

$$\frac{dp_{Lc}N_2}{d\tau} = \frac{1}{V_{Lc}\alpha_3}(\alpha_3(Q - Q_{sh})(p_{\bar{v}}N_2 - p_{Lc}N_2) + G_AN_2),$$

where Q, Q_{sh} — are volumetric rates of systemic circulation and circulation in conditions of the lungs bypass; α_1 α_2 α_3 — are coefficients of gases solubility in the blood plasma; *Hb*, *BH* — hemoglobin and buffer concentrations in the blood; γ, γ_{BH} — are Güfner constants, and the degree of oxygen saturation is determined by the ratios (20)–(23) relatively to the blood of pulmonary capillaries.

The equations of tensions change for gases and studied chemical compounds in the blood of arterial vessels were obtained in the same way. It is necessary to note only that the levels of gases tensions are formed as a result of quick mixing of their flows, coming from the blood of pulmonary capillaries and mixed venous blood with the gases in arterial vessels. That is why

$$\frac{dp_aO_2}{d\tau}=\frac{1}{V_a(\alpha_1+\gamma\cdot Hb\dfrac{\partial\eta_a}{\partial p_aO_2})}[\alpha_1(Q-Q_{sh})p_{Lc}O_2+\gamma\cdot Hb\cdot(Q-Q_{sh})(\eta_{Lc}-\eta_a)+$$
$$+\alpha_1Q_{sh}p_{\bar{v}}O_2]+\frac{1}{V_a(\alpha_1+\gamma\cdot Hb\dfrac{\partial\eta_a}{\partial p_aO_2})}+[\gamma\cdot BH\cdot Q_{sh}\eta_{\bar{v}}-\alpha_1Qp_aO_2-\gamma\cdot BH\cdot q\,\eta_a] \quad (11)$$

$$\frac{dp_aCO_2}{d\tau}=\frac{1}{V_c(\alpha_2+\gamma_{BH}\cdot BH\dfrac{\partial z_a}{\partial p_aCO_2}+\gamma\cdot Hb(1-\eta_a)\dfrac{\partial z_a}{\partial p_aCO_2})}\cdot$$
$$[\alpha_2(Q-Q_{sh}p_{Lc}CO_2)+\alpha_2Q_{sh}p_{\bar{v}}+(Q-Q_{sh})\cdot\gamma_{BH}\cdot BH\cdot Q_{t_i}\cdot(z_{Lc_i}-z_a)+(1-\eta_{Lc})\cdot\gamma_{BH}\cdot \quad (12)$$
$$\frac{(1-\eta_c)\cdot\gamma\cdot Hb\cdot(Q-Q_{sh})\cdot z_{Lc}+(1-\eta_{\bar{v}})\cdot\gamma\cdot Hb\cdot Q_{sh}\cdot\cdot z_{\bar{v}}-(1-\eta_c\cdot\gamma\cdot Hb\cdot Q\cdot z_a}{V_c(\alpha_2+\gamma_{BH}\cdot BH\dfrac{\partial z_a}{\partial p_aCO_2}+\gamma\cdot Hb(1-\eta_a)\dfrac{\partial z_a}{\partial p_aCO_2})}.$$

$$\frac{dp_aN_2}{d\tau}=\frac{1}{V_a\alpha_3}(\alpha_3(Q-Q_{sh})p_{Lc}N_2-\alpha_3\cdot Q_{sh}\cdot p_{\bar{v}}N_2\cdot Q_{t_i}-\alpha_3\cdot Q\cdot p_aN_2) \quad (13)$$

Here is an equation that characterizes the changes in the tensions of respiratory gases in the blood of tissue capillaries and tissue fluid of the organ:

$$\frac{dp_{ct_i}O_2}{d\tau}=\frac{1}{V_{ct_i}(\alpha_1+\gamma\cdot Hb\dfrac{\partial\eta_{ct_i}}{\partial p_{ct_i}O_2})}(\alpha_1Q_{t_i}(p_aO_2-p_{ct_i}O_2)+\gamma\cdot Hb\cdot Q_{t_i}(\eta_a-\eta_{ct_i})-G_{t_i}O_2), \quad (14)$$

$$\frac{dp_{ct_i}CO_2}{d\tau}=\frac{1}{V_{ct_i}(\alpha_{21}+\gamma_{BH}\cdot BH\dfrac{\partial z_{ct_i}}{\partial p_{ct_i}CO_2})}(\alpha_2Q_{t_i}(p_aCO_2-p_{ct_i}CO_2)+ \quad (15)$$
$$+\gamma_{BH}\cdot BH\cdot Q_{t_i}\cdot Hb\cdot Q_tz_a-G_{t_i}CO_2)-(\alpha_2Q_{t_i}-(1-\eta_{ct})\cdot\gamma_{Hb}\cdot Hb\cdot V_{ct\,i}\frac{\partial\eta_{ct\,i}}{\partial\tau})$$

$$\frac{dp_{ct_i}N_2}{d\tau}=\frac{1}{V_{ct_i}\alpha_3}(\alpha_3 Q_{t_i}p_aN_2-\alpha_3 p_{ct_i}N_2\cdot Q_{t_i}-G_{t_i}N_2), \tag{16}$$

$$\frac{dp_{t_i}O_2}{d\tau}=\frac{1}{V_{t_i}(\alpha_1+\gamma_{Mb}\cdot Mb\dfrac{\partial\eta_{t_i}}{\partial p_{t_i}O_2})}(G_{t_i}O_2-q_{t_i}O_2) \tag{17}$$

$$\frac{dp_{t_i}CO_2}{d\tau}=\frac{1}{V_{t_i}\alpha_2}(G_{t_i}CO_2+q_{t_i}CO_2) \tag{18}$$

$$\frac{dp_{t_i}N_2}{d\tau}=\frac{G_{t_i}N_2}{V_{t_i}\alpha_3}, \tag{19}$$

where

$$\eta_{ct_i}=1-1{,}75\exp(-0{,}052m_{ct_i}p_{ct_i}O_2)+0{,}75\exp(-0{,}12m_{ct_i}p_{ct_i}O_2) \tag{20}$$

$$m_{ct_i}=0{,}25(pH_{ct_i}-7{,}4)+1 \tag{21}$$

$$pH_{ct_i}=6{,}1+\lg\frac{BH}{\alpha_2 p_{ct_i}CO_2}, \tag{22}$$

$$z_{ct_i}=\frac{p_{ct_i}CO_2}{p_{ct_i}CO_2+35} \tag{23}$$

α_1, α_2, α_3, α_{1t_i}, α_{2t_i}, α_{3t_i} are solubility coefficients of respiratory gases in blood and tissue fluid; Q_{t_i} — volume circulation velocity in the capillary channel of the tissue reservoir; t_i, V_{ct_i}, V_{t_i} — volume of blood and tissue fluid, respectively.

Tissue blood which partially gave off oxygen and saturated with carbon dioxide, returns to the lungs through circulation. There tissue blood is enriched with oxygen, but left the carbon dioxide during each respiratory cycle. Respiratory gas tension equations for mixed venous blood can be written as:

$$\frac{dp_{\bar{v}}O_2}{d\tau}=\frac{1}{V_{\bar{v}}(\alpha_1+\gamma\cdot Hb\dfrac{\partial\eta_{\bar{v}}}{\partial p_{\bar{v}}O_2})}[\alpha_1(\sum_{ti}Q_{ti}\cdot p_{ct}O_2-Q\cdot p_{\bar{v}}O_2)-\gamma\cdot Hb\cdot Q\cdot\eta_{\bar{v}}], \tag{24}$$

$$\frac{dp_{\bar{v}}CO_2}{d\tau} = \frac{1}{V_{\bar{v}}(\alpha_2 + \gamma_{BH} \cdot BH \frac{\partial z_{\bar{v}}}{\partial p_{\bar{v}}CO_2})}[\alpha_2(\sum_{t_i} Q_{t_i} - Qp_{\bar{v}}CO_2) + (\sum_{t_i} \gamma_{BH} \cdot BH \cdot Q_{t_i} \cdot z_{2ct_i} -$$

$$\gamma_{BH} \cdot BH \cdot Q \cdot z_{2\bar{v}}) + (\sum_{t_i} (1 - \eta_{ct_i}) \cdot \gamma_{Hb} \cdot Hb \cdot Q \cdot z_{\bar{v}} - (1 - \eta_{\bar{v}}) \cdot \gamma_{Hb} \cdot Hb \cdot Q \cdot z_{\bar{v}}) + \quad (25)$$

$$+ \sum_{t_i} \gamma_{Hb} \cdot Hb \cdot V_{ct_i} \frac{\partial \eta_{ct_i}}{\partial \tau}$$

$$\frac{dp_{\bar{v}}N_2}{d\tau} = \frac{1}{V_{\bar{v}}\alpha_3}(\sum_{t_i} \alpha_3 \cdot Q_{t_i} \cdot p_{ct_i}N_2 - \alpha_3 \cdot p_{\bar{v}}N_2 \cdot Q_{t_i}). \quad (26)$$

System (1)–(26) for given $\dot{V}$, Q, Q_t, describes changes in the partial pressures and tensions of respiratory gases in the blood and tissue fluids of organism regions and organs during the respiratory cycle; η is the degree of hemoglobin saturation with oxygen; Q — is volumetric rate of systemic and Q_t — of local blood flows; $q_{t_i}O_2$ — is velocity of oxygen consumption by *i*-th tissue reservoir; $q_{t_i}CO_2$ — is velocity of carbon dioxide emission in *i*-th tissue reservoir. Velocities $G_{t_i}O_2$ of oxygen flow from the blood into the tissue and $G_{t_i}CO_2$ — of the carbon dioxide from the tissue to the blood are determined by the ratio

$$G_{t_i} = D_{t_i}S_{t_i}(p_{ct_i} - p_{t_i}), \quad (27)$$

where D_{t_i} — coefficients of gas permeability through the aerohematic barrier, S_{t_i} is area of the surface of gas exchange.

The task of optimal control. The purpose of control [12] is to output the perturbed system to a steady state mode, where following relations are true:

$$|G_{t_i}O_2 - q_{t_i}O_2| \le \varepsilon_1, \quad |G_{t_i}CO_2 + q_{t_i}CO_2| \le \varepsilon_2, \quad (28)$$

where, ε_1 and ε_2 are sufficiently small positive numbers that were stated in advance. In this case, the control parameters are in limits:

$$0 \le \dot{V} \le \dot{V}_{\max}, \; 0 \le Q \le Q_{\max}, \; 0 \le Q_{t_i} \le Q, \; \sum_{i=1}^{m} Q_{t_i} = Q, \quad (29)$$

where m — is the number of tissue reservoirs in organism.

In addition, to resolve the conflict situation between the executive organs of regulation (respiratory muscles, cardiac muscles and smooth muscles of vessels), being at that time consumers of oxygen, and other tissues and organs, following relations were suggested

$$q_{resp.m}O_2 = f(V)\ q_{card.m}O_2 = \varphi(Q)\ q_{smooth.m}O_2 = \psi(Q)\,. \tag{30}$$

We consider following functional as a criterion for regulation

$$I = \min_{\substack{0\le \dot V \le \dot V_{\max} \\ 0\le Q_{t_i} \le Q_{\max}}} \int_{\tau_0}^{T} [\rho_1 \sum_{t_i} \lambda_{t_i} (G_{t_i}O_2 - q_{t_i}O_2)^2 + \rho_2 \sum_{t_i} \lambda_{t_i} (G_{t_i}CO_2 + q_{t_i}CO_2)^2]d\tau\,, \tag{31}$$

where τ_0 is moment of the start of perturbated influence on the system, T is the duration of this effect, ρ_1 and ρ_2 — the coefficients characterizing the sensitivity of individual organism to hypoxia and hypercapnia, λ_{t_i} are coefficients reflecting the morphological features of the individual tissue reservoir i, $i = \overline{1,m}$.

Such control minimizes the total oxygen consumption in organism and in each tissue region, as well as accumulation of carbon dioxide.

Mathematical model of studied substances transport in organism. Let's denote $c_{f_{rw}}$ as concentration of organic substance in respiratory tract (in moles), and as d_f — its dose, then the equation of the dynamics of respiratory gases in the respiratory tract (1)–(31) should be supplemented by the equations of studied organic compound concentration [8–10]:

$$\frac{dc_{f_{RW}}}{d\tau} = \frac{\dot V}{V}(\tilde c_{f_{RW}} - \tilde c_{f_A}) \tag{32}$$

$$\tilde c_{f_{RW}} = \begin{cases} \xi d_f, \xi = 1, with\ inhalation of\ the\ drug (\dot V > 0) \\ \xi = 0, in\ the absence of\ inhalation during\ a\ respiratory\ break\ (\dot V > 0) \\ \tilde c f_{RW}, at\ \dot V \le 0 \end{cases} \tag{33}$$

$$\tilde c f_A = \begin{cases} c f_{RW}\ npu\ \dot V > 0 \\ c f_A\ npu\ \dot V \le 0 \end{cases}. \tag{34}$$

The level p_AO_2, p_ACO_2, p_AN_2 as well as c_{f_A} in alveolar space is formed due to the mixing of the gases and dispersion of studied organic compounds coming from the airways into the alveoli with those ones that are present in the alveolar space, and taking into account the flows of gases and chemical substances through the alveolar-capillary membrane. Then the equation of the dynamics of respiratory gases in the alveolar space (6) should be supplemented by the equations

$$\frac{dc_{f_A}}{d\tau} = \frac{1}{V_L}(\tilde{c}_{f_A}(\tau)\dot{V} - G_{f_A} - c_{f_A}\frac{dV_L}{d\tau}) \tag{35}$$

$$G_{j_A} = D_j S(p_{f_A} - p_{j_{lc}}) \tag{36}$$

$$G_{f_A} = D_f S(c_{f_A} - c_{j_{lc}}), \tag{37}$$

where D_j, are coefficients of permeability of gases and studied organic compound through the alveolar-capillary membrane with the surface area S

It should be noted that respiratory gases are transported by the blood in different ways: being dissolved in blood plasma and chemically bound to hemoglobin (*Hb*) carbon dioxide in dissolved plasma and chemically bound to bicarbonate compounds (*BH*); nitrogen is transported in dissolved form only. We assume that studied organic compound is transported in the blood too.

Using the principles of material balance and continuity of flow it is possible to obtain the equations of changes in gases tensions and concentrations of studied organic molecules in the blood of pulmonary capillaries, supplementing equations (8)–(10) by the equation

$$\frac{dc_{f_{lc}}}{d\tau} = \frac{1}{V_{lc}}((Q - Q_{sh})(c_{f_{\bar{v}}} - c_{f_{lc}}) - G_{f_A}. \tag{38}$$

The equations of tensions changes of respiratory gases and studied organic compound in the blood of arterial vessels can be written in the same way. Only it should be taken into account that the levels of gases tensions and concentrations of studied organic compounds can be formed as a result of instantaneous mixing of streams coming from the blood of pulmonary capillaries and mixed venous blood with gases and substance in arterial vessel. Then equations (11)–(13) for portions of arterial blood have to be supplemented by the equation.

$$\frac{dc_{f_a}}{d\tau} = \frac{1}{V_a}((Q - Q_{sh})c_{f_{lc}} + Q_{sh}c_{f_{\bar{v}}} - Qc_{f_a}. \tag{39}$$

The arterial blood flow branches to the microcirculatory networks of organs and tissues. The classical mathematical model of mass transfer and mass exchange of respiratory gases describes the dynamics of tensions of respiratory gases in ***m*** tissue reservoirs among which, as a rule, there are tissues of the brain, kidneys, liver, gastrointestinal tract, cardiac and skeletal muscles, bone and fat tissues. The structure of tissue reservoir is described usually as “Krog cylinder” whose axis is a generalized capillary. Equations (14)–(16) describing changes in tensions of respiratory gases in the blood washing the tissue, and in the tissue fluid of the reservoir can be supplemented by following equations of studied substances’ concentrations for the blood of tissue capillaries:

$$\frac{dc_{f_{ct_i}}}{d\tau} = \frac{1}{V_{ct_i}}(Q_{t_i}(c_{f_a} - c_{f_{ct_i}}) - G_{f_{t_i}}) \tag{40}$$

and for tissue fluid we supplement equations (16)–(18) with the expression

$$\frac{dc_{f_{t_i}}}{d\tau} = \frac{G_{f_{t_i}}}{V_{t_i}}, \tag{41}$$

where

$$G_{f_{t_i}} = D_{f_{t_i}} S_{t_i}(c_{f_{ct_i}} - c_{f_{t_i}}). \tag{42}$$

During the development of mathematical model for the transport and mass exchange of respiratory gases and aromatic derivatives, it was assumed that this substance does not participate directly in the metabolic processes.

In the venous vessels, the blood from organs and tissues is mixed and transported to the lungs for oxygen enrichment. Therefore, the equations for respiratory gases transport in mixed venous blood (24)–(26) are supplemented by the equation of concentration of the substance

$$\frac{dc_{f_v}}{d\tau} = \frac{1}{V_{\bar{v}}}(\sum_{t_i} Q_{t_i} c_{f_{t_i}} + c_{f_a} Q_{f_{t_i}} - Q c_{f_v}). \tag{43}$$

It is assumed that the excretion of organic compounds f from organism is carried out through the kidneys. The changes in concentrations of this compound f in the renal tissue are determined by the equation

$$\alpha_{f_i} V_{t_i} \frac{dc_{f_{t_i}}}{d\tau} = G_{f_{i_i}} - \alpha_{t_i} Q_f c_{t_i}, \tag{44}$$

where Q_f is velocity of the liquid filtration. It was assumed that the value of volumetric filtration rate was 0, 035 mg / s.

Then the iterative procedure for studying the effect of organic matter on the human respiratory system can be represented as follows (Fig. 2).

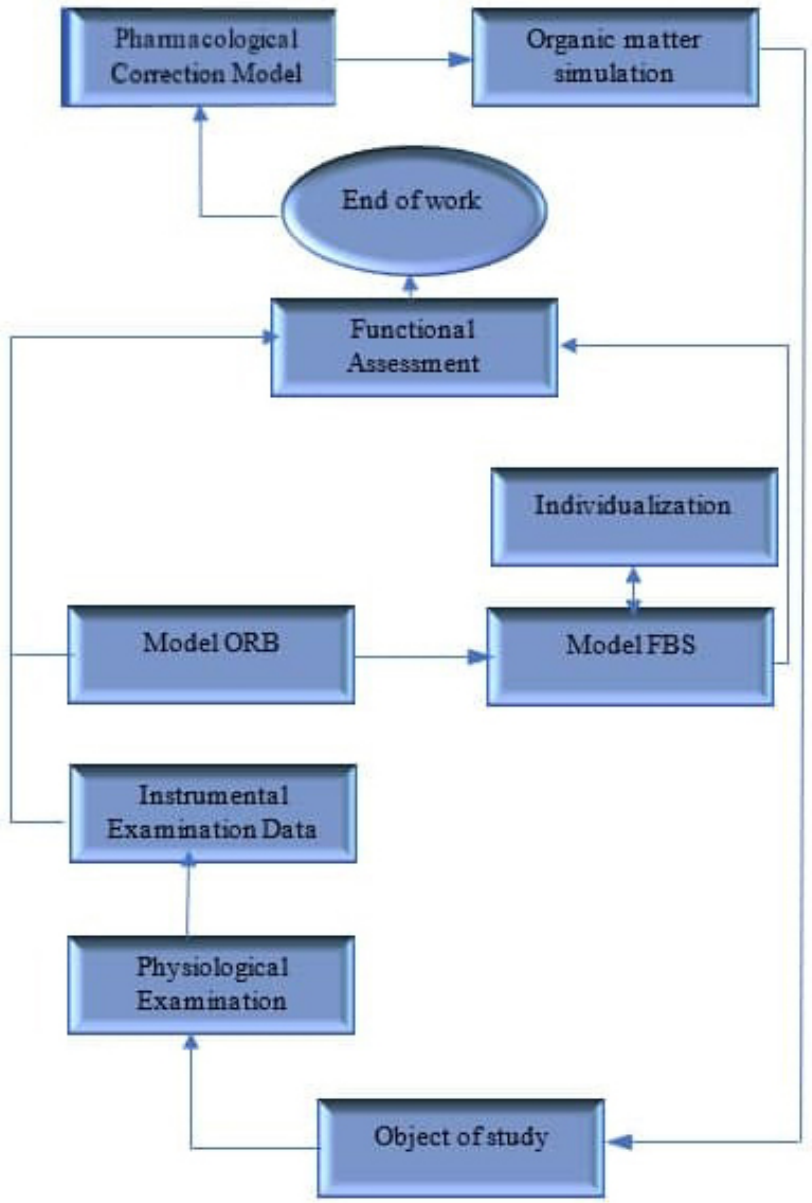

Fig. 2. Iterative procedure for studying the effect of organic matter on the human respiratory system

The iterative procedure for applying the proposed software package in this case will be:

1. An instrumental examination of the patient is carried out. We get data on lung ventilation, composition of the alveolar and exhaled air, respiratory rate, blood pressure, heart rate, hemoglobin, blood acidity etc., which are the source for the model of oxygen regimes of the body (ORB)[8, 13–15].

2. Based on the data of instrumental examination, we calculate indicators such as minute volume of respiration, minute volume of blood, rate of oxygen

consumption by the body, profitability, intensity and effectiveness of oxygen modes of the body, data characterizing the hypoxic state.

3. The data of instrumental examination and part of the data obtained in the calculation of the oxygen regimes of the body are used as the source for the model of respiratory gas transport. Thus, individualization of the model is carried out.

4. We simulate the introduction of organic matter into the body of a particular person on an individualized model [8, 16]. We obtain the values of the stresses of oxygen and carbon dioxide in the tissues of individual organs, which allow us to judge the degree of tissue hypoxia and get information about the state of seven groups of tissues represented in the mathematical model.

CONCLUSIONS

Proposed mathematical model for studying of organic compounds transport in human organism, consisting from the equations of mass transfer and mass exchange of respiratory gases, mathematical model of self-organization of respiration functional system and equations of substances transport in the systems of respiration and circulation have only theoretical value for today. However, in case of obtaining of experimental data array, these models will allow to monitor the state of respiratory system and blood circulation when harmful organic compounds enter the human organism. Presented models will allow the physicians to optimize the strategy and tactics of medical treatment.

REFERENCES

1. Isayenko V.M., Lisichenko G.V., Dudar T.V., Franchuk G.M. et al. Monitoring and methods of measuring the parameters of the environment. Kyiv: NAU-druck. 2009, 312 p. (In Ukrainian)
2. Franchuk G.M., Zaporozhets O.A., Arkhipova G.I. Urban ecology and technoecology. Kyiv: NAU-druck. 2011, 496 p. (In Ukrainian)
3. Franchuk G.M. Isayenko V.M. Ecology, aviation and space. Kyiv. NAU-druck. 2005, 456 p. (In Ukrainian)
4. Klyuchko O.M., Biletsky A.Ya. Computer recognition of chemical substances based on their electrophysiological characteristics. *Biotechnologia Acta*, 2019 (12), N 5, pp. 5–28.
5. Klyuchko O.M. Information and computer technologies in biology and medicine. Kyiv: NAU-druck. 2008. 252 p. (In Ukrainian)
6. Onopchuk Yu.N. Homeostasis of functional respiratory system as a result of intersystem and system-medium informational interaction. *Bioecomedicine. Uniform information space* /Ed. by V.I. Gritsenko. Kyiv. 2001, pp. 59–84 (In Russian)
7. Onopchuk Yu.N. Homeostasis of the functional circulatory system as a result of intersystem and system-medium informational interaction. *Bioecomedicine. Uniform information space* / Ed. by V.I. Gritsenko. Kyiv. 2001, pp. 85–104 (In Russian)
8. Aralova N.I. Mathematical models of functional respiratory system for solving the applied problems in occupational medicine and sports. Saarbrücken: LAP LAMBERT Academic Publishing GmbH&Co, KG. 2019, 368 p.
9. Lyashko N.I., Onopchuk G.Yu. Pharmacological correction of organism states. Mathematical model and its analysis. *Computer mathematics.* 2005. N 1. P. 127–134 (In Russian)
10. Aralova N.I.Information Technologies of Decision Making Support for Rehabilitation of Sportsmen Engaged in Combat Sports **DOI:** 10.1615/JAutomatInfScien.v48.i6.70 pages 68–78.
11. Maslenikova L.D., Ivanov S.V., Fabulyak F.G. et al. Physical chemistry of polymers. Kyiv: NAU-druck. 2009. 312 p. (In Ukrainian)
12. Polynkievich K.B., Onopchuk Yu.N. Conflict situations during the regulation of the main function of organism respiratory system and mathematical models of their resolution.*Cybernetics*.1986. No. 3. P. 100–104 (In Russian)

13. Aralova A.A., Aralova N.I., Klyuchko O.M., Mashkin V.I., Mashkina I.V. Information system for the examination of organism adaptation characteristics of flight crews' personnel. *Electronics and control systems.* 2018. 2. P. 106–113. DOI: 10.18372/1990-5548.52.11882
14. Klyuchko O.M., Aralova N.I., Aralova A.A. Electronic automated work places for biological investigations *Biotechnologia Acta.* 2019. V. 12. № 2. P. 5–26
15. Onopchuk Yu.N., Aralova N.I., Beloshitsky P.V., Podlivaev B. A., Mastucash Yu. I. Forecasting of wrestler' state in the combat on the base of mathematic model of functional respiratory system. *Computer mathematics*. 2005. № 2. P. 69–79 (In Russian)
16. Aralova N.I., Shakhlina L.Ya.-G., Futornyi S.M., Kalytka S.V. Information Technologies for Substantiation of the Optimal Course of Interval Hypoxic Training in Practice of Sports Training of Highly Qualified Sportswomen. 2020. *Journal of Automation and Information Sciences* DOI: 10.1615/JAutomatInfScien.v52.i1.50 pages 41–55.

Received 04.11.2020

ЛІТЕРАТУРА

1. Ісаєнко В. М., Лисиченко Г. В., Дудар Т. В., Франчук Г. М. та ін. Моніторинг і методи вимірювання параметрів навколишнього середовища. Київ: НАУ-друк. 2009. 312 с.
2. Франчук Г. М., Запорожець О. А., Архіпова Г. І. Урбоекологія і техноекологія. Київ: НАУ-друк. 2011. 496 с.
3. Франчук Г. М., Ісаєнко В. М. Екологія, авіація і космос. Київ: НАУ-друк. 2005. 456 с.
4. Klyuchko O.M., Biletsky A.Ya. Computer recognition of chemical substances based on their electrophysiological characteristics. *Biotechnologia Acta*, 2019 (12). N 5. P. 5–28.
5. Ключко О.М. Інформаційно-комп'ютерні технології в біології та медицині. Київ: НАУ-друк. 2008. 252 с.
6. Онопчук Ю.Н. Гомеостаз функциональной системы дыхания как результат внутрисистемного и системно-средового информационного взаимодействия. *Биоэкомедицина. Единое информационное пространство* /ред. В.И. Гриценко. К.:Наук.думка. 2001. С. 59–81.
7. Онопчук Ю.Н. Гомеостаз функциональной системы кровообращения как результат внутрисистемного и системно-средового информационного взаимодействия. *Биоэкомедицина. Единое информационное пространство.*Ред. В.И. Гриценко. К.:Наук.думка. 2001. С. 82–104.
8. Аралова Н.И. Математические модели функциональной системы дыхания для решения прикладных задач медицины труда и спорта. Saarbrücken: LAP LAMBERT Academic Publishing GmbH&Co, KG. 2019. 368 с. ISBN 978-613-4-97998-6
9. Ляшко Н.И., Онопчук Г.Ю. Фармакологическая коррекция состояний организма. Математическая модель и ее анализ. *Компьютерная математика.* 2005. № 1. С. 127–134.
10. Aralova N.I.Information Technologies of Decision Making Support for Rehabilita tion of Sportsmen Engaged in Combat Sports **DOI:**10.1615/JAutomatInfScien.v48.i6.70 pages 68–78
11. Масленнікова Л. Д., Іванов С. В., Фабуляк Ф. Г. та ін. Фізико-хімія полімерів. Київ: НАУ-друк. 2009. 312 с.
12. Полинкевич К.Б., Онопчук Ю.Н. Конфликтные ситуации при регулировании основной функции системы дыхания организма и математические модели их разрешения. *Кибернетика*. 1986. 3. С. 100–104.
13. Aralova A.A., Aralova N.I., Klyuchko O.M., Mashkin V.I., Mashkina I.V. Information system for the examination of organism adaptation characteristics of flight crews' personnel**.** *Electronics and control systems.* 2018. 2. P. 106–113. DOI: 10.18372/1990-5548.52.11882
14. Klyuchko O.M., Aralova N.I., Aralova A.A. Electronic automated work places for biological investigations *Biotechnologia Acta.* 2019. V. 12. № 2. P. 5–26
15. Онопчук Ю.Н., Аралова Н.И., Мастыкаш Ю.И., Подливаев Б.А., Белошицкий П.В. Прогнозирование состояния борца в процессе поединка на основе математической модели функциональной системы дыхания. *Компьютерная математика. 2*005. № 2. С. 69–79.

16. Aralova N.I., Shakhlina L.Ya.-G., Futornyi S.M., Kalytka S.V. Information Technologies for Substantiation of the Optimal Course of Interval Hypoxic Training in Practice of Sports Training of Highly Qualified Sportswomen. 2020. *Journal of Automation and Information Sciences* DOI: 10.1615/JAutomatInfScien.v52.i1.50 pages 41–55

Отримано 04.11.2020

Аралова Н.І.[1], д-т.техн.наук,
старш. наук. співроб. відд. оптимізації керованих процесів,
ORCID: 0000-0002-7246-2736
mail: aralova@ukr.net
Ключко О.М.[2], канд.біол.наук, доцент,
доцент фак-ту аеронавігації,
ORCID: 0000-0003-4982 7490
mail: kelenaXX@nau.edu.ua
Машкін В.Й.[1], канд.техн.наук, старш. наук. співроб.,
старш. наук. співр. відд. оптимізації керованих процесів,
ORCID: 0000-0002-4479-6498
mail: mashkin_v@ukr.net
Машкіна І.В.[3], канд.техн.наук, доцент,
доцент факультету інформаційних технологій та менеджменту,
ORCID: 0000-0002-0667-5749
mail: mashkina@kubg.edu.ua
[1] Інститут кібернетики імені В.М. Глушкова НАН України
пр. Глушкова, 40, Київ, 03680, Україна
[2] Інститут електроніки і телекомунікацій Національного авіаційного університету,
пр. Л. Гузара, 1, Київ, 03058, Україна
[3] Київський університет імені Бориса Грінченка
вул. Бульварно-Кудрявська, 18/2, Київ, 04053, Україна

МАТЕМАТИЧНА МОДЕЛЬ ФУНКЦІОНАЛЬНОЇ СИСТЕМИ ДИХАННЯ ДЛЯ ДОСЛІДЖЕННЯ ВПЛИВУ ШКІДЛИВИХ ОРГАНІЧНИХ СПОЛУК У ПРОМИСЛОВИХ РЕГІОНАХ

Вступ. Території навколо промислових об’єктів, а натепер і в місцях проведення бойових дій характеризуються підвищеним вмістом сполук-забруднювачів, якісний спектр яких є надзвичайно широким та містить як неорганічні, так і органічні елементи та сполуки. Зокрема, відбувається забруднення атмосфери вуглеводнями широкого спектру хімічної будови, дослідження яких є дуже важливим внаслідок їхньої токсичної дії на живі організми. Методики, які наразі застосовують в медицині, дають лише деякий зріз поточного патологічного стану організму, проте не можуть прогнозувати довготермінові наслідки такого ураження. Саме тому видається доцільним застосувати математичні моделі, які дають змогу імітувати процес пересування органічної сполуки системою дихання та кровообігу і тим самим прогнозувати можливі патології в органах та тканинах, спричинені гіпоксичним станом, який виникає внаслідок ураження цих органів та тканин.

Мета. Побудувати математичну модель функціональної системи дихання, яка імітує вплив зовнішнього середовища на параметри самоорганізації системи дихання людини в динаміці дихального циклу і таким чином дає змогу прогнозувати гіпоксичні стани внаслідок ураження тканини вуглеводнями.

Результати. Надано математичну модель транспорту та масообміну респіраторних газів в організмі людини як систему диференційних рівнянь, яка є керованою динамічною системою, стани якої визначаються у кожен момент часу рівнями напруження кисню та вуглекислого газу в кожній структурній ланці системи дихання (альвеолах, крові, тканинах). Модель доповнено рівняннями транспорту речовини у кожній структурній ланці і математичною моделлю регулювання кисневих режимів організму.

У моделі передбачено сім груп тканин — тканини мозку, серця, печінки та ШКТ, нирок, м'язові тканини тощо. Наведено алгоритм роботи та ітераційну процедуру дослідження із застосуванням запропонованого комплексу.

Висновки. Запропонована математична модель для вивчення транспорту органічних речовин в організмі людини, яка складається з диференційних рівнянь транспорту та масообміну респіраторних газів в організмі людини і транспорту органічної сполуки, наразі має лише теоретичний характер. Проте за наявності відповідного масиву експериментальних даних вона надасть можливість відстежити стан функціональної системи дихання у разі потрапляння патогенних органічних сполук, що може виявитися корисним для вибору стратегії та тактики лікування конкретного ураження організму.

Ключові слова: *функціональна система дихання, регулювання кисневих режимів організму, шкідливі органічні речовини, гіпоксичний стан, математична модель системи дихання, транспорт газів кров'ю, саморегуляція системи дихання.*

DOI: https://doi.org/10.15407/kvt203.01.077

УДК 004.75+004.932.2:616

KRYVOVA O.A., Researcher,
Medical Information Systems Department
ORCID: 0000-0002-4407-5990
e-mail: ol.kryvova@gmail.com
KOZAK L.M., DSc (Biology), Senior Researcher,
Leading Researcher of the Medical Information Systems Department
ORCID: 0000-0002-7412-3041
e-mail: lmkozak52@gmail.com
International Research and Training Center for Information Technologies
and Systems of the National Academy of Sciences of Ukraine
and Ministry of Education and Science of Ukraine,
40, Acad. Glushkov av., Kyiv, 03187, Ukraine

INFORMATION TECHNOLOGY FOR CLASSIFICATION OF DONOSOLOGICAL AND PATHOLOGICAL STATES USING THE ENSEMBLE OF DATA MINING METHODS

Introduction. *The digital technologies implementation provides registration of large amounts of bio-medical data (ECG, EEG, electronic medical records) as a basis for assessing and predicting the patients` condition. Data Mining methods allow to identify the most informative indicators and typological groups, to classify the person` functional state and the patients` disease stages to predict their changes.*

The purpose *of the paper is to develop information technology for the classification of human health states using an set of Data Mining methods and to carry out its validation on examples of a operators` functional state and patient's disease severity.*

Results. *The developed IT unites several stages: I — data pre-processing; II — clustering, selecting the homogeneous groups (data segmentation); III — predictors` identification; IV — classifying the studied states, development of predictive models using machine learning algorithms (Decision trees, Support vector machines, neural networks) and the method cross-validation. The proposed IT was used to classify the operators` functional state and the patients` severity in case of disease progression.*

Conclusions. *The IT use to assess the operators` activity successes made it possible to identify the most informative HRV indicators, changes in which can predict the operators` reliability, taking into account the type of vegetative regulation. Assessing the disease activity of children with dysplasia with IT use made it possible to identify diagnostic markers of CCC and develop diagnostic rules for determining the stages of the disease by ECG parameters (T wave symmetry, an integral indicator of the ST_T segment shape).*

Keywords: *information technology, Data Mining, machine learning models, severity of the patient.*

INTRODUCTION

At the current stage of digital medicine development, accompanied by the use of multifunctional monitoring systems, individual mobile health monitoring devices, there is a problem of interpretation of untreated primary arrays of heterogeneous medical data. One approach to solving it is to develop and apply information technology using Data Mining methods. The basic definition of Data Mining is the process of identifying patterns in data arrays (previously unknown) and using them to predict health states and make decisions [1].

In recent years, more and more researches have been done to improve patients' health. Multilevel schemes are developed, which use different types and methods of adaptive learning and combine various sources of clinical information (EHR, laboratory data, monitors, medical images). In recent decades, researchers have noted that the direction of Data Mining application and machine learning methods, namely the patients' classification into risk groups to predict treatment outcomes, mortality, disease stages etc., was formed [2–10]. Analysis of the literature data for 2008–2019 leads to the conclusion that in terms of accuracy and clarity of the results the intellectual analysis methods, which integrate hybrid methods and previous models of clinical risk stratification, should be prefered [11].

PROBLEM STATEMENT

In the early 2000s, examples of successful use of Data Mining for biomedical data analysis appeared [2]. The research was mainly aimed at improving the diagnostic accuracy of the diseases identification by medical databases [3] and at developing the decision support systems [4] and diferent studies by medical and biological information [8].

Different types of machine learning methods are used to develop classification diagnostic models: logistic regression, decision tree methods, random forest (RF), support vector machine (SVM) or ensembles of classification models, genetic algorithms, artificial neural or deep learning networks [4–7].

Among the growing number of works on the application of Data Mining and machine learning technologies, the trend of the clinical direction of predictive models, which use new multi-sensory, multi-resource and multiprocessor information merging schemes, stands out. The architecture of such systems consists of hybrid multilevel schemes, combines uncontrolled and controlled teaching methods and methods of features selection. This approach makes it possible to identify clinically significant patterns using data of monitoring, clinical measures, tools and treatment outcomes [9–11].

For almost 30 years, more than twenty classical tools (systems) for assessing and forecasting the patients' condition have been developed and updated [12–16]. Among them are severity scores, which quantitatively or qualitatively determine the severity of the patient's condition and classify him into specific risk group based on the analysis of deviations of anatomical, physiological, biochemical parameters. Determining the severity of the condition the decision to hospitalize the patient in the intensive care unit can be made. For example, in intensive care units in the United States and the EC use scoring systems to assess the patients' condition. These are several scales: Simplified Acute Physiology Score (SAPS II) [14], Acute

Physiology and Chronic Health Evaluations (APACHE II and III) [15], Mortality Probability Models (MPM II-24) [16]. In addition to standardized scales designed for the general population, a number of specialized scales have been developed to assess the activity (stages, severity) of individual diseases.

A number of studies on the stratification of patients into risk groups according to clinical data and treatment outcomes have demonstrated the superiority of models developed by Data Mining methods over classical scales [17–19].

Much attention is paid to the choice of informative characteristics for the analysis of prenosological and pathological human conditions. Many researchers have determined that the cardiovascular system (CVC) is one of the main indicators of adaptive capacity and responses of the whole organism [20, 21].

One of the most common methods of studying the mechanisms of regulation of the cardiovascular system is the analysis of heart rate variability, which has become a reliable and powerful tool for research in cardiology, assessment of human functional status (FS) [21]. It is proved that the adaptive reactions of the heart to constantly changing physiological conditions are reflected in changes in heart rate variability, which provides information about the systemic reactions of the body during deteriorating health and under the influence of external stress. It is the CVS functioning level that can determine the boundary between the prenosological state (health) and the disease, as well as affect the disease severity.

Methods of HRV analysis are being actively developed [21–29], the technology of analysis is being improved, mathematical approaches to the analysis of nonlinear dynamics of heart rhythm are involved, which has expanded the list of informative indicators for assessing the human condition. Currently, studies of this condition (norm and pathology) are carried out using estimates of irregularity and chaotic rhythm, such as fractal dimension, entropy parameters [27]. The following approaches are proposed for use: wavelet transform [28], the method of multispectral analysis of CVC [29], analysis in the phase plane [23, 24]. Thus, one of the common and effective approaches to detecting changes in human health is to assess the relationship of this condition with the CVS state, which allows to determine functional changes in physiological systems, identify the boundary between prenosological state (health) and disease, as well as affect the disease severity.

The purpouse of the paper is to develop information technology for the classification of human health using sets of Data Mining methods by objective and expert characteristics.

DEVELOPMENT OF INFORMATION TECHNOLOGY FOR CLASSIFICATION OF FUNCTIONAL CONDITION AND HEALTH STATE

Large amounts of information, the need for it adequate analysis with the possibility of further forecasting and planning of appropriate activities necessitate the development and application of new technologies for assessing the current state of both individual health and population health of Ukraine on objective and expert indicators.

Note the effectiveness of the use of Data Mining methods to determine the risk groups according to clinical data, to assign patients to the appropriate group by health markers with further prediction of its changes and evaluation of the effectiveness of treatment. We have developed a method for detecting markers of the cardiovascular system state, which is based on Data Mining models,

which are based on the analysis of heart rate variability (HRV) [30]. The development of the method takes into account the experience of using the constructed Data Mining models to determine population health clusters that are homogeneous in terms of medical and demographic indicators [31].

We have formed an ensemble of Data Mining methods, developed a research scheme that uses a combination of filtering methods, cluster analysis algorithms (*k*-means, EM) and classification (Decision Trees, Neural networks, SVM) using informative ECG features. The application of these methods makes it possible to combine the possibilities of solving specific tasks at the stages of analysis: reducing the sample size, selecting criteria / markers of the appropriate health level and classification of a particular subject / patient to the appropriate group according to his health.

Let consider in more detail an ensemble of used Data Mining methods.

Selection of informative parameters (filtering). The choice of variables follows from two tasks: 1) to find informative variables strongly connected with the target feature, 2) to define a small parameters subset, keeping enough information on initial indicators.

A peculiarity of the initial data in our study was a large number of indicators — ECG parameters. The multilevel system of indicators, calculated by automated ECG analysis, had a total of 240 features. Such a large amount of primary data is characteristic of many tasks in various fields of medical research. The correlation matrix was calculated among the predictors to avoid the problem of multicollinearity. The correlation coefficient ($R > 0,7$) is used as criteria for deciding whether variable may be excluded from the analysis because another input variable contains the same information.

As you know, there are several reasons for the negative impact of a large number of non-informative parameters on the learning algorithm quality, three of which are considered basic [32]. One important reason is that as the parameters number increases, more learning objects are needed for reliable classification. In addition, with increasing parameters number decreases the statistical reliability of the algorithm on the control data. The advantage of selecting informative features is the increase in the accuracy of the classification algorithm, generalization ability, achieving the possibility for the best interpretation of data.

Usually a preliminary selection of parameters is carried out before the start of machine learning algorithms. Statistical criteria for correlation of each of the primary features with the target feature and ordering (for example, by the size and significance of Chi-Square Pearson, F — Fisher) are used. Further selection of a set (combinations) of informative parameters is performed using classification algorithms for greater accuracy [33].

Clustering. One of the effective methods of data processing is their segmentation using cluster analysis methods (unsupervised learning). The clustering process divides the data set into cluster groups or subclasses [3]. Clustering (subgroups) allows you to use all available information to build multiple models, and then make more accurate predictions for the model.

We used two most popular algorithms, namely *k*-means, EM, which are implemented in the module Data Miner STATISTICA 10 [35, 36].

K–means method. The patients were divided into groups using the generalized *k*–means method. This method makes it possible to distribute observations (from space *Xn*) into k clusters according to the following criteria.

The first criterion for recalculating cluster centers is the minimization of the objective function (F_1) by the sum of the squares of the distances between each object x_i and the center of the cluster μ_n, to which it belonged at each iteration:

$$F_1 = \sum_{n=1}^{k} \sum_{x \in X_n} \left\| x_i - \mu_i \right\|^2 \to \min, \tag{1}$$

where x_i is the set of n observations, n is the number of objects to be divided into k groups (clusters), μ_n — cluster centers.

And the second criterion (F2) determines that the distances sum between the clusters should be as large as possible:

$$F_2 = \sum_{n,i=1}^{k} \left\| \mu_i - \mu_n \right\|^2 \to \max. \tag{2}$$

Additionally, in contrast to the classical method k–means, a cross-check is performed on N random samples, which allows to minimize the error and to select the optimal number of clusters. If the error function (average distance between cluster centers) for a solution k+1 clusters is not 5% better than the solution for k clusters, then the solution with k clusters will be final (optimal).

Fuzzy clustering algorithm (EM). The expectation-maximization (EM) algorithm assumes that the data correspond to a linear combination of distributions (normal, lognormal, binomial):

$$P(x) = \sum_{i=1}^{k} w_i \cdot p_i(x), \sum_{i=1}^{k} w_i = 1, w_i \geq 0, \tag{3}$$

where k is a number of components in a mixture of distributions $P(x)$, w_i — is weights of components, $p_i(x)$ — distribution density of components.

At each step of the iterative process, the expectation parameters are estimated and the likelihood function is calculated until the maximum of logarithmic likelihood is reached. The k-fold cross-validation use with the error function evaluation (loglikelihood) helps to determine the final number of clusters.

One of the accepted methods of estimating the required number of clusters is the Cluster Validity Indices method [37].

Classification and Regression Trees (CART). Decision trees have become the most common approach to solving the problem of assessing the patient's condition [17], to detect ischemia of the heart [38], to classify the stages of heart disease [39], as well as to identify changes in human functional states [30].

The advantage of the decision tree method is that there are no requirements for data distribution, their type. This approach facilitates the interpretation of the results, the model is displayed as a tree, the structure of which is determined by logical rules (IF — THAT). Its purpose is to predict the target variable based on other features known as predictors, which makes it possible to detect complex interactions.

We used the CART algorithm, a recursive method that allows us to develop classification and regression models. According to the CART algorithm, the data set is distributed across all variables sequentially into segments. The purpose of sequential segmentation is to obtain uniformity of data on the selected attribute, reducing uncertainty in the partition node.

In the CART algorithm for predictor selection and division into two nodes, the index as a measure of uncertainty (*Gini*) is used:

$$Gini(d) = 1 - \sum_{i \neq j}^{k} (P_i^d)(P_j^d), \tag{4}$$

where P_i is the probability of classification in node d as i or j.

In each node, the reduction of the impurity is maximized.

To summarize the result, the optimal size tree is selected by cutting branches in combination with the method of estimating the error of cross-checking (algorithms minimal cost-complexity tree pruning, V-fold cross-validation).

The method of **Support Vector Machine** is based on vector space model, which aims to find such a surface distribution between classes, which is the most remote from all points of the learning set any of the classes. If we denote the learning data set $D = \{X_i, y_i\}$, where X is the vector of the i-point and y_i is the corresponding class label, then the linear classifier has the form:

$$f(x) = sign(W^T X_i + b), \tag{5}$$

where W^T is weight vector and b is constant.

The optimization problem is solved, namely, the task of achieving the maximum gap between the reference points:

$$\frac{1}{2} W^T W \to \min. \tag{6}$$

For all $(X_i, y_i) \in D$ is satisfied when

$$y_i (W^T X_i + b) \geq 1. \tag{7}$$

This method is implemented in STATISTICA Data Mining module, there is a possibility of transition to a nonlinear model using other core functions.

ANN Neural network is a mathematical apparatus that simulates the work of a network of brain neurons. The components of the neural network consist of inputs x_i, which are fed to the neurons synapses that are connected by axons in several hidden layers and the final outputs y_i. The neuron state is described by a function

$$S = \sum_{i}^{n} x_i w_i, \tag{8}$$

where n is a number of inputs, w_i — weights i — synapse. The output value of the axon is

$$Y = f(S), \tag{9}$$

where $f(S)$ is the activation function.

When learning the network, the task is to minimize the objective error function by the method of least squares:

$$E(w) = \frac{1}{2}\sum_{j=1}^{k}(y_j - d_j)^2, \tag{10}$$

where y_j is the value of the j^{th} output of the neural network, d_j — target value of the j^{th} output, k — is a number of neurons in the output layer.

Classification quality indicators. To evaluate the performance of the proposed model the sensitivity, specificity, accuracy, and *F*-score are calculated.

The sensitivity is the proportion of positive instances that are correctly classified as positive. The specificity is the proportion of negative instances that are correctly classified as negative. The accuracy is the proportion of instances that are correctly classified.

$$Sensitivity\,(Recall) = \frac{TP}{TP + FN}, \tag{11}$$

$$Precision = \frac{TP}{TP + FP}, \tag{12}$$

$$Specificity = \frac{TN}{FP + TN}, \tag{13}$$

$$predicive\ Accuracy = \frac{TP + TN}{TP + TN + FP + FN}, \tag{14}$$

$$F\,score = \frac{2 \times Recall \times Precision}{Recall + Precision}, \tag{15}$$

where — *TP*, *TN*, *FP* and *FN* are the numbers of true positives, true negatives, false positives and false negatives respectively.

For multiclass case, these measures can be obtained from the confusion matrix by comparing numbers of instances for each class in the matrix against instances of all the other classes. *F*-score, since it combines precision and recall into a single number evaluating the whole system performance [40].

To solve the tasks for a particular subject of analysis, the formation of an appropriate ensemble of the considered set of methods was done. The initial data were indicators of heart rate variability, objective indicators of the studied physiological systems and expert assessments of the human health state.

The proposed information technology for the classification of functional states and human health consists of four main stages (Fig. 1).

Stage 1. Data pre-processing. At stage 1, the input data is pre-processed, checked for completeness, the presence of emissions, type compliance, reformatting. The target feature is determined by the specific task of the analysis: information about the response of body systems to external influences, expert data on the severity of the condition (disease activity) of patients and so on. At this stage, the number of primary HRV indicators was reduced and the most informative ones were selected regarding the target feature using filtration methods.

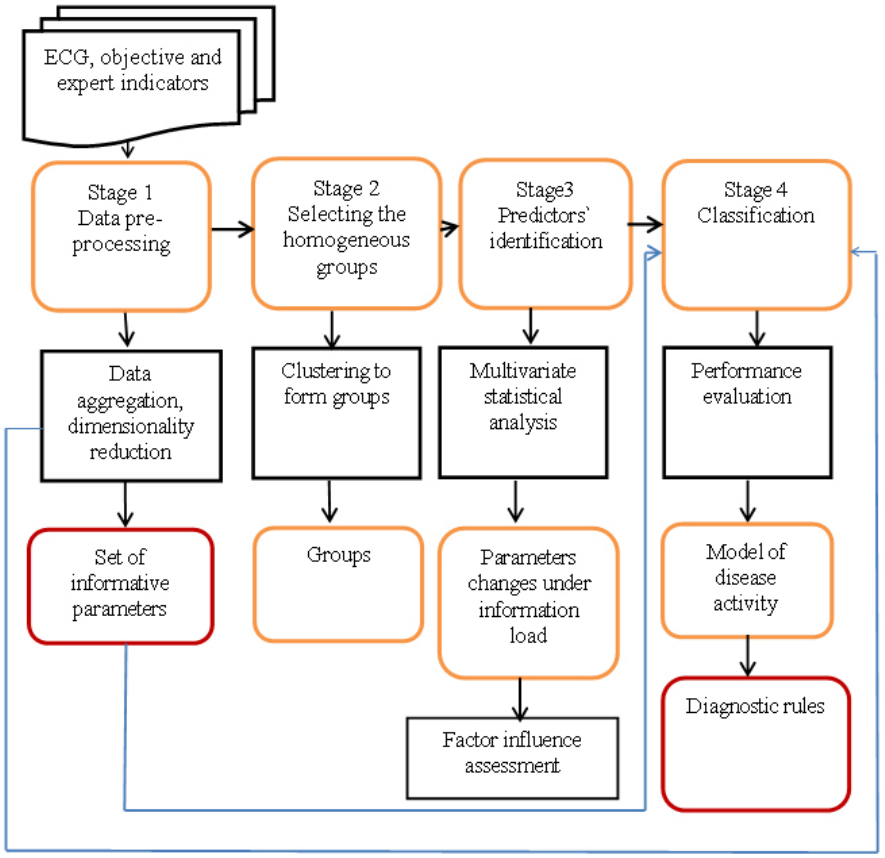

Fig. 1. Stages of information technology for the classification of functional states and human health

At this stage, the primary selection methods of informative parameters are used with statistical correlation criteria (Pearson's Chi-Square, *F*), that results in a reduction in the study volume to further determine the classification groups for the gradation of studied state changes.

In *stage 2 — clustering to form groups*, the number and composition of typological groups were determined by sets of informative indicators. At this stage, cluster analysis methods (*k* –means, EM) are used.

Stage 3. Predictors` identification. The transition to step 3 is carried out if there is a need for analysis of the repeated measurements. That is, when the purpose of the study is to identify changes in the informative indicators associated with changes in the factor (e.g., response to exercise). Methods of repeated analysis of variance (RepANOVA) are used, which allows to determine differences in informative indicators changes in certain subgroups, as well as to provide a statistical assessment of the factor influence. The result obtained at this stage will be a set of informative features that are statistically significantly related to the factor.

Stage 4. Classification of the human condition severity. In this stage, informative indicators set were tested, which are predictors of the CVS state as attributes of the state classification model. This step is performed if the initial data contains the target attribute (class label) provided by the experts.

Algorithms CART, ANN, and SVM were used. Comparisons of classification features sets selected by different models and general classification accuracy of different models were performed. The efficiency indicators of the models for each class were calculated (sensitivity, specificity, accuracy).

For samples of small number, cross-validation (10 -fold) was used to optimize the complexity of the model. The model was chosen according to two criteria: high enough accuracy and optimal complexity.

Calculated according to the CART algorithm, the decision tree with the optimal size allows to formulate classification rules for health of each severity (logical conditions for the values of a small set of ECG parameters).

If the classification quality is unsatisfactory, it is possible to return to the previous stages 1, 2, 3 using other selection methods of features subsets (or model parameters). In the presence of a test sample, the quality of classification models is checked on it.

The end result is the classification rules according to the informative set of ECG parameters, which determine the patient's condition severity.

During the development, the procedures of the Data Miner module of the STATISTICA 10 package were used. Note that the Data Mining algorithms are implanted in the Weka, RapidMiner, SAS Enterprise Miner software and in the modern design tool Python, R.

STUDY OF FUNCTIONAL STATE AND HUMAN HEALTH WITH THE USE OF DEVELOPED INFORMATION TECHNOLOGY

The proposed IT is used to solve problems aimed at studying the operators` functional state (prenozological state) and to classify the patients` severity in case of disease progression.

Determination of specific changes in operators` HRV indicators (prenosological state). Verification of the developed IT was carried out according to the experimental study of the reliability of operator activity under information load, which was performed by employees of the Research Institute of Military Medicine of the Armed Forces of Ukraine [41].

The condition of CVS regulatory mechanisms was studied by ECG recording (for 2 min) using Cardio Sens AIC (KHAI Medica, Kharkiv). The analysis was performed on the main HRV indicators, which belong to the generally accepted informative characteristic set of human functional state (statistical characteristics, spectral analysis, spectral components in the ranges ULF, VLF, LF, HF).

The professionally important qualities of military operators and their reliability of activities were assessed by tests consisted of information-intensive tasks: the dynamic memorization quality test (DMQ); the test of determining the speed and accuracy of the reaction to a moving object (RMO); the attention concentration and short-term memory test (ACSM). Factors influencing the operators` FS were determined according to the training process stages: 1 — rest state; 2 — QDM; 3 — RMO; 4 — ACSM; 5 — recovery state [42].

At the preparatory stage of each test, the individual optimal load level (τ_{lim}), which the operator can still perform without errors, was determined. At the training stage, the tasks complexity increased by 10 % of the determined individual optimal level. The percentage of errors made was used as an indicator of the operator activity reliability at different levels of test task complexity. The technique of the training cycle is described in detail in the works [41, 42].

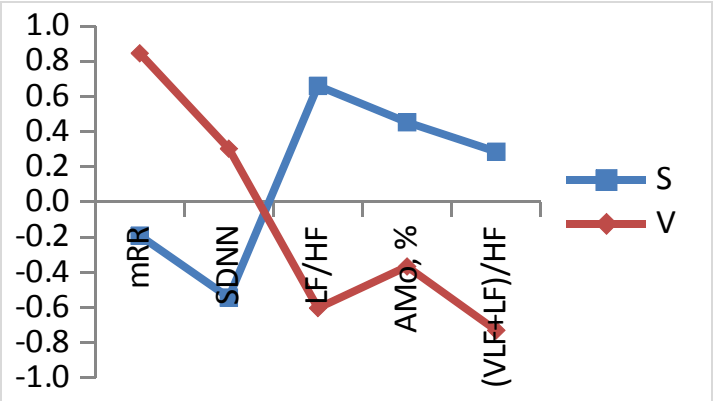

Fig. 2. Graf of means of indicators in two groups (S — sympathonics, V — vagotonics)

At the IT first stage the complex of the HRV main indicators on groups is defined:

— statistical characteristics: mode of RR-intervals (M_0RR), amplitude mode (AMo, %), standard deviation of RR-intervals (SDNN), stress index (SI);

— spectral indicators: total spectral power of the TP spectrum (0.003–0.4 Hz), spectral components in the bands ULF (< 0.015 Hz), VLF (0.015–0.04 Hz), LF (0.04–0,15 Hz), HF (0.15–0.4 Hz), the activation indices of subcortical centers VLF/HF, index centralization IC = (VLF + LF)/HF.

At the second stage of IT with the help of cluster analysis the group at rest state (1) was determined by the vegetative regulation type: 1) predominance of sympathetic division (S, sympathonics), 2) predominance of parasympathetic division (V, vagotonics). In fig. 2 standardized average values of indicators for which clustering was performed are provided. The group of sympathonics (S) includes 42, vagotonics (V) 28 operators.

Heart rate parameters in groups with different types of vegatative regulation, which differed significantly at rest stage (1), undergo significant changes during the training cycle, and at the stage of recovery (5) there is no significant difference between the two typological groups (Fig. 3).

If at the initial stage (1) the spectrum was dominated by components of the activity of the autonomous control loop (HF, LF), then after performing tests in both groups there is a redistribution of power spectrum against the background of decreasing mode of RR-intervals. The power of the high-frequency component (HF) decreases, the low-frequency component of the spectrum (VLF) increases, and the LF (first-order slow-wave power) increases, which reflects the activity of the vasomotor center.

At the same time, it was determined that the test loads of dynamic memory (DMQ) and rapid response (RMO) cause greater changes in HRV than the activation of attention concentration and memory (ACSM). Characteristically, after performing all test loads (step 5), the components of the heart rate spectrum return to values at rest state (1), except for the spectrum total power (TP) due to an increase in the LF component in the sympathonics` group.

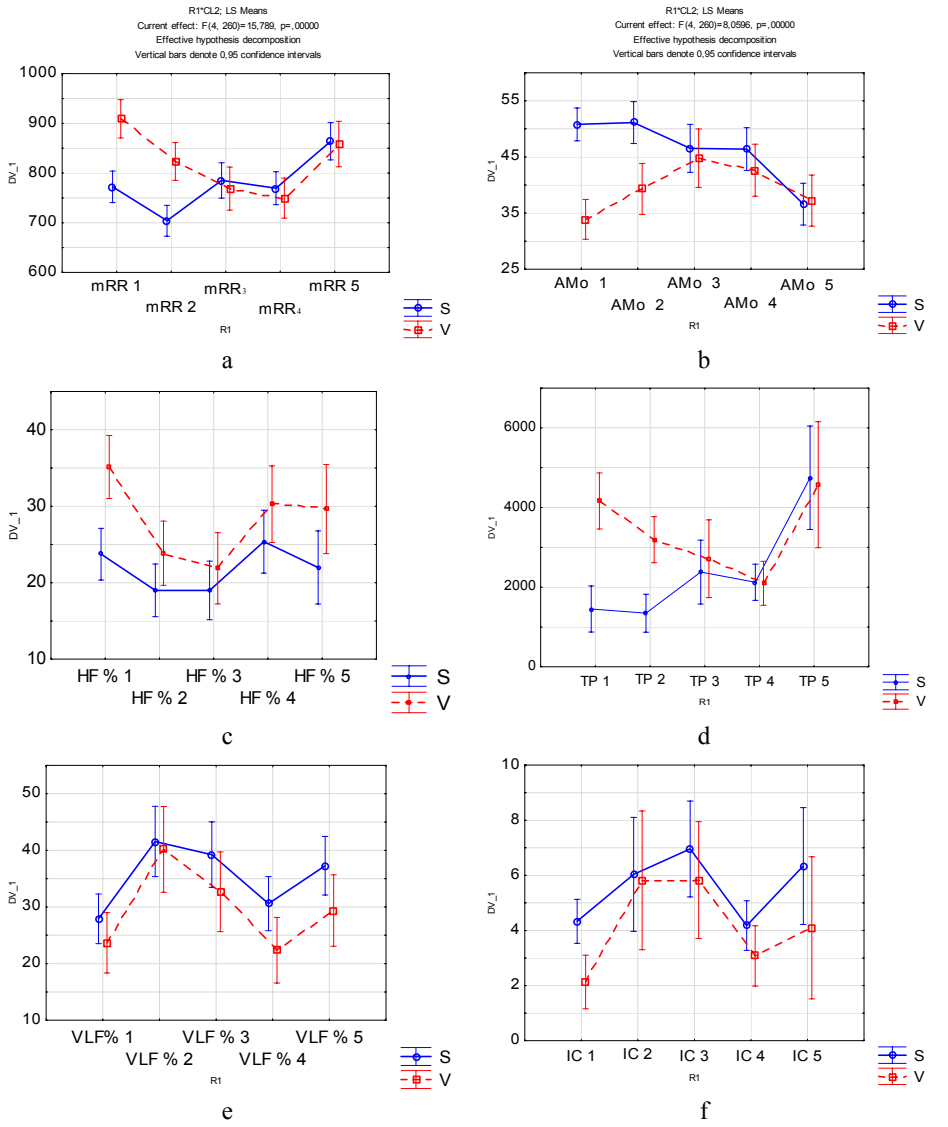

Fig. 3. Changes in spectral components at the stages of training (1, 2, 3, 4, 5) in sympathonics and vagotonics: a) mode; b) the RR mode amplitude; c) HF - high frequency component; d) TP — total power; e) VLF — power in the region of very low frequencies; f) (VLF + LF) / HF — centralization index

At the same time, it was determined that the test loads of dynamic memory (DMQ) and rapid response (RMO) cause greater changes in HRV than the activation of attention concentration and memory (ACSM). Characteristically, after performing all test loads (step 5), the components of the heart rate spectrum return to values at rest state (1), except for the spectrum total power (TP) due to an increase in the LF component in the sympathonics` group.

According to the literature, it is known that in the bases of mechanisms of formation of the low-frequency component (VLF) are stressors that activate the renin-angiotensin-aldosterone system and increase the catecholamines concen-

tration in plasma. The VLF component power is associated with the activity of suprasegmental (hypothalamic) centers of vegetative regulation, which are transmitted through the sympathetic part of the VNS [21].

Thus, after performing NPS and PPO tests changes in heart rate regulation occur, namely: acceleration of heart rate (decrease in MoRR), increase in low-frequency (VLF) and high-frequency (HF) heart rate fluctuations, increase in the centralization index (influence of the central control loop), indicating the stressful nature of these loads and significant psycho-emotional stress of the operators.

Development of a classification model of disease activity in children with dysplasia. Connective tissue dysplasia (CTD) is a systemic disease that arises at an early age, has many manifestations in the cardiovascular system, musculoskeletal system and other organs. To predict the disease development, it is important to know the diagnostic criteria that characterize the stages of disease activity. The purpose of the study is to determine these criteria according to the system of ECG indicators.

The classification of the severity of the condition of children with CTD was developed according to the arrays of ECG indicators, as well as indicators of the severity of the condition of patients determined by expert physicians. The final indicator of CVS state is the final assessment (FA), which is formed from complex assessments of lower level: health rate regulation, myocardial status and additional features (quantitative and qualitative assessments of different coding systems, arrhythmias, risk of sudden cardiac events etc.). Complex indicators are calculated in points (0–100).

The study was based on data from laboratory and clinical examination of 25 children with CTD manifestations. Disease activity was measured by the Juvenile Arthritis Activity Scale (JADAS) [43]. 6-channel ECG recording was performed for 5–20 minutes using a Cardio Plus P device.

Cluster analysis methods (*k*-means with 10-fold cross-validation) allowed identifying two typological groups for comprehensive assessments of the CVS regulation, myocardium condition and its reserves:

- group 1 (16 children) had a low level of complex assessment: $FA_1 = 58.3 \pm 8.1$;
- group 2 (9 children) - significantly differed by higher complex assessment: $FA_2 = 68.3 \pm 5,2$. ($I = 68,3 \pm 5,2$).

The optimal set of CVS state predictors is determined. The set of predictors consists of the following primary ECG parameters: cardiac arrhythmia (Heart rhythm disorders), T-wave amplitude (lead II), integrated indicator of the STT form (lead II), QRS — alpha angle, T-wave symmetry ratio. The error of the regression model (by CART algorithm) for a set of 5 parameters ECG is 18.8 %, the correlation coefficient $R = 0.88$.

Classification models of disease activity stages were developed. CVS FA predictors were tested as attributes on CART, Neural network, SVM models. The target variable — disease activity was determined by 3 gradations provided by experts (1 — the initial stage of activity, 2, 3 — subsequent stages of inflammation increasing). The quality comparison of 3 models in the training sample gave such training errors: CART — 0 %, Neural network — 24 %, SVM — 44%. That is, for a small sample, the best result was for the C&RT decision tree model — 100% classification accuracy.

After 10-fold cross-validation of the CART models revealed 4 indicators, which determine the disease activity with an overall classification accuracy of 88 %. The most significant attributes of the disease activity model and their contribution to the CART model (by rank) is shown (Tab. 1).

The optimal classification tree, which was determined after 10-fold cross-validation is given (Fig.4). It should be noted that the distribution of the training sample into groups with different activity was unbalanced.

The quality measures of the classification of these disease stages are shown (Tab.2). The average F-score = 0,94.

The quality measures of the classification of these disease stages. Thus according to the optimal model, the CTD stages are classified with high accuracy.

In accordance with the tree splitting conditions, logical rules for the severity classification of the condition are formulated, in particular the basic classification rules are:

- Low disease activity level D_1:
  if Ind STT > 49,5 and Ind STT ≤ 84,0 and Amp T(II) ≤ -160,5 then $D_1 = 1$
  if Ind STT > 49,5 and Ind STT ≤ 84,0 and Amp T(II) > -160,5 and α-QRS ≤ 75,5 and SimmT(I) ≤ -0,57 then $D_1 = 1$
- Middle disease activity level $D_2 = 2$:
  if Ind STT > 49,5 and ≤ 84,0 and Amp T(II) > -160,5 and α-QRS > 75,5 then D2 = 2
  if Ind STT > 49,5 and Ind STT ≤ 84,0 and Amp T(II) > -160,5 and α-QRS ≤ 75,5 and SimmT(I) > 0,57 then $D_2 = 2$
- High disease activity level D3 =3:
  if Ind STT ≤ 49,5 then $D_3 = 3$
  if Ind STT > 49,5 and Ind STT > 84,0 then $D_3 = 3$.

Table 1. **Predictor importance for the classification of CTD activity stages**

The best predictors	Variable importance rank
T - wave symmet ratio (I)	100
Ampl. T (II)	86
Ind. form STT (II)	76
α QRS	68

Table 2. **Classification results for CTD activity detection**

Measures (%)	Disease activity		
	1	2	3
Sensitivity	100	81,8	100
Specificity	85,7	100	100
Predictive Accuracy	92	92	100

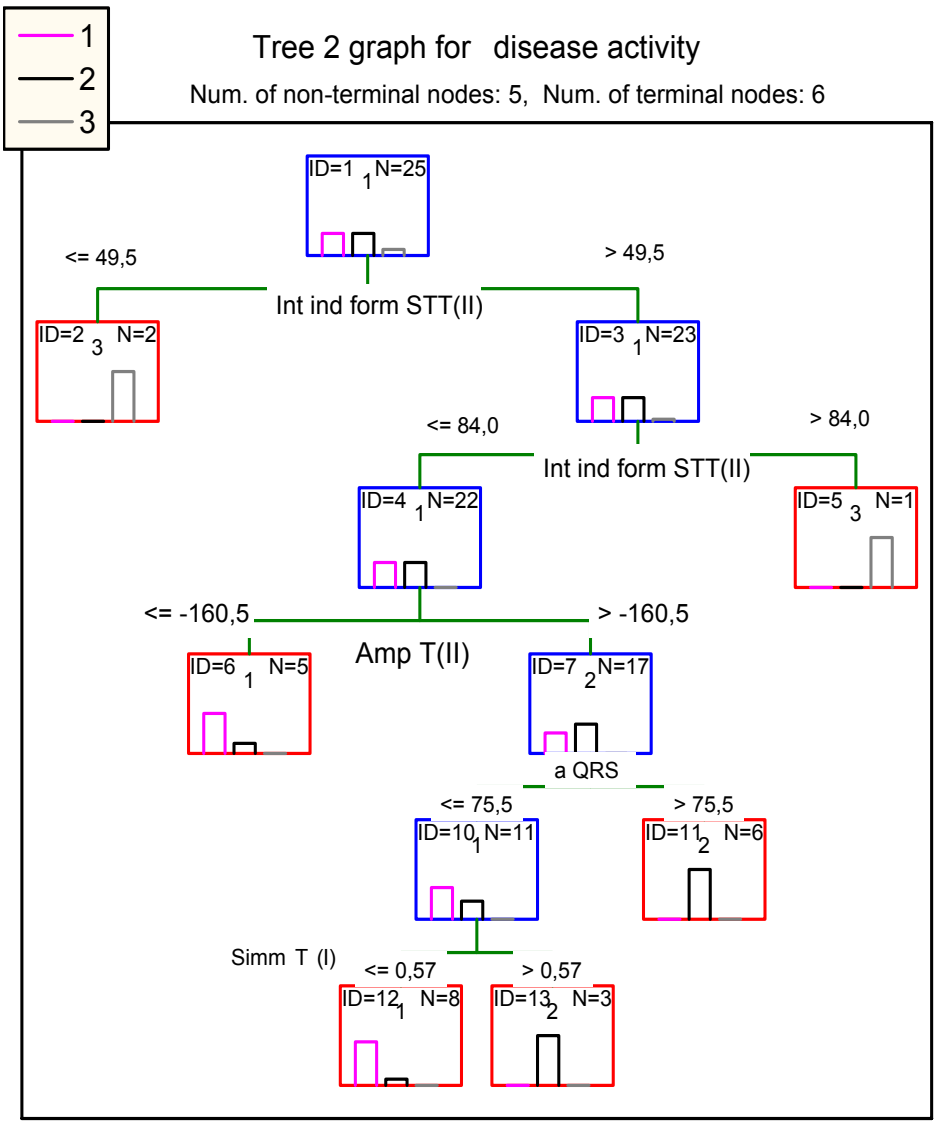

Fig. 4. Classification tree of CTD activity

Thus, with the help of the developed information technology the ECG indicators are determined, the changes of which can be markers of CVS disorders in the case of inflammatory processes in children diagnosed with juvenile arthritis, rheumatic disease. Markers of the initial stages of activity were determined by the following ECG parameters: α-QRS angle, chahge of the the T–wave (I) symmetry ratio.

Changes in the STT form (less than 49,5 or more than 84 points) indicates increased disease activity.

According to experts, the use of the proposed information technology to determine the CTD activity according the ECG parameters will allow the physician to identify the initial stages of the process in an outpatient setting. The advantage of this approach is the possibility of simultaneous assessment of CVS functional

changes and the disease activity level before the clinical manifestations of the inflammatory process. The STT shape indicator gives an opportunity to select a group of children with apropriate changes in the STT segment. Such changes reflect dysmetabolic, hypoxic changes of the myocardium that accompany the manifestations of inflammatory processes [44]. At the same time, it is also necessary to take into account changes in the T wave amplitude, changes in the angle alpha angle QRS, the T wave symmetry index.

Prospects for solving the problem of physician` information support. Further development of a clinical desition support system in disease severity determining will be aimed at analyzing large arrays of clinical, laboratory and instrumental data in order to improve the classification accuracy for an extended range of tasks.

CONCLUSIONS

The created information technology, which combines the generalized stages: data pre-processing to reduce the studied data set, clustering (data segmentation, likelihood function biulding), predictors` identification by analysis of Data Mining models and classification of human condition with formation of final characteristics allows to determine pecularities of human functional state change under external factors influence and severity patients by analysis of heart rate variability and expert characteristics.

The combination of Data Mining methods used at different stages of IT allows solving consistently the necessary tasks: by filtering indicators, the relevant features are determined; the use of clustering provides the homogeneous groups detection; the decision tree method (CART algorithm) makes it possible to build a classification rules and high classification accuracy.

Using the developed IT, specific changes in HRV indicators in operators, which occur under the influence of various types of information loads, are determined taking into account the type of vegetative regulation. Loads of dynamic memorization and rapid response cause greater changes in HRV than activation of attention concentration and short-term memory. Thus, the following shifts in HRV regulation occur during the performance of these tasks: acceleration of heart rate (decrease in MoRR), increase of low-frequency (VLF) and high-frequency (HF) heart rate fluctuations, increase of centralization index (influence of central regulation loop), which indicates stress loads and significant psycho-emotional strain in operators. In the recovery state after all test loads, only in sympathonics, the spectrum total power (due to an increase in the LF component) does not return to the initial values.

The use of developed models and technologies to classify the patients` severity allowed to assess the CVS state of children with dysplasia, identify markers of stages of different disease activity and build diagnostic rules, the use of which make it possible to predict the disease severity and to adjust treatment tactics.

REFERENCES

1. Ian H. Data Mining Practical Machine Learning Tools and Techniques Witten, Eibe Frank and Mark A. Hall Data Mining: Practical Machine Learning Tools and Techniques. 3rd Edition. Morgan Kaufmann, 2011, 665 p.
2. Yoo I., Alafaireet P., Marinov M., Pena-Hernandez K., Gopidi R., Chang J. F. Data Mining in Healthcare and Biomedicine: A Survey of the Literature. *Journal of medical systems*. 2012, no 36(4), pp. 2431–2448.
3. Chen M., Hao Y. , Hwang K., Wang L., Wang L. Disease Prediction by Machine Learning Over Big Data From Healthcare Communities. *IEEE Access 2017*;5:8869-8879.
4. Safdar S., Zafar S., Zafar N., Khan N.F. Machine learning based decision support systems (DSS) for heart disease diagnosis: a review. *Artificial Intelligence Review*. 2018, 50 (4), pp. 597–623.
5. Roopa C. K., Harish B. S. Survey on various Machine Learning Approaches for ECG Analysis. *International Journal of Computer Applications*. 2017, no 9, vol. 163, pp.25–33.
6. Mohan S., Thirumalai C., Srivastava G. Effective heart disease prediction using hybrid machine learning techniques. *IEEE Access*, 2019. 7:81542–81554.
7. Goldstein B.A., Navar A.M., Pencina M.J., Ioannidis J.P. Opportunities and challenges in developing risk prediction models with electronic health records data: a systematic review. *J Am Med Inform Assoc*. 2017, Jan; 24(1):198-208.
8. Antomonov M.Yu. Algorithmization of the choice of adequate mathematical methods in the analysis of medical and biological data. *Kibernetika i vyčislitel`naâ tehnika*. 2007, Iss. 153, pp. 12–23. (In Russian)
9. Georga E.I., Tachos N.S., Sakellarios A.I., Kigka V.I., Exarchos T.P., Pelosi G. Artificial intelligence and data mining methods for cardiovascular risk prediction Cardiovascular Computing. *Methodologies and Clinical Applications*. 2019, pp. 279–301
10. Amin M., Chiam Y. Identification of significant features and data mining techniques in predicting heart disease. *Telematics and Informatics*. 2019, Vol. 36, pp. 82–93.
11. Kaieski N., da Costa C.A., da Rosa Righi R., Lora P.S. Application of artificial intelligence methods in vital signs analysis of hospitalized patients: A systematic literature review. *Applied Soft Computing*. 2020, Vol. 96,
12. Owens W.D., Felts J.A., et al. A physical status classification: A study of consistency of ratings. *Anesthesiology*. 1978, Vol. 49, pp. 239–243.
13. Lemeshow S., Le Gall J.R: Modeling the severity of illness of ICU patients. *JAMA*. 1994, Vol 272, pp.1049–1055.
14. Le Gall J.R., Lemeshow S., Saulnier F: A new simplified acute physiology score (SAPS II) based on a European/North American multicenter study. *JAMA*. 1993, 270 (24), pp. 2957–2963.
15. Knaus W.A., Draper E.A., Wagner D.P., Zimmerman J.E: APACHE II: A severity of disease classification system. *Cri.t Care Med* .1985, 13:818-829.
16. Lemeshow S., Teres D., Klar J., Avrunin J.S., Gehlbach S.H., Rapoport J. Mortality probability models (MPM II) based on an international cohort of intensive care unit patients. *JAMA* 1993, 270, pp. 2478-86
17. Trujillano J., Badia M, Serviá L. Stratification of the severity of critically ill patients with classification trees. *BMC medical research methodology*. 2009, V 9, no 7, pp. 83–95.
18. Kim S., Kim W., Park R.W. A Comparison of intensive care unit mortality prediction models through the use of Data Mining Techniques. *Health Inform Res* 2011,17, pp. 232–43.
19. Allyn J. et all. A comparison of a machine learning model with EuroSCORE II in predicting mortality after elective cardiac surgery: a decision curve analysis. *PLoS one* 2017, 12(1), pp. 1–12.
20. Amosov N.M. Thinking about health. Moskow: 1978, 178 p. (In Russian)
21. Baevsky R.M., Berseneva A.P. Introduction to prenosological diagnostics. Moskow: Slovo, 2008, 174 p. (In Russian)
22. HRV analysis software URL: http://www.nevrokard.eu/maini/hrv.html (last access 20.10.2020)
23. Fainzilberg L.S. Computer diagnostics based on the phase portrait of an electrocardiogram. Kyiv: Osvita Ukrainy. 2013, 191 p. (In Russian)

24. Gritsenko V.I., Fainzilberg L.S. Intelligent information technologies in digital medicine on the example of phasagraphy. Kyiv: Naukova Dumka. 2019, 423 p. (In Russian)
25. Fainzilberg L.S., Dykach Ju.R. Linguistic approach for estimation of electrocardiograms's subtle changes based on the Levenstein distance. *Cybernetics and Computer Engineering*. 2019, no. 2 (196), pp. 3–26.
26. Gritsenko V.I., Fainzilberg L.S. Current state and prospects for the development of digital medicine. *Cybernetics and Computer Engineering*. 2020, no. 1 (199), pp. 59–84.
27. Richman J.S. Randall M.J. Physiological time–series analysis using approximate entropy and sample entropy. *Am J. Physiol. Heart Circ. Physiol*. 2000, Vol. 278, № 6, pp. H22039–H2049.
28. İşler Y., Kuntalp M. Combining classical HRV indices with wavelet entropy measures improves to performance in diagnosing congestive heart failure. *Computers in Biology and Medicine*. 2007, Vol. 37, no. 10, pp. 1502–1510.
29. Valupadasu R., Chunduri B. R., Chanagoni V. Identification of Cardiac Ischemia using bispectral analysis of ECG. *Biomedical Engineering and Sciences* (IECBES). 2012: IEEE EMBS Conference on, Langkawi. 2012, pp. 999–1003.
30. Romanyuk O.A., Kozak L.M., Kovalenko A.S., Kryvova O.A. Digital transformation in medicine: from formalized medical documents to information technologies of digital medicine. *Cybernetics and Computer Engineering.* 2018, no. 4(194), pp. 61–78.
31. Krivova O.A., Kozak L.M. Comprehensive assessment of regional demographic development. *Kibernetika i vyčislitel`naâ tehnika*. 2015, Iss 182, pp. 70–84 (In Russian)
32. Wolf L., Shashua A. Features Selection for Unsupervised and Supervised Inference: The Emergence of Sparsity in a Weight-Based Approach. *J. Machine Learning Res*. 2005, V. 6, pp. 1855–1887.
33. Guyon I., Elisseeff A. An Introduction to Variable and Feature Selection. *Journal of Machine Learning Research*. 2003, V 3, pp. 1157–1182.
34. Mandel I.D. Cluster analysis. Moscow: Finance and Statistics. 1988. 128 p. (In Russian)
35. Tzortzis G., Likas A. The MinMax k-Means clustering algorithm. *Pattern Recognition*. 2014, no 47 (7), pp. 2505–2516.
36. McLachlan G. Krishnan T. *The EM algorithm and extensions*. New York, United States: Wiley. 1997, 274 p.
37. Wang K., Wang B., Peng L. CVAP: Validation for cluster analyses. *Data Science Journal*. 2009, no 8, pp. 88–93.
38. Fayn J. A classification tree approach for cardiac ischemia detection using spatiotemporal information from three standard ECG leads. *IEEE Trans. Biomed. Eng*. 2011, V. 58, no 1, pp. 95–102.
39. Pecchia L., Melillo P. Bracale M. Remote health monitoring of heart failure with data mining via CART method on HRV features. *IEEE Transactions Biomedical Engineering*. 2011, V. 58(3), pp. 800–804.
40. Sokolova M., Lapalme G. A systematic analysis of performance measures for classification tasks. *Information processing & management*. 2009, V. 45, N 4, pp. 427–437.
41. Kalnish V.V., Shvets A.V. Information technology for psychophysiological support of high reliability of operator activities. *Kibernetika i vyčislitel`naâ tehnika*. 2014, Iss. 177, pp. 54–67. (In Russian)
42. Shvets A.V., Kalnysh V.V. Features of influence of various psychophysiological states on reliability of operator` activity. *Military medicine of Ukraine*. 2009, no 1, pp. 84–91. (In Ukrainian)
43. Consolaro A., Ruperto N, Bazso A. Development and validation of a composite disease activity score for juvenile idiopathic arthritis. *Arthritis & Rheumatism*, 2009, vol. 61, pp. 658–666.
44. Ansari S., Farzaneh N, Duda M, Horan K. A review of automated methods for detection of myocardial ischemia and infarction using electrocardiogram and electronic health records. *IEEE reviews in biomedical engineering*. 2017, Vol. 10, pp. 264–298.

Received 31.11.2020

ЛІТЕРАТУРА

1. Ian H. Data Mining Practical Machine Learning Tools and Techniques Witten, Eibe Frank and Mark A. Hall Data Mining: Practical Machine Learning Tools and Techniques. 3rd Edition. Morgan Kaufmann, 2011. 665 p.
2. Yoo I., Alafaireet P., Marinov M., Pena-Hernandez K., Gopidi R., Chang J. F. Data Mining in Healthcare and Biomedicine: A Survey of the Literature. *Journal of medical systems*. 2012. No 36(4). P. 2431–2448.
3. Chen M., Hao Y. , Hwang K., Wang L., Wang L. Disease Prediction by Machine Learning Over Big Data From Healthcare Communities. *IEEE Access*. 2017;5:8869-8879.
4. Safdar S., Zafar S., Zafar N., Khan N.F. Machine learning based decision support systems (DSS) for heart disease diagnosis: a review. *Artificial Intelligence Review*. 2018, 50 (4), 597-623.
5. Roopa C. K., Harish B. S. Survey on various Machine Learning Approaches for ECG Analysis. *International Journal of Computer Applications*. 2017. no 9. Vol. 163. pp.25–33.
6. Mohan S., Thirumalai C., Srivastava G. Effective heart disease prediction using hybrid machine learning techniques. *IEEE Access*, 2019. 7:81542–81554.
7. Goldstein B.A., Navar A.M., Pencina M.J., Ioannidis J.P. Opportunities and challenges in developing risk prediction models with electronic health records data: a systematic review. *J Am Med Inform Assoc*. 2017, Jan; 24(1):198-208.
8. Антомонов М.Ю. Алгоритмизация выбора адекватных математических методов при анализе медико-биологических данных. *Кибернетика и вычислительная техника*. 2007. Вып. 153. С. 12–23.
9. Georga E.I., Tachos N.S., Sakellarios A.I., Kigka V.I., Exarchos T.P., Pelosi G. Artificial intelligence and data mining methods for cardiovascular risk prediction Cardiovascular Computing. *Methodologies and Clinical Applications*. 2019. P. 279–301
10. Amin M., Chiam Y. Identification of significant features and data mining techniques in predicting heart disease. *Telematics and Informatics*. 2019. Vol. 36. P. 82–93.
11. Kaieski N., da Costa C.A., da Rosa Righi R., Lora P.S. Application of artificial intelligence methods in vital signs analysis of hospitalized patients: A systematic literature review. *Applied Soft Computing*. 2020. Vol. 96.
12. Owens W.D., Felts J.A., et al. A physical status classification: A study of consistency of ratings. *Anesthesiology*. 1978. Vol. 49. P. 239–243.
13. Lemeshow S., Le Gall J.R: Modeling the severity of illness of ICU patients. *JAMA*. 1994, Vol 272. P.1049–1055.
14. Le Gall J.R., Lemeshow S., Saulnier F: A new simplified acute physiology score (SAPS II) based on a European/North American multicenter study. *JAMA*. 1993, 270 (24). P.: 2957–2963.
15. Knaus W.A., Draper E.A., Wagner D.P., Zimmerman J.E: APACHE II: A severity of disease classification system. *Cri.t Care Med* .1985. 13:818-829.
16. Lemeshow S., Teres D., Klar J., Avrunin J.S., Gehlbach S.H., Rapoport J. Mortality probability models (MPM II) based on an international cohort of intensive care unit patients. *JAMA*.1993. 270:2478-86
17. Trujillano J., Badia M, Serviá L. Stratification of the severity of critically ill patients with classification trees. *BMC medical research methodology*. 2009. V 9. no 7. P. 83–95.
18. Kim S., Kim W., Park R.W. A Comparison of intensive care unit mortality prediction models through the use of Data Mining Techniques. *Health Inform Res* 2011;17:232-43.
19. Allyn J. et all. A comparison of a machine learning model with EuroSCORE II in predicting mortality after elective cardiac surgery: a decision curve analysis. *PloS one* 2017. 12(1). P. 1–12.
20. Амосов Н.М. Раздумья о здоровье — М: 1978. 178 с.
21. Баевский Р.М., Берсенева А.П. Введение в донозологическую диагностику. М.: Слово, 2008. 174 с.
22. HRV analysis software. URL: http://www.nevrokard.eu/maini/hrv.html (дата звернення: 20.10.2020)
23. Файнзильберг Л.С. Компьютерная диагностика по фазовому портрету электрокардиограммы. К.: Освита Украины, 2013. 191 с.

24. Гриценко В.И., Файнзильберг Л.С. Интеллектуальные информационные технологии в цифровой медицине на примере фазаграфии. Киев: Наукова Думка, 2019. 423 с.
25. Fainzilberg L.S., Dykach Ju.R. Linguistic approach for estimation of electrocardiograms's subtle changes based on the Levenstein distance. *Cybernetics and Computer Engineering*. 2019. No. 2 (196). P. 3–26.
26. Gritsenko V.I., Fainzilberg L.S. Current state and prospects for the development of digital medicine. *Cybernetics and Computer Engineering*. 2020. No. 1 (199). P. 59–84.
27. Richman J.S. , Randall M.J.Physiological time–series analysis using approximate entropy and sample entropy. *Am J. Physiol. Heart Circ. Physiol.* 2000. Vol. 278. № 6. P. H22039–H2049.
28. İşler Y., Kuntalp M. Combining classical HRV indices with wavelet entropy measures improves to performance in diagnosing congestive heart failure. *Computers in Biology and Medicine*. 2007. Vol. 37. No. 10. P. 1502–1510.
29. Valupadasu R., Chunduri B. R., Chanagoni V. Identification of Cardiac Ischemia using bispectral analysis of ECG. *Biomedical Engineering and Sciences* (IECBES). 2012: IEEE EMBS Conference on, Langkawi. 2012. P. 999–1003.
30. Romanyuk O.A., Kozak L.M., Kovalenko A.S., Kryvova O.A. Digital transformation in medicine: from formalized medical documents to information technologies of digital medicine. *Cybernetics and Computer Engineering.* 2018. No. 4(194). P. 61–78.
31. Кривова О.А., Козак Л.М. Комплексная оценка регионального демографического развития. *Киб.и выч.техн.*, 2015. Вып 182. С. 70–84.
32. Wolf L., Shashua A. Features Selection for Unsupervised and Supervised Inference: The Emergence of Sparsity in a Weight-Based Approach. *J. Machine Learning Res*. 2005. V. 6. P. 1855–1887.
33. Guyon I., Elisseeff A. An Introduction to Variable and Feature Selection. *Journal of Machine Learning Research*. 2003. V 3. P. 1157–1182.
34. Мандель И.Д. Кластерный анализ. М.: Финансы и статистика. 1988. 128 с.
35. Tzortzis G., Likas A. The MinMax k-Means clustering algorithm. *Pattern Recognition*. 2014. No 47 (7). Pp 2505–2516.
36. McLachlan G. Krishnan T. *The EM algorithm and extensions*. New York, United States: Wiley. (1997) 274 p.
37. Wang K., Wang B., Peng L. CVAP: Validation for cluster analyses. *Data Science Journal*. 2009. No 8. Pp. 88–93.
38. Fayn J. A classification tree approach for cardiac ischemia detection using spatiotemporal information from three standard ECG leads. *IEEE Trans. Biomed. Eng*. 2011. V. 58. no 1. P. 95–102.
39. Pecchia L., Melillo P. Bracale M. Remote health monitoring of heart failure with data mining via CART method on HRV features. *IEEE Transactions Biomedical Engineering*, 2011 V. 58(3). P. 800–804.
40. Sokolova M., Lapalme G. A systematic analysis of performance measures for classification tasks. *Information processing & management*. 2009 (45). N 4. V. 45. P. 427–437.
41. Кальниш В.В., Швец А.В. Информационная технология психофизиологического обеспечения высокой надежности операторской деятельности. *Киберн. И выч. техн.* 2014. Вып. 177. С. 54–67.
42. Швець А.В., Кальниш В.В. Особливості впливу різних психофізіологічних станів на надійність операторської діяльності. *Військова медицина України*. 2009. № 1. С. 84–91.
43. Consolaro A., Ruperto N, Bazso A. Development and validation of a composite disease activity score for juvenile idiopathic arthritis. *Arthritis & Rheumatism*. 2009. Vol. 61. P. 658–666.
44. Ansari S., Farzaneh N, Duda M, Horan K. A review of automated methods for detection of myocardial ischemia and infarction using electrocardiogram and electronic health records. *IEEE reviews in biomedical engineering*. 2017. Vol. 10. P. 264–298.

Отримано 31.11.2020

Кривова О.А., наук. співроб.
відд. медичних інформаційних систем
ORCID: 0000-0002-4407-5990
e-mail: ol.kryvova@gmail.com
Козак Л.М., д-р біол. наук, старш. наук. співроб.,
провід. наук. співроб. відд. медичних інформаційних систем
ORCID: 0000-0002-7412-3041
e-mail: lmkozak52@gmail.com
Міжнародний науково-навчальний центр інформаційних
технологій та систем НАН України та МОН України,
пр. Акад. Глушкова, 40, м. Київ, 03187, Україна

ІНФОРМАЦІЙНА ТЕХНОЛОГІЯ КЛАСИФІКАЦІЇ ДОНОЗОЛОГІЧНИХ ТА ПАТОЛОГІЧНИХ СТАНІВ ЗДОРОВ'Я З ВИКОРИСТАННЯМ АНСАМБЛЮ МЕТОДІВ DATA MINING

Вступ. Впровадження цифрових технологій забезпечує реєстрацію великих обсягів біомедичних даних (ЕКГ, ЕЕГ, електронних медичних записів) як основи для оцінювання і прогнозування стану пацієнтів. Методи Data Mining дають змогу виявити найбільш інформативні показники, типологічні групи, класифікувати функційний стан людини і стадії захворювання для прогнозування їхніх змін.

Метою роботи є розроблення інформаційної технології класифікації стану здоров'я людини за допомогою комплексу методів Data Mining за об'єктивними та експертними характеристиками.

Результати. Розроблена інформаційна технологія об'єднує кілька етапів: I — попереднє оброблення даних; II — кластеризація, вибір однорідних груп (сегментація даних); III — ідентифікація предикторів; IV — класифікація досліджуваних станів, розроблення прогнозних моделей за допомогою алгоритмів машинного навчання (дерев рішень (Decision trees, опорних векторних машин Support vector machine, нейронних мереж) та методу перевірки навчальної вибірки (cross-validation). Запропоновану ІТ використано для дослідження функційного стану операторів та класифікації тяжкості стану пацієнтів у разі прогресування захворювання.

Висновки. Використання інформаційної технології для оцінювання успішності діяльності операторів дало можливість виділити найінформативніші показники ВРС, за змінами яких можна прогнозувати надійність діяльності операторів з урахуванням типу вегетативної регуляції. Оцінювання активності захворювання дітей з дисплазією з використанням ІТ дало змогу ідентифікувати діагностичні маркери ССС та розробити діагностичні правила для визначення стадій захворювання за параметрами ЕКГ (симетрія зубця Т, інтегральний показник форми сегмента STT).

Ключові слова: *інформаційна технологія, Data Mining, моделі машинного навчання, тяжкість стану пацієнта.*

ДО УВАГИ АВТОРІВ!

У журналі надано результати досліджень у галузях теорії та практики інтелектуального керування, інформатики та інформаційних технологій, а також біологічної та медичної кібернетики.

Цільова аудиторія — науковці, інженери, аспіранти та студенти вищих навчальних закладів відповідного фаху.

Вимоги до рукописів статей

1. Рукопис надають на папері у двох примірниках (мова — англійська, українська, 17–22 с.) та електронна версія. До рукопису додають:

• анотації — українською та англійською мовами (прізвище, ініціали автора/ів, місце роботи, місто, країна, назва статті, текст 250–300 слів, з виділенням рубрик: вступ, мета, результати, висновки, ключові слова 5–8 слів);

• список літератури мовою оригіналу — у порядку згадування в тексті, за стандартом ДСТУ 8302:2015;

• список літератури — переклад джерел англійською мовою, прізвища та ініціали авторів — транслітерація;

• ліцензійний договір;

• відомості про автора/ів українською та англійською мовами повинні містити: ПІБ, вчений ступінь, наукове звання, посада, відділ, місце роботи, поштова адреса організації, телефон (для зв’язку редактора), авторські ідентифікатори ORCID або ResearcherID, E-mail.

2. Текст статті подають з обов'язковими рубриками: вступ, постановка завдання/проблеми, мета, результати, чітко сформульовані висновки.

Вимоги до текстового файлу

Формат файлу * .doc, * .rtf. Файл повинен бути підготовлений за допомоги текстового редактора Microsoft Word.

Використовувані стилі: шрифт Times New Roman, 12 пт, міжрядковий інтервал – 1,5. Формат паперу А4, всі береги — 2 см.

Формули набирають у редакторах формул Microsoft Equation Editor 3.0. та MathType 6.9b. Опції редактора формул — (10,5; 8,5; 7,5; 14; 10). **Ширина формул — до 12 см**.

Рисунки повинні бути якісними, створені вбудованим редактором рисунків Word Picture або іншими Windows-додатками (рисунки надають окремими файлами відповідних форматів). **Ширина рисунків — до 12 см**.

Таблиці виконують стандартним вбудованим у Word інструментарієм «Таблиця». **Ширина таблиці — до 12 см**.

Передплату на журнал (друкована версія) в Україні здійснюють:

- за «Каталогом видань України», індекс передплати друкованої версії — 86598;
- за допомоги передплатної агенції «Укрінформнаука» НАН України, ukrinformnauka@gmail.com, індекс журналу — 10029